Title

The Role of Abiotic and Biotic Processes in Regulating Benthic Ecosystem Function along a Productivity Gradient

Author

Framsted, Nicholas

Publication Date

2022

Peer reviewed|Thesis/dissertation

The Role of Abiotic and Biotic Processes in Regulating Benthic Ecosystem Function along a Productivity Gradient

By

NICHOLAS FRAMSTED
THESIS

Submitted in partial satisfaction of the requirements for the degree of

MASTER OF SCIENCE

in

Ecology

in the

OFFICE OF GRADUATE STUDIES

of the

UNIVERSITY OF CALIFORNIA

DAVIS

Approved:

Steven Sadro, Chair

Geoffrey Schladow

Mark Buetel

Committee in Charge

2022

Abstract

The benthic zone of lakes can be a hotspot for lake energy flows and nutrient cycling. Indeed, the notion of benthic "ooze" and its role in the recycling of nutrients forms a conceptual cornerstone of ecology (Lindeman 1942). Benthic habitats can vary from soft, muddy sediments rich in organic matter and nutrients to bare rock covered by thin biofilms. These habitats form the linkage between lake and watershed, and support a range of ecosystem processes—from exchange of groundwater nutrients, internal nutrient cycling, mineralization of organic matter, heterotrophic respiration, and benthic algal production—that each vary in importance between different waterbodies. Clear Lake, CA, and Lake Tahoe represent two systems that span a gradient in trophic level, depth, and underlying geology. The former is shallow, and extremely productive, while the latter is deep and has nutrient concentrations near detection limit. Both, however, are large lakes and are extremely important water resources in California. We set out to characterize two very different, but nevertheless important, benthic processes that are adversely affecting water quality in each lake.

Benthic algae, or periphyton, blooms may be increasing in oligotrophic, clear water lakes globally in response to increases in water temperature and nutrient loads, often associated with climate change. In many regions, climate change is altering the duration of snow cover, the frequency and severity of drought, and storm intensity, all of which have the potential to affect periphyton growth rates. Lake Tahoe, located in the Sierra Nevada Mountains of California and Nevada, has anecdotal reports that the frequency and severity of nearshore periphyton blooms have increased in recent years. Such blooms decrease both water quality and the aesthetic value of nearshore areas. While recent studies have documented changes in periphyton biomass, it is difficult for *in situ* studies to disentangle the individual and interactive effects of temperature and nutrients on periphyton growth rates. Consequently, we used laboratory experiments to examine 1) seasonal variability in periphyton biomass and metabolism, 2) the role of temperature, nutrients, and their interactive effects on determining

periphyton metabolic rates, and 3) seasonal variability of the aforementioned temperature and nutrient effects. By measuring changes in dissolved oxygen in sealed incubation chambers containing rocks collected from the nearshore, we quantified rates of gross primary production (GPP), ecosystem respiration (ER), and net ecosystem production (NEP). Our experiments had two nutrient treatments (ambient and augmented with nitrogen and phosphorus) and four temperature treatments (ambient, +3, +6, and +9 °C above ambient) to simulate warming during different seasons, and nutrient loading associated with increased runoff. We found that temperature drove the majority of variability in periphyton metabolic rates and increased GPP, ER, and NEP by 4-7% per 1°C of warming. The effect of warming varied seasonally with larger effects in colder months. Warming also stimulated ER more so than GPP, with decreasing trends of NEP with warming during summer months. Nutrient additions had variable effects on rates of GPP, ER and NEP, but increased ER rates by 6-7% at maximum nutrient concentrations observed in the field. However, in contrast to our expectations, we found little evidence for interactive effects between temperature and nutrients for GPP and NEP, and a small, negative, inhibitory interaction for ER. In all, these experiments provide evidence that warming can increase periphyton metabolic rates in oligotrophic systems even in the absence of increased nutrient loads in cases where periphyton are not nutrient limited. These effects on littoral zones of lakes will have important consequences for ecosystem structure and function, and management efforts to curb nutrients will be crucial for limiting periphyton blooms under climate change.

Eutrophication continues to be a problem in aquatic systems globally, resulting from excessive nutrients such as phosphorus and nitrogen. Nutrient sources can be external (i.e. runoff) or from within the lake (internal loading). In the case of phosphorus, internal loading can occur several ways: 1) chemically reduced conditions at the sediment-water interface of lake bottoms (usually induced by anoxic conditions) facilitate the reductive dissolution of phosphorus from the sediments to the overlying water, 2) mineralization of organic matter, and 3) physical resuspension of shallow sediments, and 4)

elevated pH (commonly the result of intensive algal productivity) that results in ion exchange in sediments. Efforts to restore Clear Lake, a hypereutrophic lake located in Lake County, CA, have largely focused on external nutrient inputs as the cause of excessive phosphorus concentrations. This study provided the first direct measure of internal phosphorus fluxes from the nutrient-rich lake-bottom sediments to the overlying water column using incubations of intact sediment cores. Similar to other studies, soluble reactive phosphorus (SRP) flux rates from sediments ranged from 8.8 to 26.7 mg SRP m^{-2} d^{-1} in anoxic treatments and from -4.2 to 0.9 mg SRP m^{-2} d^{-1} in oxygenated treatments. We found little seasonal variation in anoxic SRP flux rates between winter and summer incubations despite large temperature differences between these two seasons. We hypothesize that early summer drawdown of redox-sensitive sediment P pools can potentially limit sediment phosphorus flux rates later in the season despite the positive effects of warmer summer temperatures on SRP flux. Thus, characterizing phenology of sediment P pools is important for estimating annual internal phosphorus loads in lakes. Large internal fluxes of P in this system were largely ignored during establishment of nutrient TMDLs for the watershed. This study highlights the importance of measuring internal fluxes of P and its seasonality when setting nutrient TMDLs or designing restoration strategies for a watershed.

Acknowledgements

I am grateful for financial support from the Lahontan Regional Water Quality Control Board and Assembly Bill 707, and the Blue Ribbon Committee for the Rehabilitation of Clear Lake.

This work would not have been possible without the dedicated folks who braved cold weather, early mornings, and late nights to carry out these experiments. I would like to thank Alice Tung, China Granger, Anne Le, Sarah Martin, Paloma Herrera-Thomas, and a special thanks to Kendal Hiemke and Lindsay Vaughan for their incredible support and dedication during experiments. Thank you to Karen Atkins, Scott Hackley, Brandt Allen, Brandon Berry, Katie Senft, Anne Liston, Steven Sesma, Aaron Vanderpool, Sergio Valbuena, Tina Hammell, Christopher Dunbar, Ruth Thirkill, Micah Swann, and the

rest of TERC staff whose work formed the foundation for my research and made everything possible. I would like to thank Andrew Blandino and Wesley Brooks for their advice and consult on statistics, which was incredibly helpful. I would also like to thank the UC Davis Center for Aquatic Biology and Aquaculture, Dennis Cocherell, Linda Deanovic, Matthew Stone for providing excellent support for building and maintaining our incubation facility. I would like to thank the Durand lab for lending dissolved oxygen equipment. We acknowledge the land on which the UC Davis main campus and the Tahoe Environmental Research Center are located, the historic homeland of the Patwin and Washoe peoples.

I would also like to thank my mentor and advisor Steve Sadro for his constant support and guidance these last 3 years. Your advice and leadership have taught me that good science does not have to be complicated or flashy, but is best when the story is simple and understandable. Our conversations taught me more than how to be a good scientist, but also how to be the person I want to be.

Dedication

To my parents, who inspired me to become a scientist and supported my work since day one.

Table of Contents

Chapter 1: Disentangling Temperature and Nutrient Effects on Nearshore Periphyton Metabolism in a Large, Oligotrophic Lake

Introduction

Periphyton, or benthic algae, form the base of littoral food webs in lakes (Hecky and Hesslein 1995, Yoshii 1999) and can account for a majority of total production, especially in clear-water, oligotrophic lakes (Cattaneo and Kalff 1980, Loeb et al. 1983, McCormick et al. 1997, Vadeboncoeur and Steinman 2002). Recent studies indicate that periphyton blooms are increasing in frequency and severity in clear-water lakes globally (Jacoby et al. 1991, Hawes and Smith 1994, Kravtsova et al. 2014, Cantonati et al. 2016, Ozersky et al. 2018, Vadeboncoeur et al. 2021). This potential trend is worrying as periphyton blooms can degrade both water quality and aesthetic value of pristine lakes, especially in nearshore areas with high visibility to the public. For example, in Lake Baikal periphyton blooms have caused extensive beach fouling that require human removal as blooms senesce, slough off the benthos, and wash up on beaches (Vadeboncoeur et al. 2021). With climate change expected to raise both mean surface air temperatures by 2-4°C by 2100 (IPCC 2013) and nutrient inputs to inland waters through increasing storm intensity (Cisneros et al. 2014), few studies quantify how these changes will potentially affect future periphyton growth and biomass (Cao et al. 2017, Oleksy et al. 2020).

Oligotrophic lakes are especially sensitive to climate change effects as perturbations in nutrient inputs and temperature can induce large ecosystem-level changes (Nõges et al. 2011a, McCullough et al. 2019, Sadro et al. 2019, Ward et al. 2020, Oleksy et al. 2020). This is particularly true in high elevation regions where elevation dependent climate change is causing temperature to increase disproportionately (Mountain Research Initiative Edw Working Group et al. 2015, Pepin et al. 2022), increase storm intensity, and cause decreased snowpack (Berg and Hall 2017) with earlier melt-off (Sadro et al. 2019). Taken together, these changes will potentially result in even more drastic increases

in nutrient availability and water temperatures in these regions, all of which are likely to increase periphyton bloom frequency and severity in clear water lakes (Cao et al. 2017, Oleksy et al. 2020). Additionally, temperature-nutrient effects have large implications for cold-water adapted assemblages since metabolic rate response to warming is more sensitive at lower temperatures (Hargrave 1969). As a result, oligotrophic, cold-water assemblages—which are also more vulnerable to the effects of eutrophication—are potentially doubly vulnerable to climate change impacts.

Adding another layer of complexity to climate change effects on periphyton metabolism is that we also expect warming and precipitation patterns to be seasonally variable, with some seasons experiencing a greater degree of warming or precipitation than others. For example, in the Emerald Lake Basin of the Sierra Nevada Mountains of California, summer warming rates outpaced fall and winter warming rates by 35% and 54% respectively from 1986-2015 (Melack et al. 2020) which could have important implications for summertime periphyton growth in this region. Similarly, future precipitation patterns in California are also expected to become increasingly extreme, with wetter winters, dryer falls and springs (Swain et al. 2018), and a higher proportion of precipitation falling as rain vs. snow (Melack et al. 2020)--though annual precipitation averages are not expected to change significantly (Swain et al. 2018). Consequently, nutrient inputs from runoff may become more pronounced during the winter months and potentially increase periphyton growth during this season, while nutrients may become more limiting during the rest of the year with less runoff. While these patterns may be specific to California, it is likely that many regions globally will also experience increasing extremes in seasonality as well. Changes in these ecosystem-level drivers will likely affect oligotrophic lakes globally, making it increasingly important to understand seasonal variation in temperature and nutrient effects on periphyton growth and metabolism.

Our current understanding of climate change impacts on periphyton is mainly limited to observational studies of periphyton blooms (Jacoby et al. 1991, Hawes and Smith 1994, Higgins et al.

2008, Kravtsova et al. 2014, Cantonati et al. 2016). While these studies corroborate an increase in periphyton blooms globally, it is difficult at times to assign specific causes of these events. While no single mechanism appears to be responsible for widespread blooms (Vadeboncoeur et al. 2021), nutrient concentrations and temperature are two known important regulators of periphyton growth. Nutrients such as nitrogen (N) and phosphorus (P) are essential for production of new biomass, and rates of organismal growth and reproduction depend on supply of these resources relative to demand (Sterner and Elser 2002). Alternatively, temperature exerts strong control over metabolic rates (e.g. primary production and respiration) (Arrhenius 1889) through regulating enzymatic activity and kinetic energy of the system (Johnson et al. 1974, Gillooly et al. 2001). While the individual effects of each of these fundamental variables are well understood if not often described, the strength and nature of their interactive effects are not as well established (Cross et al. 2015). Temperature and nutrients rarely operate in isolation in natural systems, and rates of metabolic reactions are largely determined in conjunction by both reactant (nutrient) concentrations and temperature (Gillooly et al. 2001). Thus it is important to understand their interactions on metabolic processes (Cross et al. 2015).

There are several mechanisms through which interactive effects between temperature and nutrients may arise. First is that nutrient uptake itself may be temperature dependent. Temperature regulates the active transport of nutrients across cellular membranes (Quinn 1988, Clarkson et al. 1988, Reay et al. 1999), and the rates of biochemical reactions with which nutrients are incorporated into new biomass (Cross et al. 2015). Similarly, nutrient use efficiency (NUE; productivity rates normalized by associated nutrient use; Oleksy et al. 2020) and nutrient demand (Rhee and Gotham 1981, Thomas et al. 2017) can vary as a function of temperature in aquatic primary producers, leading to varying reliance on nutrient resources across a range of temperatures (Thomas et al. 2017). Each of these potential mechanisms makes it likely that temperature and nutrient effects interact to influence metabolic rates in natural systems.

In this paper, we explore mechanistic linkages between water temperature and nutrients on periphyton growth and how they vary seasonally within a clear water lake. We seek to answer three questions with this study: 1) how do periphyton metabolic rates vary seasonally, 2) to what extent do nutrients, warming, and their interactive effects influence rates of gross primary production, respiration, and net ecosystem metabolism, and 3) do water temperature and nutrient effects on periphyton metabolism vary seasonally? For temperature effects on metabolic rates, we hypothesize that during the winter months, when *in situ* water temperatures are colder, warming will induce a larger increase in periphyton metabolic rates relative to the warmer spring, summer, and fall months due to the increased sensitivity of metabolic rates to warming at lower temperatures. For nutrient effects on periphyton metabolic rates, we hypothesize that nutrient enrichment effects will be larger during fall months when *in situ* concentrations of nutrients are at a minimum and periphyton growth may be limited by nutrient availability. In addition to seasonal variation in nutrient levels, temperature, and incident solar radiation, we also expect seasonal succession in periphyton taxonomic composition—the balance between stalked diatoms, cyanobacteria, and green filamentous algae in the case of Lake Tahoe (Aloi 1986, Atkins et al. 2021)—to contribute to seasonality in temperature and nutrient effects on periphyton metabolism. We also predict that temperature nutrient interactions will be positive for all 3 metabolic rates, since warmer temperatures should stimulate increased uptake of nutrients that will in turn fuel higher rates of production and respiration.

To answer these questions, we performed our study on Lake Tahoe—an ideal system in which to study these dynamics as there is a rich, long-term dataset of periphyton research and monitoring for the past 37 years by the Tahoe Environmental Research Center (TERC) of UC Davis. Lake Tahoe also allows us to investigate potential drivers and controls of periphyton blooms since the lake is currently experiencing similar changes to ecosystem structure and function as in other exceptionally clear, oligotrophic lakes worldwide. We develop statistical mixed effects models to estimate the relative

strength of temperature-nutrient effects on aquatic primary producers. Such models have implications for predicting how fundamental aspects of near-shore food web structure and energy flow may change as a result of climate change, and are extremely valuable to managers seeking to control and combat widespread periphyton blooms.

Methods

Site Description

Lake Tahoe is a deep, subalpine (1898m amsl), oligotrophic lake located in the northern Sierra Nevada Mountains and shares a border with both California and Nevada. The lake has 116km of shoreline, a maximum depth and average depth of 505m (average depth of 313m), and a surface area of approximately 500km^2 (Goldman 1988). Formed by a graben basin, Lake Tahoe is characterized by its largely granitic basin and low watershed to lake area ratio of 1.6 (Hyne et al. 1972, Jassby et al. 1999). Its bathymetry is defined by a flat bottom surrounded by steep sides. Forest cover makes up the bulk of land cover within the watershed (~85%), yet significant residential developments surround much of the lakes (Jassby et al. 1999).

Water levels in Lake Tahoe fluctuate up to 2.5m/year (Atkins et al. 2021) creating a eulittoral zone that is periodically submerged and a sublittoral zone that remains submerged year round, each with distinctive periphyton communities present (Aloi 1986). These seasonal fluctuations in water level affect the locations of our sampling sites since periphyton was consistently sampled from 0.5m depth throughout the year.

Our field site, hereafter referred to as Pineland, is located on the west central shore of Tahoe (Fig. 1.1A), and was chosen due the availability of historical data on periphyton biomass at this site since 1982 as part of TERC routine periphyton monitoring and a USGS groundwater monitoring site (Naranjo et al. 2019). This site also supports some of the largest periphyton biomass at Lake Tahoe with stalked

diatoms and cyanobacteria usually making up the majority of the community (TERC 2019, Atkins et al. 2021). Pineland is also located next to a residential development (Atkins et al. 2021). Periphyton biomass at this site is correlated to groundwater-derived nutrients, suggesting that these communities are mainly supported by this nutrient subsidy (Loeb 1987, Naranjo et al. 2019). Photosynthetically active radiation (PAR) at this site ranged from ~1800µmol s^{-1} m^{-2} to ~635µmol s^{-1} m^{-2} during collection times. Daily water temperature fluctuations nearshore at this site were generally 3-4°C, with temperatures ranging from 4°C in February and 21°C in August (Fig. 1.1D). Annual periphyton biomass trends in Lake Tahoe are characterized by winter bloom onset, with peak biomass occurring in March-April, followed by a summer die-off (Fig. 1.1A & C) (TERC 2019, Naranjo et al. 2019, Atkins et al. 2021). After peak biomass in the spring, periphyton begin to senesce due to lack of groundwater nutrients and photochemical bleaching caused by elevated summer UV radiation (Naranjo et al. 2019), the latter of which has been shown to inhibit periphyton growth in clear, alpine lakes (Vinebrooke and Leavitt 1996, Higley et al. 2001).

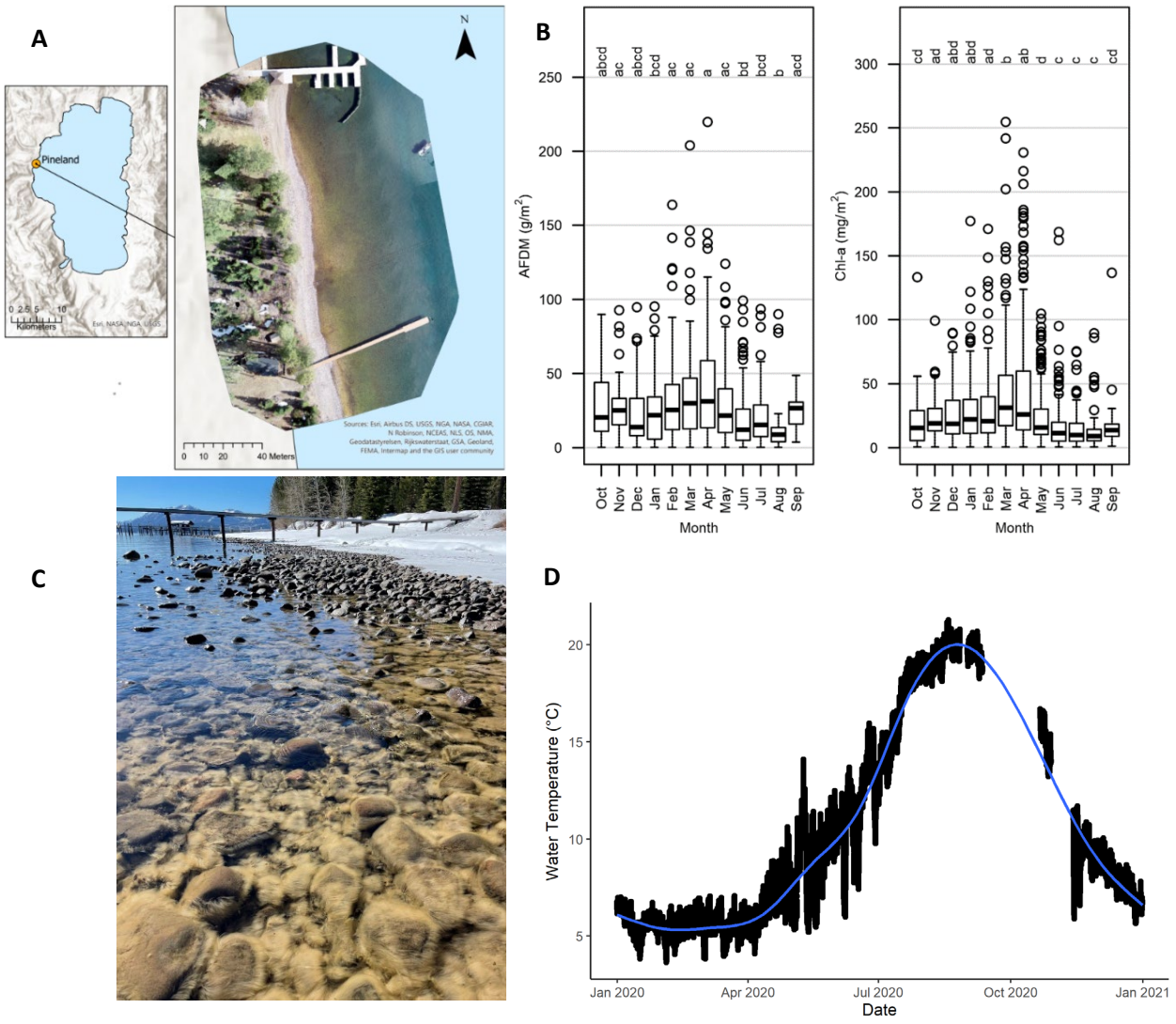

Figure 1.1: *A) Map depicting Pineland site in orange, where periphyton samples were taken for this study. Inset map is drone imagery of the shoreline at the Pineland site taken on 4/22/2021, during peak periphyton biomass at the site. B) Annual patterns in biomass (AFDW and Chl-a) of periphyton in Lake Tahoe since 1982 (taken from Atkins et al. 2021). C) Photo of periphyton mat at Pineland site during peak biomass taken 2/27/2022. D) Nearshore water temperature time series from nearby Homewood in Lake Tahoe.*

Experimental Design

To investigate nutrient concentration, water temperature, and their interactive effects on intact periphyton communities we used a 2x4 factorial incomplete block design with 4 temperature treatments (defined as control, +3°C, +6°C, and +9°C above *in situ* water temperatures at the time of collection) and 2 nutrient treatments (control (*in situ*), and enriched) to incubate periphyton covered rocks (Fig. 1.2B). We chose temperature treatments based on both projected regional warming trends of ~4°C in the next half century (Melack et al. 2020), and to encompass a greater range of temperatures relative to the 3-4°C daily fluctuations in the nearshore of Lake Tahoe (Fig. 1.1D). To capture the potential seasonality of temperature and nutrient effects we performed 7 experiments approximately bimonthly from March 2021 to February 2022; however, the first 2 experiments are only treated as pilot experiments due to subsequent improvements in the experimental design. For each of the 5 experiments used in in this study, 16 individual rocks, each contained within a sealed chamber, were randomly assigned to one temperature treatment and were measured for metabolic rates under ambient nutrient conditions. After the first trial each of the same 16 rocks were subsequently enriched with nutrients, re-assigned to an additional temperature treatment, and allowed to equilibrate overnight. The following morning, metabolic rates were re-measured under enriched nutrient conditions such that each rock experienced 1-2 temperature levels and both nutrient levels. For enriched incubations, the ambient water was enriched to ~6.5 times average *in situ* groundwater concentrations with respect to NO_3, NH_4, and SRP (~400µg/L NH_4-N, 400µg/L NO_3-N, and 318µg/L SRP; Naranjo et al. 2019) to promote peak periphyton metabolic rates at nutrient-saturated conditions. We also chose nutrient concentrations that promote maximum N-absorption rates and prevent nutrient depletion during the nutrient uptake experiments (Reuter et al. 1986). Individual rocks were assigned randomly to temperature treatments and sequentially exposed to *in situ* and enriched nutrient levels in order to prevent potential nutrient contamination between trials.

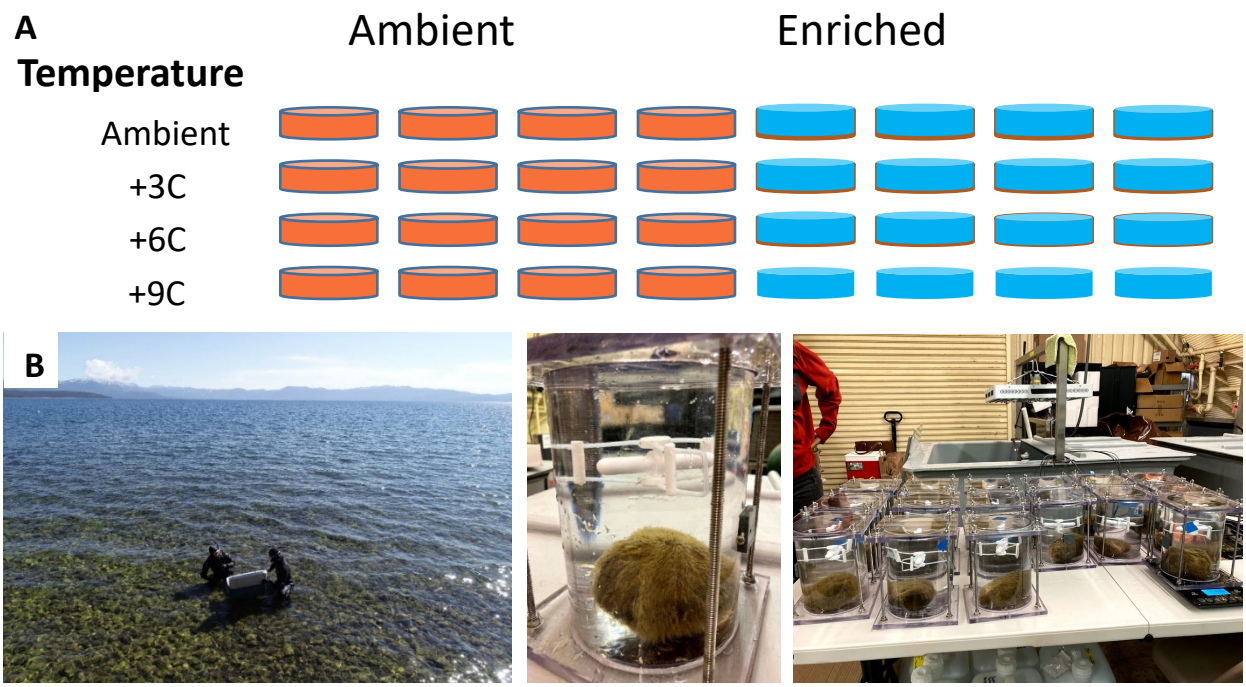

Figure 1.2: *A) Experimental design of the periphyton incubations with 4 temperature levels and 2 nutrient levels with n=4 at each treatment combination. B) Left panel shows researchers collecting periphyton-covered rocks for experiments, center panel shows a rock sealed inside an incubation equipped with a magnetic stirrer, and finally the right panel shows a set of 16 periphyton samples with one of four temperature-controlled water baths used to control temperature in the background.*

Field Measurements and Collections

We collected 16-32 cobble-sized rocks in coolers and 65L of ambient lake water from the Pineland site from 0.5m depth. The site and depth was chosen to coincide with historic routine periphyton monitoring conducted at this site (TERC 2019). Samples were immediately transported back to a research facility in Davis, CA, and ambient water was filtered to 0.45µm to remove phytoplankton and bacterioplankton. Background metabolism of filtered water was negligible and was verified by incubating water-filled chambers with periphyton absent for subset of experiments (Appendix A2).

We measured photosynthetically active radiation (PAR) using a PME miniPAR Logger for March and April 2020 experiments, and a Licor LI-250A light meter for all subsequent experiments, both equipped with Licor LI-192 underwater quantum sensors. We used the same instruments to verify that PAR intensities during laboratory experiments were similar to *in situ* intensities. We based experimental temperature treatments on *in situ* water temperatures measured at the time of sampling at 0.5m depth using a HOBO Water Temperature Pro V2 Data Logger for March and April 2020 experiments, and a YSI Professional Series Pro 30 Conductivity Probe for all subsequent experiments. Seasonal temperature data collected for Figure 1.1 was collected using a RBR Maestro conductivity-temperature-depth probe detailed in Roberts et al. (2019).

Metabolism Measurements

We quantified periphyton metabolic rates using an oxygen mass balance. We measured dissolved oxygen (DO) concentrations inside sealed chambers equipped with homogenizing stirrers and optical oxygen sensor spots (PreSens) in both light (PAR levels matched *in situ* intensities of ~800-1000µmol s^{-1} m^{-2}) and darkness using multi-channel optical oxygen data loggers (Presens Oxy-4 SMA G3 and OXY-10 SMA). We measured DO at 3-second intervals during dark periods of the incubations, but only measured before and after DO concentrations during light periods due to artificial noise introduced in the DO data likely caused by interference of DO sensors associated with well-lit conditions. We then calculated metabolic rates from rates of change of DO concentrations during both production (light-exposed) and respiration (dark) periods. To calculate net ecosystem production (NEP) and ecosystem respiration (ER) rates, we fit simple linear regressions to trends in DO evolution through time during the light and dark incubation periods respectively. The resulting linear regression coefficients then yielded rates of NEP and ER. Since NEP represents the net balance between DO gains via production and DO losses via respiration, we calculated gross primary production (GPP) rates as the sum of measured NEP

and ER rates using the Equation 1.1. For quality control, we only included metabolic rate regressions with $R^2 > 0.75$.

Equation 1.1:

$$GPP = NEP + ER$$

Rates were normalized for each sample according to surface area and periphyton biomass (ash free dry weight-AFDW) to allow comparison among samples and model variation across sites and temperatures.

Water Chemistry

Water chemistry samples were filtered (Whatman GF/F) within 24 hours of collection. Filters were subsequently analyzed for particulate constituents and while dissolved constituents were collected in 250ml acid-washed HDPE bottles, stored on ice, and sent for analysis at TERC. Dissolved NH_4 concentrations were determined using the Idophenol method adapted from Liddicoat et al. and Solorzano et al. (Solórzano 1969, Liddicoat et al. 1975) and has a method detection limit (MDL) of 2µg/L. Dissolved NO_2 + NO_3 concentrations were analyzed using the Hydrazine/Sodium Pyrophosphate Method adapted from Kamphake et al. and Strickland & Parsons (MDL 2µg/L) to avoid potential interference with Ca^{2+} and Mg^{2+} ions from groundwater sources (Kamphake et al. 1967, Strickland and Parsons 1972). Soluble reactive phosphate (SRP) concentrations were determined using a method adapted from Murphy & Riley (MDL 1ug/L) (Murphy and Riley 1962). Particulate phosphorus concentrations are measured from sample collected on GF/F filters using the reactive phosphorus method (MDL 0.02µg P) (Solórzano and Sharp 1980).

Periphyton Sampling

We harvested periphyton from rocks into DI water post-incubation using stiff-bristled brushes. We then filtered the periphyton biomass from the resulting slurry using 80µm Nitex mesh and subsampled for ash-free dry weight (AFDW), chl-a, particulate phosphorus, particulate carbon, and

particulate nitrogen from the resulting periphyton pellet. AFDW samples were dried for 24 hours at 60°C and combusted for one hour at 500°C. Chlorophyll-a samples were kept frozen until analysis, freeze-dried, and then extracted in 90% ethanol at 78°C for 10 minutes. We then allowed extracted samples to reach room temp for 2 hours and measured via EPA method 445.0 using a Turner Designs Trilogy fluorometer. We calculated the surface area of rocks by treating them as an ellipsoid from the measured rock length, width, and height and assumed an average of 67% periphyton coverage on rocks (Appendix Table A1). We also harvested and composited periphyton from a single rock during each experiment for community composition and preserved samples using Lugol's solution. Predominant periphyton taxa were determined qualitatively through analyzing samples under a microscope.

Nutrient Uptake Rates

Nutrient concentrations in *in situ* lake water were too low to measure uptake rates in the control treatments; consequently, uptake rates were only measured in the nutrient amended treatments. To measure nutrient uptake rates of periphyton communities, we measured initial concentrations of NO_3, NH_4, and SRP in the homogenized, nutrient-amended water used to fill chambers used for the nutrient-enriched portion of metabolism experiments and then allowed periphyton samples to incubate in the enriched water for an 11-24hr period before measuring final concentrations in each chamber. During these incubations, samples sat in darkness during this period except for a 1hr period of light as part of the primary production measurements of the metabolism experiment. To confirm that background nutrient uptake rates by bacterioplankton and phytoplankton were negligible, we incubated the same water in chambers in which periphyton was absent (Appendix A2).

Statistical Modeling: Metabolic Response to Temperature, Nutrients, and Season

To test for the relative strengths of temperature, nutrient, and seasonal effects on GPP, ER, and NEP we used linear mixed effects (LME) models. Using Zuur et al. (2009) protocols for model fitting, we assessed random effects with set fixed effects that were tested in the experiment (Zuur et al. 2009). The

resulting model included temperature, nutrient level, month, and their interactions as fixed effects regressed against log-transformed metabolic rates. We also accounted for random differences between periphyton-covered rocks in our repeated measures design by including rock ID as a random effect. To account for non-constant variance between experiments, we normalized the variance of each experiment using the *weights* option of the *nlme* package (Pinheiro et al. 2022). To ensure models were appropriate we created a list of candidate models including an intercept-only model, a simple linear regression with all fixed effects we deemed experimentally relevant, and linear mixed effects models that included different combinations of random effects (Appendix A4). We then chose the model with the lowest Akiake Information Criterion (AIC), a goodness-of-fit metric that penalizes models with more parameters (Zuur et al. 2009). All statistical analyses were conducted in R version 4.0.2 (R Core Team 2020) and with the *nlme* package (Pinheiro et al. 2020) to perform linear mixed effects analysis. To assess significant interactions between fixed effects in the models, we used the emmeans() and emtrends() functions of the *emmeans* package (Lenth et al. 2022). To verify model assumptions were met, plots of residuals vs. fitted as well as residuals vs. predictors were visually assessed.

Results

Within-lake seasonal trends in periphyton

Seasonal variation in periphyton biomass and community structure

Periphyton biomass data from our experiments largely follow this same trend as long-term data (Fig. 1.1B) with a March-April peak followed by consistent decreases throughout the summer until reaching a late-summer minimum and entering a period of regrowth beginning in the fall (Fig. 1.3). The periphyton community was dominated by diatoms and stalked diatom taxa in the spring and early summer of 2021, but dominance shifted towards cyanobacteria in the late summer through the following spring of 2022 (Appendix A9). Chlorophyll-a concentrations—a more sensitive proxy for living

autotrophic material than AFDW (Atkins et al. 2021)—was highest in February with a median of 0.1g m^{-2} and lowest in June with a median of 0.01g m^{-2} (Fig. 1.3A). Another proxy for algal biomass, AFDW (which can characterize the accumulation of biomass between months, independent of photosynthetic tissues) was highest in March with a median of 55.1g m^{-2}—over double that of the minimum AFDW in August with a median of 19.7g m^{-2} (Fig. 1.3B). Periphyton autotrophic index, or (AI), which refers to the ratio of AFDW to chlorophyll-a and represents the ratio of autotrophic biomass to heterotrophic or detrital mass within the periphyton mat (Biggs and Close 1989, Biggs and Kilroy 2000), was highest during the June experiment and decreased until reaching a minimum during the February experiment (Fig. 1.3C). Temperature varied significantly over the course of the experiments, with a maximum of 19.5°C and minimum of 6°C during the August and February experiments respectively (Fig. 1.3D). Taken together, these data indicate that periphyton was more heterotrophic/detrital matter-dominated during April and June, then transitioned to being more autotrophic-dominated during peak bloom conditions in February (Fig. 1.3C).

Seasonal variation in periphyton metabolism

Periphyton metabolic rates varied across seasons, and both biomass normalized and areal NEP rates remained positive over all seasons (Fig. 1.4). Mean aerial rates of GPP, NEP, and ER of control treatments were 2476, 1930, and 545mgO_2 d^{-1} m^{-2} respectively. Areal metabolic rates of NEP and GPP were highest in the fall (medians of 2848 and 2291mgO_2 d^{-1} m^{-2} for GPP and NEP respectively), and lowest in June (medians of 2046 and 1444mgO_2 d^{-1} m^{-2} for GPP and NEP respectively) (Fig. 1.4B). The highest areal rates of ER occurred in the spring during the April experiment (median of 765mgO_2 d^{-1} m^{-2}) and the lowest during the February experiment (median of 331mgO_2 d^{-1} m^{-2}) (Fig. 1.4B).

The largest biomass (AFDW) normalized metabolic rates occurred in the June experiment (medians of 36, 126, and 97mgO_2 d^{-1} g$AFDW^{-1}$ for ER, GPP, and NEP respectively), and the lowest AFDW-

normalized rates occurred during the April experiment (medians of 12, 40, and 29mgO_2 d^{-1} $gAFDW^{-1}$ for ER, GPP, and NEP respectively) (Fig. 1.4A).

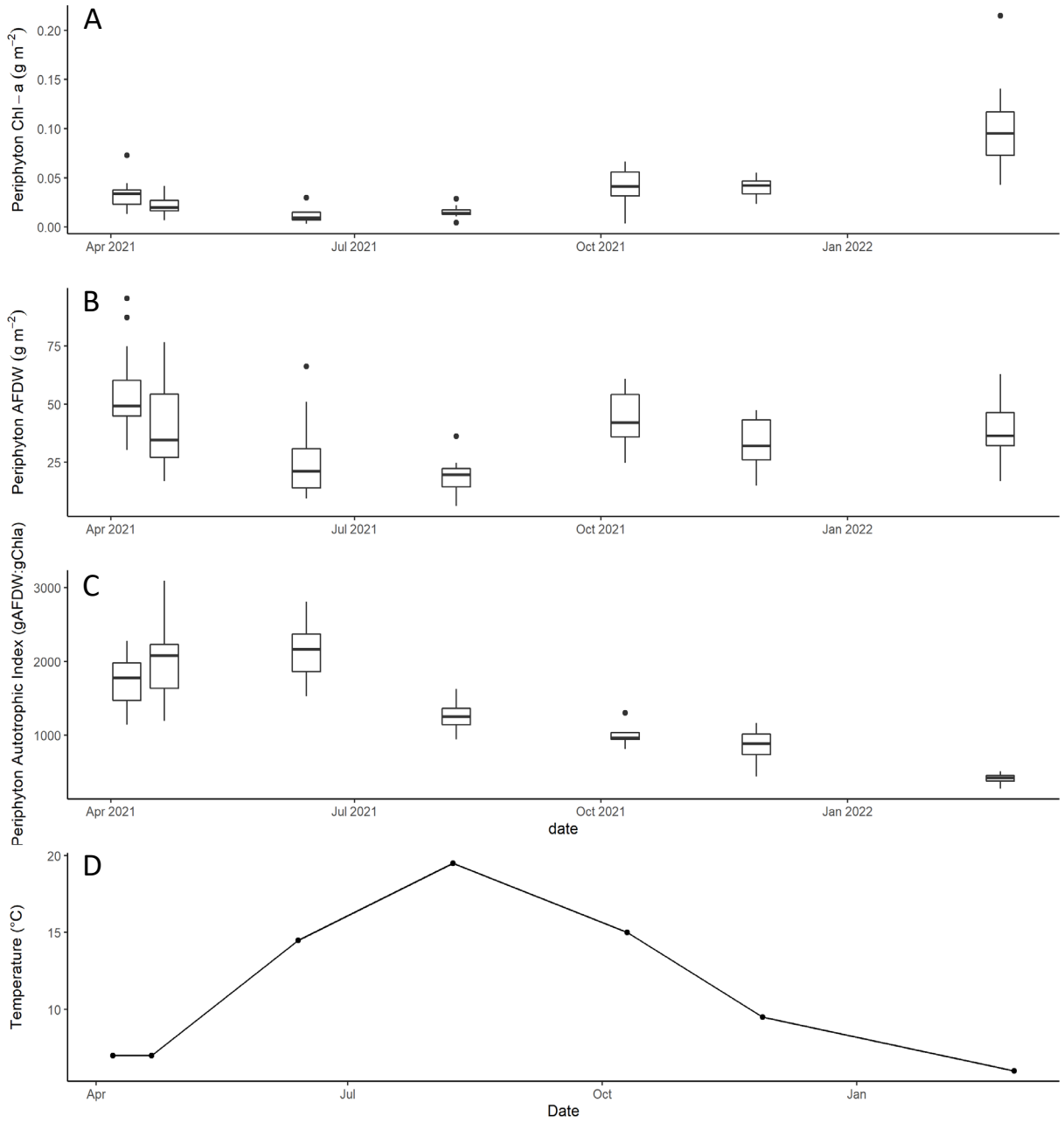

Figure 1.3: *Seasonal trends of A) periphyton chlorophyll-a, B) periphyton AFDW, C) autotrophic index (AI), and D)* in situ *temperature at the Pineland site over the duration of the study. We include data from the April pilot studies to demonstrate seasonal variability in periphyton biomass. Boxes in A-C denote the*

interquartile range, lines in the middle represent the median, whiskers denote the range of values, and points outside represent outlier data points.

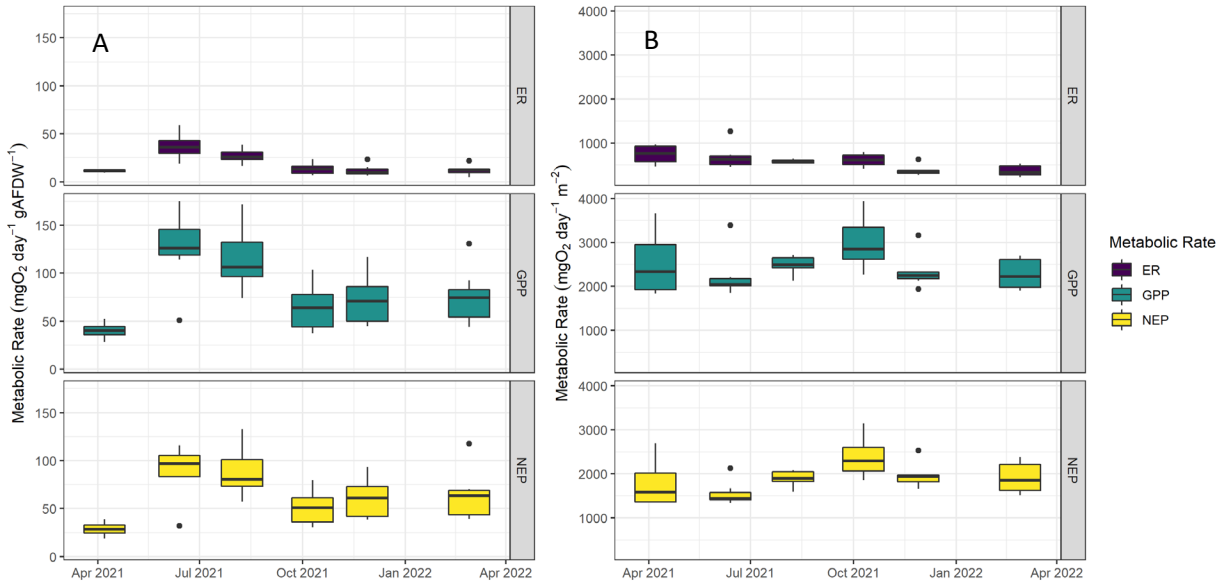

Figure 1.4: *Seasonal trends in "control" metabolic rates at* in situ *temperatures. A) AFDW-normalized metabolic rates and B) areal metabolic rates at Pineland. We include data from the April pilot study to demonstrate seasonal variability in control metabolic rates. Boxes denote the interquartile range, lines in the middle represent the median, whiskers denote the range of values, and points outside represent outlier data points.*

Analysis of temperature and nutrient effects in experiments

Temperature effects on periphyton metabolic rates

Overall, temperature was found to have a significant, positive effect on periphyton GPP, NEP, and ER averaged across all months and nutrient levels (Table 1.2). Temperature alone induced large increases in growth rates, with or without nutrient enrichment. Of all the metabolic rates, temperature had the largest stimulatory effect on ER with an average rate increase of 7% for each 1°C of warming ($p < 0.001$) relative to 4.5% and 3.6% for GPP and NEP respectively ($p < 0.001$ for both results). The effect of temperature on GPP varied seasonally, with warmer months showing reduced or slightly negative trends and colder months showing strong, positive trends (Fig. 1.5). Temperature effects on all three metabolic rates were largest in February, with an average increase of 9.5%, 11%, and 9.5% per 1°C of warming for GPP, ER, and NEP respectively. Temperature effects on GPP and NEP were lowest in August with only a 0.7% increase and 1% decrease per 1°C of warming respectively, while temperature effects on ER rates were lowest in June with rate increases of only 4.2% per 1°C of warming.

Nutrient enrichment effects on periphyton metabolic rates

The effect of nutrient enrichment on metabolic rates varied both through time and among the different metabolic rates measured. Enrichment increased rates of GPP by 6%, but this effect was not statistically significant ($p = 0.25$; Table 1.2, Fig. 1.5). For NEP rates, nutrients had a small, insignificant effect (Table 1.2). Nutrients had a large effect on ER rates, increasing rates by 25% averaged across temperature and months ($p = 0.001$; Table 1.2). Nutrient enrichment effects were found to show considerable seasonal variation, with enrichment effects varying in magnitude and direction among the metabolic rates measured. For GPP and NEP rates, enrichment induced a significant increase of 13% ($p < 0.0001$) and 11% ($p < 0.0001$) respectively during the October experiment (Table 1.1). For ER rates, nutrient enrichment induced an increase of 27% ($p < 0.0001$) and 21% ($p < 0.0001$) in June and October

experiments respectively (Table 1.1). Nutrient enrichment effects on GPP, ER, and NEP were not found to be significant in other months.

A Seasonal Variation in Nutrient Effects on Periphyton GPP

comparison	month	effect size	SE	df	null	t.ratio	p.value
enriched / ambient	february	1.1290	0.14230	60	1	0.9645	3.386e-01
enriched / ambient	june	1.0090	0.04363	60	1	0.2151	8.304e-01
enriched / ambient	august	1.0870	0.07147	60	1	1.2700	2.090e-01
enriched / ambient	october	1.1300	0.01677	60	1	8.2440	1.879e-11
enriched / ambient	november	0.9149	0.06582	60	1	-1.2370	2.210e-01

B Seasonal Variation in Nutrient Effects on Periphyton ER

comparison	month	effect size	SE	df	null	t.ratio	p.value
enriched / ambient	february	1.1060	0.2219	60	1	0.5003	6.187e-01
enriched / ambient	june	1.2690	0.0443	60	1	6.8200	5.072e-09
enriched / ambient	august	1.0580	0.1013	60	1	0.5884	5.584e-01
enriched / ambient	october	1.2060	0.0335	60	1	6.7520	6.622e-09
enriched / ambient	november	0.9889	0.1080	60	1	-0.1024	9.188e-01

C Seasonal Variation in Nutrient Effects on Periphyton NEP

comparison	month	effect size	SE	df	null	t.ratio	p.value
enriched / ambient	february	1.1380	0.14580	60	1	1.006	3.185e-01
enriched / ambient	june	0.9080	0.05283	60	1	-1.659	1.024e-01
enriched / ambient	august	1.1030	0.08937	60	1	1.216	2.288e-01
enriched / ambient	october	1.1130	0.02004	60	1	5.950	1.489e-07
enriched / ambient	november	0.8917	0.06565	60	1	-1.557	1.247e-01

Table 1.1: *Seasonal variation in nutrient effects on periphyton metabolic rates. Nutrient enrichment effect sizes are shown for each month with associated p-values.*

Temperature-nutrient interactions on periphyton metabolism

Interactive effects between temperature and nutrients differed for the three metabolic rates we measured. Averaged across all months, we found evidence of a small, but significant negative interaction for ER rates (-1%, $p = 0.03$). November ER rates exhibited the largest temperature-nutrient interaction (-5%), however, this effect was only significant at $p = 0.054$. This effect corresponds to a 5% reduction in the effect of temperature on ER rates at enriched nutrient concentrations relative to *in situ* nutrient concentrations (Fig. 1.5). Temperature-nutrient interactions were not found to be significant for either GPP or NEP (Table 1.2).

	GPP	ER	NEP
Predictors	*Estimates*	*Estimates*	*Estimates*
(Intercept)	55.17 ***	7.96 ***	49.66 ***
temp C	1.04 ***	1.07 ***	1.04 ***
nutrient trt [1]	1.06	1.25 **	1.01
month [1]	0.63 **	0.61 **	0.60 ***
month [2]	1.59 **	2.18 ***	1.56 *
month [3]	2.17 ***	1.51 *	2.53 ***
month [4]	0.58 ***	0.72 **	0.53 ***
temp C * nutrient trt [1]	1.00	0.99 *	1.00
temp C * month [1]	1.05 ***	1.04 **	1.06 ***
temp C * month [2]	0.97 ***	0.97 ***	0.97 ***
temp C * month [3]	0.96 ***	0.98 *	0.96 ***
temp C * month [4]	1.00	0.99	1.01 *
nutrient trt [1] * month [1]	0.96	1.01	0.96
nutrient trt [1] * month [2]	0.89	0.98	0.84
nutrient trt [1] * month [3]	0.93	0.90	0.92
nutrient trt [1] * month [4]	1.06	0.92	1.11
(temp C * nutrient trt [1]) * month [1]	1.00	1.00	1.01
(temp C * nutrient trt [1]) * month [2]	1.01	1.00	1.01
(temp C * nutrient trt [1]) * month [3]	1.00	1.00	1.01
(temp C * nutrient trt [1]) * month [4]	1.00	1.01	1.00
Random Effects			
σ^2	0.01	0.01	0.01
τ_{00}	0.17_{rock_ID}	0.09_{rock_ID}	0.17_{rock_ID}
τ_{11}	$0.00_{rock\_ID.temp\_C}$		$0.00_{rock\_ID.temp\_C}$
ρ_{01}	-0.83_{rock_ID}		-0.81_{rock_ID}
ICC	0.91	0.94	0.85
N	78_{rock_ID}	78_{rock_ID}	78_{rock_ID}
Observations	153	153	153
Marginal R^2 / Conditional R^2	0.661 / 0.971	0.745 / 0.984	0.655 / 0.947

*$p<0.05$ **$p<0.01$ ***$p<0.001$

Table 1.2: *Parameter estimates with their significance for LME models of periphyton GPP, ER, and NEP.*

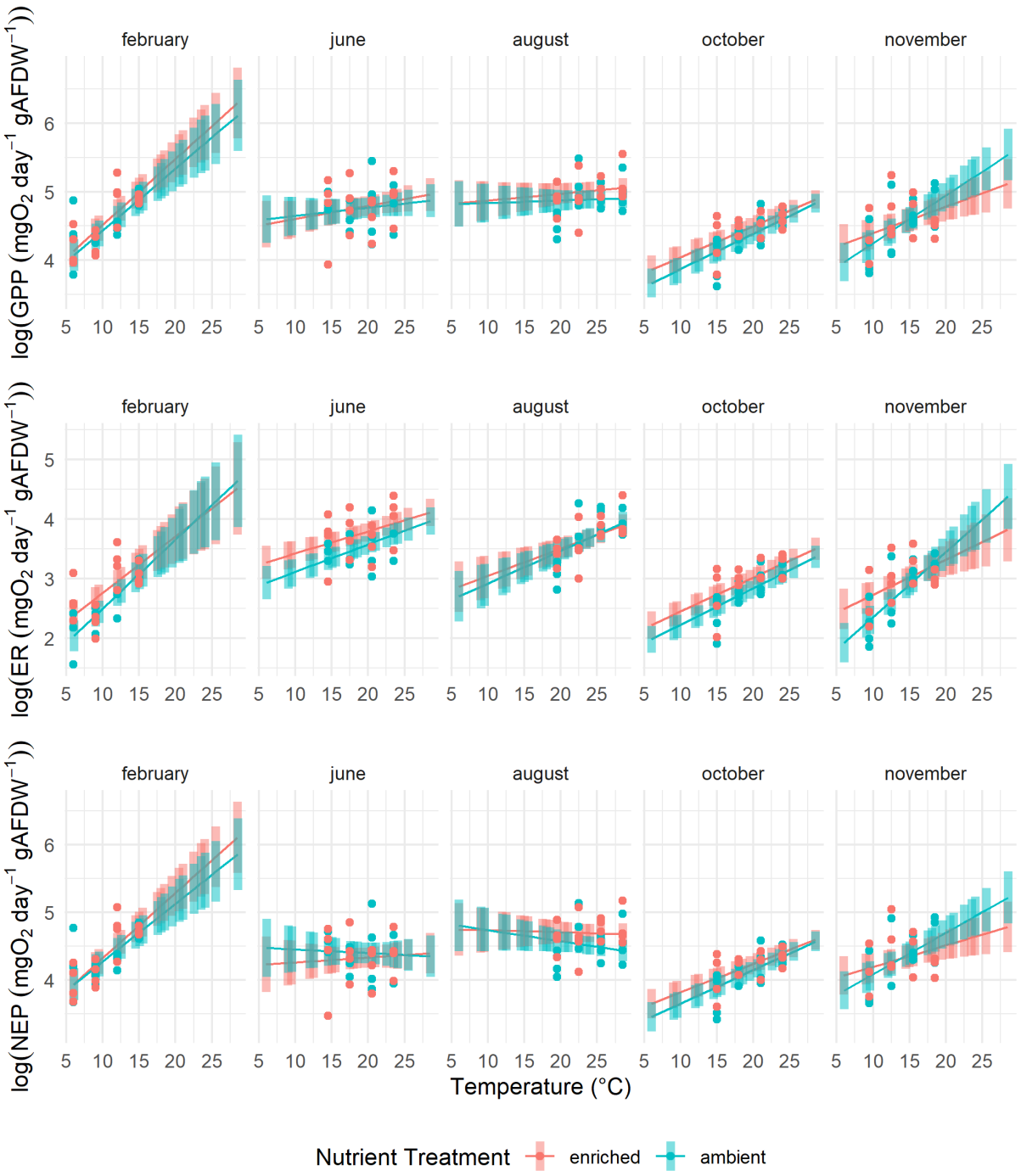

Figure 1.5: *Log-transformed metabolic GPP, ER, and NEP vs temperature separated by month. Lines represent a linear regression, with blue lines representing ambient nutrient treatments and red enriched nutrient treatments.*

Periphyton nutrient uptake

Nutrient uptake rates were seasonally highest in the summer, and declined into the fall and winter. Nutrient uptake rates for both NH_4 and SRP were highest during June and August, with average uptake rates at *in situ* temperatures of 131µgN gAFDW^{-1} hr^{-1} and 94µgP gAFDW^{-1} hr^{-1} respectively. Nutrient uptake rates were not found to be tightly associated with ambient nutrient concentrations measured at the sediment-water interface, but at low NH_4 concentrations, nutrient uptake rates tended to be higher with some exceptions (Appendix A6).

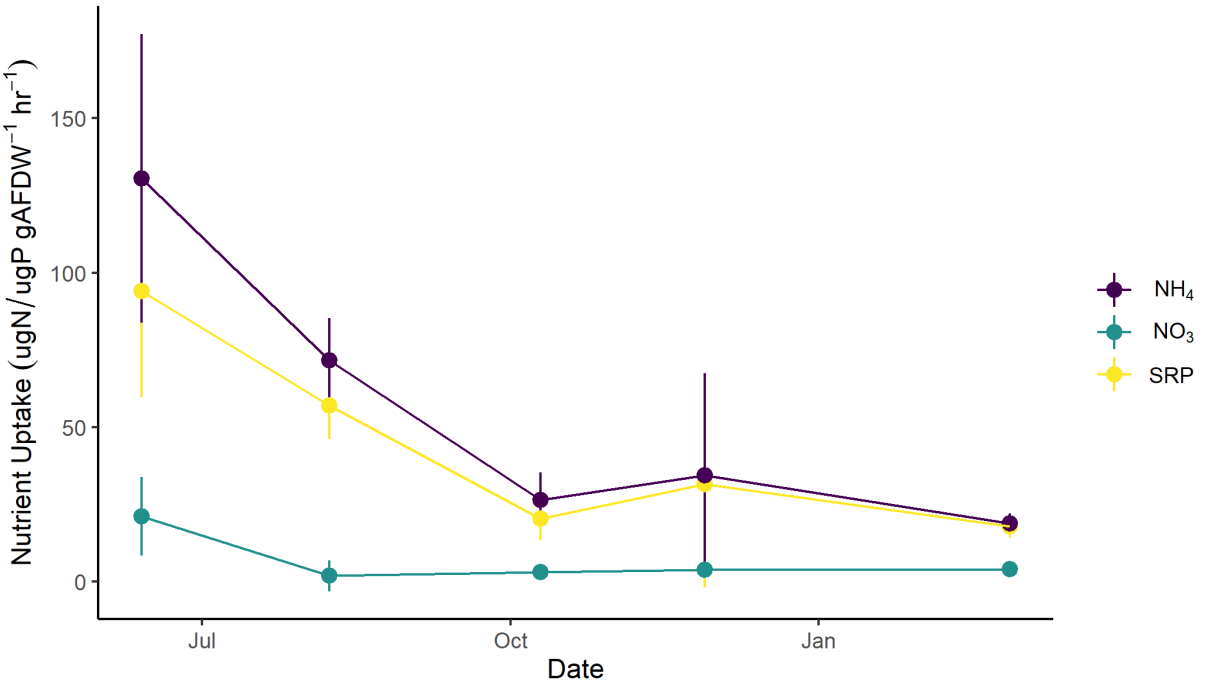

Figure 1.6: *Seasonal variation of* in situ *uptake rates of ammonium, nitrate, and SRP uptake rates show that nutrient uptake is highest in June before decreasing to baseline levels for the rest of the year. Points represent averaged values (n = 4) and error bars +/- SD.*

Temperature effects on periphyton nutrient uptake rate

Nutrient uptake rates increase with temperature, however, the relationship did not appear to be completely linear (Fig. 1.7). NH_4 uptake rates ranged from 13-176µgNH_4-N gAFDW^{-1} hr^{-1} and NO_3 uptake rates from 0-70µgNO_3-N gAFDW^{-1} (Fig. 1.7). SRP rates ranged from 11µgSRP gAFDW^{-1} hr^{-1} to 159µgSRP gAFDW^{-1} hr^{-1} (Fig. 1.7). Uptake rates of N and P tended to increase with temperature at different rates, however, there was no significant trend in the molar N:P ratio of nutrient uptake with temperature (Appendix A8).

Periphyton NUE (both N and P) tended to increase with temperature in spring in winter months, with phosphorus use efficiency increasing at a greater rate than that of nitrogen (Fig. 1.8). In the June experiment, NUE decreased at higher temperatures, leading to an overall negative correlation with temperature (Fig. 1.8).

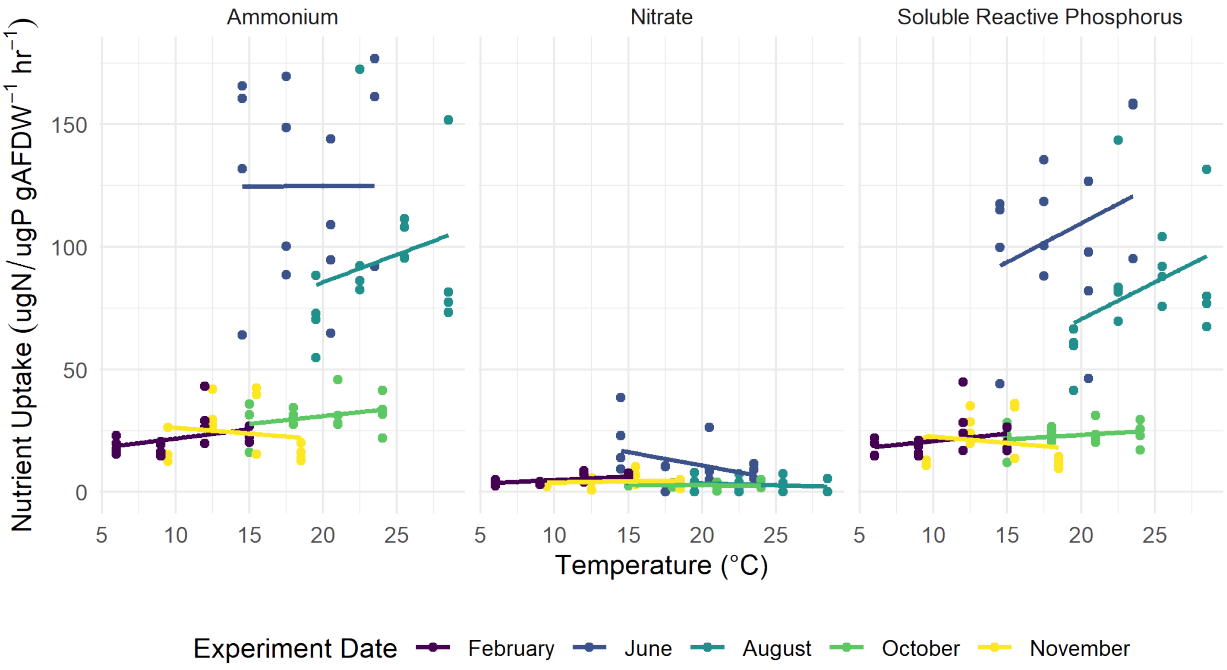

Figure 1.7: *Nutrient uptake rates for ammonium (NH_4), nitrate (NO_3), and phosphate (SRP) per gram of ash-free dry weight per hour. While temperature appears to increase nutrient uptake rates of SRP and*

NH_4, these trends exhibit considerable seasonal variation. Lines represent a linear regression with colors representing each experiment.

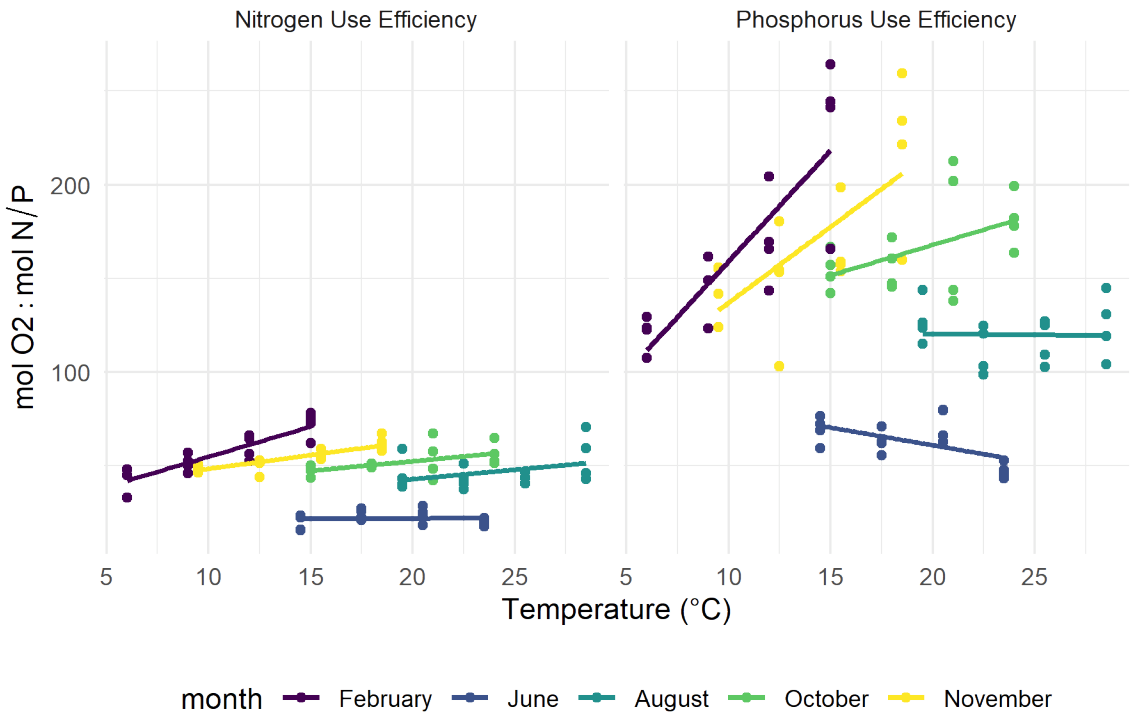

Figure 1.8: *Temperature effects on both NUE (calculated as moles of O_2 produced from NEP per moles of N or P used). Lines represent a linear regression with colors representing each experiment.*

Discussion

Seasonal differences in in situ *periphyton metabolic rates*

Periphyton metabolic rates varied across seasons, and both biomass specific and areal NEP rates remained positive over all seasons (Fig. 1.4). Biomass-specific rates can be interpreted as the organism-level seasonal changes of periphyton independent of variation in biomass. Areal rates, however, represent ecosystem-level seasonal changes that incorporate seasonal variation in periphyton biomass.

Consistent with the results of our model results regarding the effects of temperature and nutrients, biomass specific metabolic rates were most affected by *in situ* temperatures as high metabolic rates corresponded to warmer conditions (and *vice versa*) (Figs. 1.3D and 1.4A). One notable exception was the October experiment in which warmer temperatures did not correspond to higher metabolic rates (Fig. 1.4A). This discrepancy may be attributed to a shift in community composition from diatom/stalked diatom to cyanobacterial dominance during June-October 2021 (Appendix A9). Other studies have noted that cyanobacteria have lower biomass-specific productivity relative to other taxa (Abe et al. 2007)—a potential result of the sensitivity of basal growth of this species to the effects of self-shading and nutrient limitation (Hay 1981). Cyanobacteria have been found to accumulate biomass slowly in Lake Tahoe relative to other periphyton taxa (Loeb 1980) providing further support to this hypothesis. Therefore it is likely that both temperature and seasonal shifts in periphyton community composition mainly determine biomass-specific metabolic rates and bloom formation in the nearshore.

Conversely, areal metabolic rates were driven by both *in situ* temperatures and biomass levels. Areal NEP and GPP rates at *in situ* temperatures peaked in October when biomass levels were relatively high (Fig. 1.3A & 1.3B) and temperature was still relatively warm (Fig. 1.3D). Likewise, ER rates peaked in April when heterotrophic biomass was highest within the periphyton mat (i.e. high AI; Fig. 1.3C) despite the lower ambient temperatures. The effects of community composition on areal metabolic rates are less pronounced compared to biomass specific rates because periphyton biomass can override these effects (i.e. periphyton communities with low metabolic activity at high levels of biomass can produce high areal metabolic rates despite low biomass specific metabolic rates). Thus October areal rates were high despite cyanobacterial dominance (and their lower metabolic activity) because more biomass was present in a given surface area of lake bottom.

Community composition at the Pineland site varied seasonally between April 2021 and February 2022. Diatoms, stalked diatoms, and cyanobacteria taxa each dominated at some point throughout this period, and these community shifts were likely driven by changing lake levels (Atkins et al. 2021). Diatoms and stalked diatom taxa were dominant during the April and June 2021 experiments during periods of higher water levels, while cyanobacteria dominated the August 2021-February 2022 experiments which occurred mainly during periods of rapid water level decline (Appendix A10). This community shift was expected as cyanobacteria are usually more dominant in the deeper sublittoral zone that becomes exposed when water levels are low (Atkins et al. 2021). Green filamentous taxa were observed at some level during most experiments with moderate to minimal levels of dominance observed from the April-October 2021 experiments, but was absent during the November 2021 and February 2022 experiments.

Temperature effects on periphyton metabolic rate

Temperature is a master variable with respect to biological rates. These experiments indicate that temperature was very important in determining periphyton metabolism –inducing a 4% increase in GPP and NEP, and a 7% increase in ER per 1°C of warming. The corresponding Q_{10} values for these temperature effects were 1.5, 1.5, and 2 for GPP, NEP, and ER respectively, which is within the range of values reported for periphyton (Phinney and McIntire 1965, Demars et al. 2011, Brothers et al. 2013). We found ER was stimulated more by warming than GPP or NEP, and this is consistent with other studies that have investigated temperature effects on primary producers in mesocosms (Yvon-Durocher et al. 2010), laboratory incubations of periphyton communities (Oleksy et al. 2020), and in natural streams (Demars et al. 2011), and suggests that warming has the potential to significantly increase carbon exports to the atmosphere as aquatic ecosystems are significant components of the global carbon cycle (Cole et al. 2007).

We also found evidence that periphyton metabolic responses to warming are seasonally explicit. Consistent with our hypothesis, the largest temperature induced increases in GPP, ER, and NEP occurred during February—the coldest month included in this study. These data are in agreement with previous literature that notes temperature has a larger stimulatory effect on biological rate processes are lower temperatures (Hargrave 1969, Johnson et al. 1974). Therefore, significant long-term warming trends during winter months in the Sierra Nevada (Melack et al. 2020) will likely increase periphyton metabolic rates and biomass in the late winter/early spring in Lake Tahoe. These results have implications for clear water lakes globally, and warming effects will be mediated by both local scale influences of climate change, lake morphometry, and ice cover as discussed below.

In contrast, during summer months when water temperatures were already high, the effect of warming was reduced or even slightly negative (Fig. 1.5). One potential explanation for smaller temperature effects during the summer is that high levels of incident UV radiation limited periphyton growth and biomass at shallow depths in Lake Tahoe (Naranjo et al. 2019, Atkins et al. 2021). A second explanation is that summer temperatures in Tahoe are already at the upper limit of tolerance for the algal assemblages included in this study. As a result, periphyton metabolism is not likely to increase during the summer months despite significant warming trends measured during the summer in the Sierra Nevada (Melack et al. 2020). A more likely result is that periphyton community composition may shift to more warm-water species as a result of warmer average temperatures. These findings reinforce the importance of understanding temperature effects in a seasonal context in order to make more specific predictions of ecosystem level response to climate change.

Nutrient effects on periphyton metabolic rate

Nutrient effects averaged across all seasons and temperatures did not significantly affect periphyton GPP or NEP rates, but did significantly affect ER rates. These results are contrary to our expectations as nutrients such as N and P frequently induce increases in growth and production of

aquatic primary producers (Hecky and Kilham 1988, Elser et al. 1990, 2007). This evidence potentially suggests that heterotrophic components in the periphyton mat (i.e. bacteria) may outcompete primary producers for nutrients (Bernhardt and Likens 2004), thus ER increased while NEP and GPP remained unchanged. Another more likely explanation was that our experiments underestimated nutrient effects due to such short-term incubation periods. In fact, additions of nutrients have even been found to temporarily suppress production in nutrient deficient algal populations as cellular energy is first allocated to nutrient uptake and assimilation rather than to carbon-fixation upon enrichment (Healey 1979, Lean and Pick 1981, Beardall et al. 2001). This rapid nutrient uptake by periphyton would not only explain a lack of stimulation of NEP and GPP with nutrient enrichment, but also the unexpected increase ER since phosphate uptake consumes energy (Healey 1973). Thus, nutrient enrichment likely caused a spike in respiration rates in order to fuel rapid cellular nutrient uptake (Healey 1973). This phenomenon has been documented in a number of studies of phytoplankton (Healey 1979, Lean and Pick 1981, Birch et al. 1986, Elrifi and Turpin 1987), yet this is the first example of this phenomenon being documented in periphyton to our knowledge. Contrary to our findings, however, a similar study of periphyton response to short term nutrient additions found little effect on respiration, although the phosphate enrichments tended to be smaller than our experiments and may not have been sufficient to affect carbon metabolism (Rosa et al. 2013). These findings show that short-term nutrient bioassays can sometimes miss or inaccurately estimate nutrient effects on periphyton growth and metabolism (Aloi 1986), however, long-term nutrient assays increase the potential for chamber effects that can confound results (i.e. changes in initial algal community over the course of the experiment, etc.; Beardall et al. 2001). Thus, large-scale, *in situ* experiments may be the most reliable way to assess nutrient limitation (Beardall et al. 2001).

Nutrient enrichment increased ER rates by 25% averaged over all temperatures and seasons. Despite this, we enriched to nutrient-saturated conditions (~6.5 times average groundwater

concentrations with respect to NO_3 and SRP ;~400µg/L NH4-N, 400µg/L NO3-N, and 318µg/L SRP; Naranjo et al. 2019) and therefore the nutrient effect may not be representative of nutrient effects experienced in the field. If adjusted with respect to maximum nutrient concentrations measured in the field (~1.6-1.8 times average groundwater concentrations) by assuming nutrient effects are linear, the resulting nutrient stimulatory effect on ER rates decreases from 25% to between 6.2-6.9%. These adjusted rates indicate that nutrients were less important than temperature in determining ER rates in our study. One other study also found temperature to be more important relative to nutrient effects (Rosa et al. 2013), however, they also used short-term nutrient bioassays with much smaller enrichment concentrations and may have missed nutrient effects that arise over longer time scales.

We found evidence of seasonality of periphyton nutrient limitation as nutrient effects were most prominent for primary production in October and respiration in June and October (Table 1.1). Other studies also show nutrient effects on periphyton to vary seasonally (Rosa et al. 2013, Trochine et al. 2014), further highlighting the need to study these effects in a seasonal context. Consistently positive NEP rates during the incubations indicate that periphyton growth will increase until it comes into equilibrium with *in situ* nutrient levels. Thus it is important to manage nutrient inputs to lakes, especially as climate change is expected to increase rates of runoff, especially during winter seasons in regions were more snowfall is expected to fall as rain.

Temperature-nutrient interactions

Metabolic theory predicts that temperature and nutrients mediate (increase or decrease) the effects of one another as metabolic rate reactions are a product of both reactant concentration and temperature (Cross et al. 2015, Thomas et al. 2017). We found evidence of a small, but significant negative interaction for ER rates—suggesting that nutrient additions slightly reduced the impacts of warming on periphyton ER rates when averaged across all seasons and temperature treatments. Temperature and nutrients rarely operate in isolation in natural systems, thus understanding how their

interaction affects periphyton metabolism is important in predicting response to global change (Cross et al. 2015). Inconsistent with our hypothesis, we found no significant interaction between temperature and nutrients for GPP or NEP. In fact, temperature induced significant increases in metabolic rate with or without nutrient enrichments. This is consistent with predictions that primary producers exhibit a degree of plasticity in nutrient demand, therefore allowing metabolic rates to increase with warming independent of environmental nutrients concentrations (so as long as nutrients are not limiting; Cross et al. 2015). We thus do not find temperature-nutrient interactions to be a significant driver of periphyton metabolism at the nutrient levels tested in these experiments, although under nutrient-limitation a significant interaction may arise (Thomas et al. 2017).

We also acknowledge that our experiments may have underestimated temperature-nutrient interactions since short-term exposure to nutrient enrichments may not have allowed sufficient time to detect true long-term nutrient effects (Aloi 1986). Instead, results of these short-term nutrient additions tested for instantaneous nutrient limitation in periphyton metabolism. Significant temperature-nutrient interactions have been found in marine phytoplankton communities, with temperature and nutrients having a positive interaction when nutrients are not limiting, and a negative interaction under nutrient-limited conditions (Thomas et al. 2017, Anderson et al. 2022). These studies show that warming can potentially create or worsen nutrient limitation on primary producers (Thomas et al. 2017). While this relationship was significant for phytoplankton in other studies, periphyton in our study were perhaps not as susceptible to nutrient limitation due to luxury uptake of GW derived nutrients (Oleksy et al. 2020), greater nutrient retention ability relative to phytoplankton (Mazumder et al. 1989, Blumenshine et al. 1997, Vadeboncoeur and Steinman 2002), and remineralization of organic matter within the periphyton matrix (Mulholland et al. 1991). These questions may need to be addressed by longer-term studies on periphyton communities where nutrient effects are more likely to emerge (Aloi 1986), preferably *in situ* to avoid potential container effects (Beardall et al. 2001).

Seasonal variation in nutrient uptake rates and nutrient use efficiency

Periphyton nutrient uptake varied seasonally and was highest during the summer (Fig. 1.6), likely caused due to warmer temperatures (Cross et al. 2015) and increased nutrient limitation during this season. Within seasons, nutrient uptake tended to show a positive correlation with temperature, with elevated uptake rates occurring at warmer temperature treatments (with the exception of the November experiment; Fig. 1.7). Winter uptake rates of nitrogen species were on par with historic rates in Lake Tahoe, however, summer rates tended to differ. February NH_4 uptake rates were ~19µgNH_4-N gAFDW^{-1} hr^{-1} on average and were on par with historic rates reported in Lake Tahoe during March under similar temperatures, however, August NH_4 uptake was approximately 3 times larger than historic August rates with an average of ~69µgNH_4-N gAFDW^{-1} hr^{-1} (Reuter et al. 1986). Both February and August NO_3 uptake rates were consistently lower than historic rates measured during the same months and were ~3.5 and ~4 µgNO_3-N gAFDW^{-1} hr^{-1} respectively--around one-third to one-quarter of historic rates.

NUE, a metric that measures how efficiently nutrients are taken up and incorporated into new biomass, largely showed positive correlations with temperature. Variation in NUE was seasonally explicit, with low summer NUE values likely caused by high levels of UV radiation that limit periphyton productivity (Naranjo et al. 2019). Another potential cause for low summer NUE is that high summer nutrient uptake rates suppressed periphyton production rates (Healey 1979, Lean and Pick 1981, Beardall et al. 2001) and thus lowered NUE. Spring and winter nutrient use efficiency increased sharply with warming, nearly doubling over a temperature interval of 9°C (Fig. 1.8). This pattern was driven by large increases in biomass-specific NEP rates and comparatively smaller increases in N or P uptake with warming—a result of lower activation energies of nutrient uptake relative to production (Cross et al. 2015). We found N-use efficiency was mainly driven by NH_4 uptake rather than NO_3 (which was barely utilized by periphyton), since NO_3 uptake into algal cells involves a passive transport process rather than

active transport and is thus less affected by temperature increases (Reay et al. 1999). Our findings are in agreement with both theoretical predictions and whole-ecosystem manipulations that also reveal NUE to increase with temperature (Cross et al. 2015, Hood et al. 2018), but they are in disagreement with experiments on other oligotrophic systems that show NUE to decrease with temperature (Oleksy et al. 2020). Our study demonstrates that the relationship between periphyton nutrient use efficiency and temperature vary seasonally, and that warming tends to increase rates of NEP to a greater degree than nutrient uptake leading to increases in NUE.

Limitations of this study

A few caveats in this study are worthy of consideration and improvement in future studies. In any laboratory study of natural processes, recreating natural conditions is not possible. In the case of our experiments, we did not account for the effects of natural turbulence and wave action of the nearshore zone that can induce sloughing of periphyton from rocks. Additionally, to avoid potential nutrient contamination of metabolic chambers between trials, we were constrained to apply the nutrient treatments in the same order—ambient first and enriched last—rather than randomize them. As a result, nutrient treatments were pseudoreplicated which can lead to potential confounding effects associated with the order that treatments were applied. While we tried to minimize the potential for confounding effects through short holding times for samples (to avoid biomass accrual or senescence of periphyton or grazers between nutrient trials), we acknowledge that unexpected changes in periphyton samples could potentially have confounded the nutrient effects in the study. Our study also focused on bottom-up regulators of periphyton metabolism such as temperature and nutrients, however, top-down regulators are also known to exert strong control over periphyton biomass through grazing (Power et al. 1988). In Lake Tahoe, invasive crayfish represent the main grazers of periphyton, and can influence its biomass dynamics significantly through both nutrient recycling and grazing (Flint and Goldman 1975). While we did not directly measure top-down effects on periphyton metabolism, we do acknowledge

that it likely has a significant effect on seasonal periphyton growth and biomass accrual in the field. Grazer effects may also interact with temperature to influence periphyton growth, as one study found snail biomass increased with temperature (Cao et al. 2017). While not within the scope of this study, future studies would be improved by incorporating top down effects and their interaction with bottom-up effects on periphyton metabolism.

Conclusions

With climate change expected to raise global air temperatures by 2-4°C by 2100 (IPCC 2013), it is increasingly important to understand how warming and nutrient enrichment will affect oligotrophic ecosystem functioning. Periphyton, an important component of ecosystem structure and function in clear water lakes, will likely increase in growth and biomass as a result of these changes. Consistent with our hypotheses, we found that temperature drove the majority of variability in periphyton metabolic rates and was seasonally explicit—having a larger in colder months when rates were most sensitive to temperature increases. We also found that warming stimulated ER more so than GPP which is consistent with the literature (Yvon-Durocher et al. 2010, Demars et al. 2011, Oleksy et al. 2020) and could alter carbon cycling in aquatic systems with climate change. Our findings show that warming can stimulate metabolic rates even without increases in nutrient concentrations. Unexpectedly, nutrient enrichments may have suppressed periphyton metabolic activity in the short term due to energy allocation to rapid nutrient uptake rather than primary production. Despite this, consistently positive NEP suggests periphyton biomass will increase until it comes to equilibrium with elevated *in situ* nutrient concentrations in the long-term. Our study indicates that climate change will likely have the greatest impact on periphyton metabolism during the cold periods of autumn, winter, and spring that are ice free since warming had the greatest stimulatory effect at low temperatures and more precipitation is expected to fall as rain rather than snow which will increase nutrient runoff. Thus, understanding

warming and nutrient effects in a seasonally explicit context will be important for developing management efforts of periphyton under a changing climate.

Chapter 2: Measuring internal phosphorus loads: the importance of accounting for variability in sediment phosphorus pools in hypereutrophic Clear Lake, CA

Introduction

Why consider Internal Phosphorus loading?

Eutrophication is a widespread phenomenon in aquatic systems globally, mainly driven by nutrients such as nitrogen and phosphorus (Schindler et al. 1971). While external nutrient sources represent an important component in lake nutrient budgets, internal sources of nutrients (i.e. from benthic sediments) can also contribute significant amounts of nutrients, especially within shallow, polymictic systems (Søndergaard et al. 2003). This internal source of nutrients is termed internal loading, and refers to the mobilization of sediment-associated nutrients across the sediment water interface (SWI) into the overlying water column. Internal phosphorus loading can contribute greatly to eutrophication and algal blooms (Welch and Cooke 1995, Søndergaard et al. 2013) — especially in shallow, polymictic lakes where hypolimnetic nutrients are regularly mixed into the photic zone. Although lake-bottom sediments contain large pools of phosphorus (P) and can act as an important source of P into the water column, fluxes are rarely measured directly and management decisions targeting restoration are often made without considering internal loading sources.

A complex set of conditions can induce internal loading events. Internal phosphorus loading was classically thought to be driven mainly by redox conditions at the SWI that could liberate metal-bound

phosphate in sediments (Einsele 1936, Mortimer 1941, 1942). In this study, we focus on this mechanism of internal P loading, and exclude other mechanisms such as sediment resuspension and porewater nutrient flux. In this framework, P dynamics are regulated by iron-oxides (α-FeOOH). In reducing conditions, reduced iron (Fe^{2+}) is soluble and does not bind phosphate ions (HPO_4^{2-}, $H_2PO_4^-$) as readily, and thus phosphate is able to desorb from the sediments. Conversely, in oxidative conditions, iron oxides are insoluble and have high specific surface areas that easily bind phosphate ions and remove them from solution (Sulzberger et al. 1989). The oxidation/reduction of iron occurs via two pathways: redox-regulated chemical reactions and biologically-mediated reduction through use as a bacterial electron receptor (Jones et al. 1983, Sulzberger et al. 1989, Roldán et al. 2002, Hyacinthe and Van Cappellen 2004, Orihel et al. 2017). While these reactions play a large role in internal P loading mechanisms, other studies have demonstrated that interacting variables such as pH (Andersen 1975, Jensen and Andersen 1992), water hardness (Orihel et al. 2017), sediment mineral composition (McCulloch et al. 2013), dissolved nitrate concentration (Straub et al. 1996, Hauck et al. 2001, Melton et al. 2012, Matthews et al. 2013, Parsons et al. 2017), dissolved sulfate concentration (Caraco et al. 1989, Roden and Edmonds 1997), redox (Einsele 1936; Mortimer, 1941, 1942), and bioturbation (Holdren and Armstrong 1980, Matisoff and Wang 1998, Chaffin and Kane 2010) all function in regulating P flux across the SWI as well. Another important variable for internal P loading is wind mixing which can resuspend sediments—releasing P in shallow lakes (Cyr et al. 2009). Wind can also entrain P from P-rich hypolimnetic waters to the photic zone (Beutel and Horne 2018) making nutrients available to phytoplankton.

Past Clear Lake Nutrient Studies

Hypereutrophication has been a major problem in Clear Lake beginning in the 1940's, and past studies have sought to identify and manage nutrients and productivity in the lake (Goldman and Wetzel 1963, Richerson et al. 1994). Early studies identified excess phosphorus as the main cause for water

quality issues in the lake as it drove low N:P ratios and favored the proliferation of nitrogen fixing cyanobacteria (Horne and Goldman 1972, Horne 1975, Goldman and Horne 1983, Richerson et al. 1994). A large body of long-term data describing the sediments (Richerson et al. 2008, Lake County Water Resources Department 2017), water chemistry (Richerson et al. 1994), and mixing dynamics (Rueda and Schladow 2003, Rueda et al. 2003) indicate that Clear Lake likely suffers from significant internal P loading. The first comprehensive nutrient study published in 1994 as part of the Clean Lakes Project included a phosphorus mass-balance of Clear Lake that reported estimates of external P loads averaging 160 MT yr^{-1}, P exports from the system of 25 MT yr^{-1}, and internal P loads of 100-200 MT yr^{-1} in non-drought years and 500 MT yr^{-1} in drought years (likely due to more frequent anoxic events and lack of dilution during drought years; Richerson et al. 1994). A more recent report in 2009 by Tetra Tech estimated that external P loads were 90-125 MT yr^{-1}—less the 160 MT yr^{-1} reported in the Clean Lakes Project (Tetra Tech 2009). Tetra Tech attributes this discrepancy to differences in the number of samples and temporal variation between the two studies.

Despite the historic research on nutrient dynamics, a substantial knowledge gap has been the lack of direct nutrient flux measurements. In the Clean Lakes Project, internal loading rates were inferred from total water column nutrients and annual external P loads (Richerson et al. 1994). In the Tetra Tech report, no estimates of internal P loads were included, but internal loading was acknowledged to contribute significant amounts of P relative to external loads (Tetra Tech 2009). Despite this, the Tetra Tech study was used to establish the total maximum daily loads (TMDLs) of P (N was not addressed by current TMDL) to Clear Lake that currently stand (Tetra Tech 2009). Past P mass-balance efforts still leave large knowledge gaps in the extent to which internal P loading contributes to eutrophication and algal blooms. Additionally, the discrepancy between these two studies calls into question the accuracy of past P loading estimates, leaving past internal P loading estimates to Clear Lake

unclear. Nitrogen has not been the focus of TMDL controls in Clear Lake as past research suggested that managing P was the most effective way for curbing toxic harmful algal blooms.

We hypothesize that productivity in Clear Lake, an extremely hypereutrophic, polymictic, shallow lake, is fueled mainly by internal nutrient sources. We also hypothesize that summer P-flux rates from the sediment will be much higher than wintertime P-flux rates. Potential mechanisms for higher summer P flux rates include higher chemical kinetics at warmer temperatures, quicker rates of oxygen depletion at the sediment-water interface (SWI) from increased biological oxygen demand, and positive effects of high pH caused by summer productivity. We also hypothesize that sediments actively exchanging P with overlying water will be relatively shallow, only extending to about 10 cm depth (Richerson et al. 1994), and will test this by comparing P content of discrete sediment layers between oxic and anoxic cores. In this study, we present 1) the results of the first direct measure of internal P flux rates using sediment core incubations from 6 monitoring sites across Clear Lake, 2) concurrent measures of ammonium and nitrate flux from lake sediments, 3) variability in N and P flux between summer and autumn seasons, 4) spatial variability in N and P flux, and 5) the depth of active sediment P exchange within the lake.

Methods

Site Description

Clear Lake is located in the coastal range in Lake County, CA, and is the largest lake completely within California at 176 km^2 (Fig. 2.1). It is likely the oldest lake in North America, and has existed in the same basin for up to 2 million years (Richerson et al. 2008). It has endemic species such as the Clear Lake hitch (*Lavinia exilicauda chi*, a planktivorous fish), and Clear Lake gnat (*Chaoborus astictopus*)—the latter of which was targeted by heavy application of the pesticide DDD to control large swarms (featured in Rachel Carson's *Silent Spring*). Due to the lake's high productivity, Clear Lake supports a large recreational fishery for largemouth bass (*Micropterus salmoides*) along with other popular species

(Richerson et al. 1994). Historically the lake has been eutrophic, owing its high P concentrations to the volcanic, P-rich parent material (Richerson et al. 2008). Starting with European settlement, anthropogenic changes such as road construction, agriculture, gravel-dredging in streams, open-pit mining, and wetland loss have hyper-eutrophied the lake (Richerson et al. 1994, 2008). These human-induced changes have led to large algal blooms dominated by cyanobacteria (Horne 1975) that degrade aesthetics (foul-smelling, decaying algal mats), cause frequent fish kills due to hypoxia (Goldman and Wetzel 1963, Feyrer et al. 2020), and increasingly generate toxin-producing cyanobacterial blooms (Goldman and Wetzel 1963, Horne 1975, Richerson et al. 1994, Kennard 2021). The lake is an important drinking water source, and large algal blooms increase expense of water treatment (Richerson et al. 1994, Kennard 2021). Problems related to excessive algal blooms also cause multi-million dollar losses in recreation each year and periodically drive local residents from their homes (Richerson et al. 1994).

Due to the Mediterranean climate, the lake remains ice-free year-round and receives the bulk of its annual precipitation in the winter (Richerson et al. 1994). Clear Lake has 3 basins: the Upper Arm (106 km^2), the Lower Arm (30 km^2), and the Oaks Arm (15 km^2; Fig. 2.1), each differing in water and sediment chemistry (Lake County Water Resources Department 2017). During winter the lake is more turbid (due to the runoff) and all the major tributaries drain into the large Upper Arm, making this arm especially turbid (Richerson et al. 1994). Due to the large amounts of P in the system, Clear Lake is an optimal system in which to measure internal nutrient cycling because of easily-detectable, prominent internal P fluxes. Seasonal patterns that have historically been observed between sediment P and water column P concentrations after periods of anoxia strongly suggest that internal P loading in Clear Lake follows classic redox-mediated mechanisms (Richerson et al. 1994).

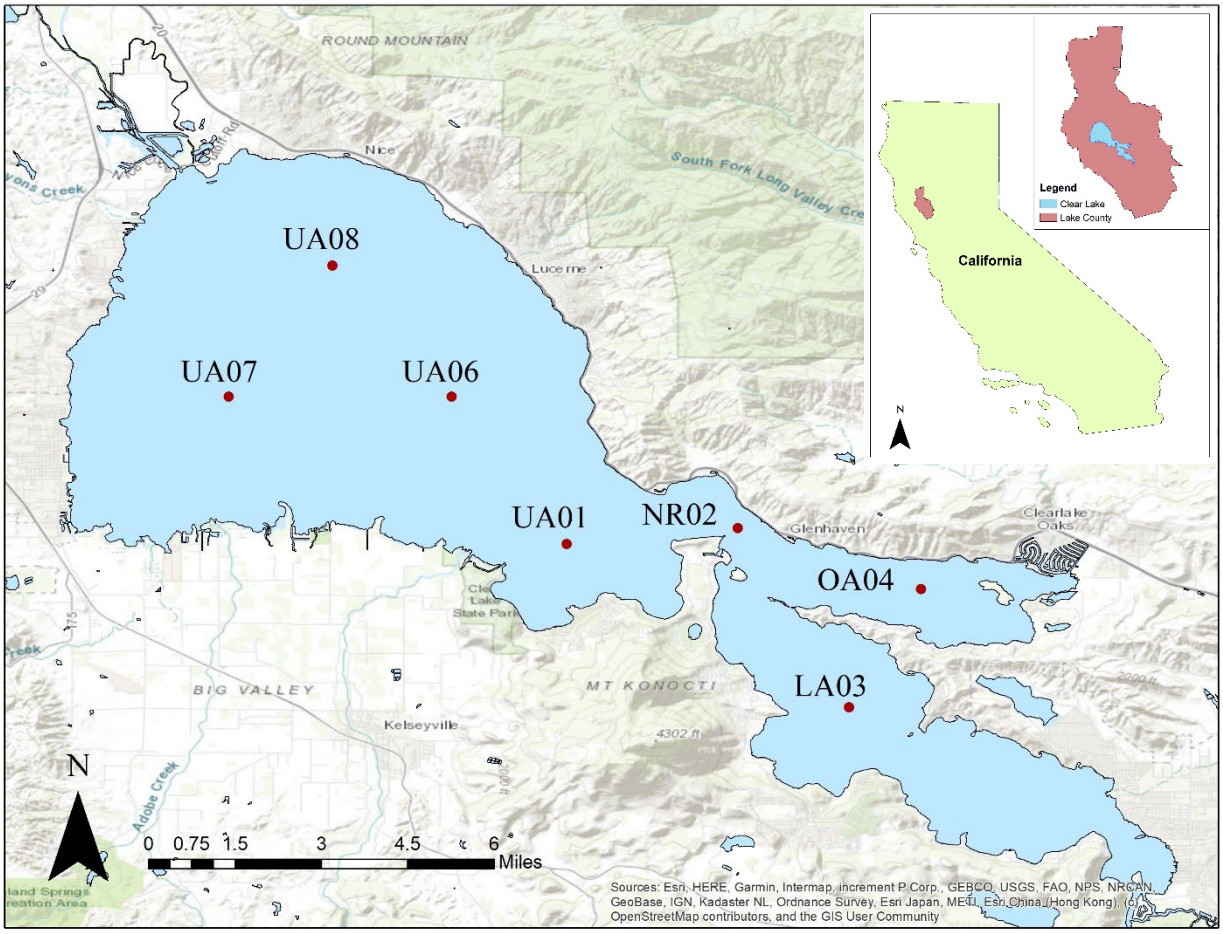

Figure 2.1: *Map of Clear Lake, CA, with six sites indicated with red points.*

Sample Collection

To determine P flux rates and compare their variability between summer and fall seasons, we used laboratory incubations of intact sediment cores during winter (November 2019) and summer (August 2020). To characterize spatial variability within the lake, we sampled from 6 sites distributed throughout each of the lakes 3 arms during the November 2019 experiment; however, we reduced the number of sites to 3 during the August 2020 experiment to focus on variability in P flux rates between summer and autumn seasons at 3 core sites. Using a large-bore gravity corer (Aquatic Research Instruments fitted with 0.5m long, 9.5 cm diameter polycarbonate cores tubes), we collected four intact sediment cores from all 6 sites (excluding UA07) for a total of 24 cores in November 2019 and 3 cores from 3 sites (UA06, LA03, and OA04) for a total of 9 cores in August 2020. Each core contained 15-25 cm of sediment

and 25-35 cm of overlying water. Cores were stored on ice during transport to the lab to maintain ambient temperature. To ensure cores had similar starting conditions at the beginning of the incubation, we siphoned off the overlying water (while minimizing disturbance of the sediment), filtered it to 0.45 µm to remove zooplankton and phytoplankton, and then pooled the filtered water by site into a carboy and homogenized. Cores were refilled from the large carboy using a peristaltic pump and placing a T-valve at the end of tubing to minimize water velocity into the sediment and prevent resuspension.

Sediment Core Incubations

After processing the cores, we placed cores in a constant temperature room set to 15.2°C for November 2019 experiments and 23°C for August 2020 experiments (ambient hypolimnion temperatures at the time of sampling). Duplicate cores were then bubbled with air for the oxic treatment, or N_2 gas balanced with 350ppm CO_2 (CO_2 added for pH buffering; Moore et al. 1998, Ogdahl et al. 2014) for the anoxic treatment (Fig. 2.2). During the August 2020 experiment, we incubated duplicate anoxic cores and one oxic core.

Bubbling rates were near one bubble per second to allow mixing of the water column without causing resuspension. The core apparatus is similar to that of Buetel et al. (2008) in that the bubbling and water sampling port extend to 5 cm above the SWI. To ensure stable starting conditions, we allowed cores to equilibrate for 24 hours before samplings began. We and sampled cores every three days for a 30-day period for a total of 11 samplings during the November 2019 experiment, and approximately every 3 days for 15 days for a total of 5 samplings during the August 2020 experiment. To verify that cores maintained steady pH conditions, we measured pH using a Fisher Scientific AP62 portable meter (calibrated with pH 4, 7, and 10 buffers before each sampling). To verify that oxic and anoxic conditions in cores, we measured redox potential (E_h) using EPA standard methods (US EPA 2017) through the access port with a Fisher Scientific Orion metallic combination electrode. We minimized oxygen contamination of headspace by sealing the access port with parafilm during redox and pH measurements.

Water and Sediment Chemistry

To characterize flux rates, cores were subsampled for water chemistry every 2-3 days. On sampling days, we removed 75 ml of water (without replacement) and filtered with a GF/F filter to 0.7 µm to remove bacterioplankton. Filtrate was then collected in 60 ml bottles without headspace to prevent potential oxidation of redox-sensitive P before analysis. We measured changes in water height throughout the incubation to account for changes in water volume in the P mass-balance calculations for each core. Samples were stored refrigerated (4˚C) for no more than 7 days before being analyzed by the Tahoe Environmental Research Center (TERC) for soluble reactive phosphorus (SRP), NO2 + NO3, NH4, and DP to characterize nutrient flux rates in cores. Dissolved NH_4 concentrations were determined using the Idophenol method adapted from Liddicoat et al. and Solorzano et al. (Solórzano 1969, Liddicoat et al. 1975) and has a method detection limit (MDL) of 2 µg/L. Dissolved NO_2 + NO_3 concentrations were analyzed using the Hydrazine Method adapted from Kamphake et al. and Strickland & Parsons (MDL 2 µg/L) (Kamphake et al. 1967, Strickland and Parsons 1972). Soluble reactive phosphate (SRP) concentrations were determined using a method adapted from Murphy & Riley (MDL 1 ug/L) (Murphy and Riley 1962). Dissolved phosphorus concentrations were determined using persulfate digestion (MDL 2 µg/L) (Strickland and Parsons 1972, Fishman and Friedman 1989).

To characterize the depth to which redox-mediated P release occurs, we measured various fractions of P species in November 2019 core sediments post-incubation and compared sediment P profiles of oxic (control) and anoxic (treatment) cores. We did not test sediment P in August 2020 cores due to resource and time constraints. Sediment samples were taken from discrete depths for each set of duplicate oxic or anoxic cores from a single site, as one replicate was sampled in 2 cm increments down to a depth of 16 cm, after which the bottom 5 cm of sediment was pooled for a final sample down to 21cm. For the remaining replicate, we sampled in 2 cm increments to a depth of 6 cm and then pooled the next 5 cm of sediment for a final sample down to 11 cm deep. Each discrete depth was then

analyzed for various metal-bound fractions using sequential extractions that test for increasingly recalcitrant forms of P in the sediments. Using methods adapted from Hieltjes and Lijklema (1980) we measured loose-bound, iron and aluminum-bound (Fe+Al-P), and calcium-bound (Ca-P) fractions of P in sediments using sequential extractions with NH_4Cl, NaOH, and HCl respectively. We then measured total phosphorus (TP) on a separate subsample using a perchloric acid digestion and characterized residual P as the difference between TP and the aforementioned P species measured during the previous set of extractions.

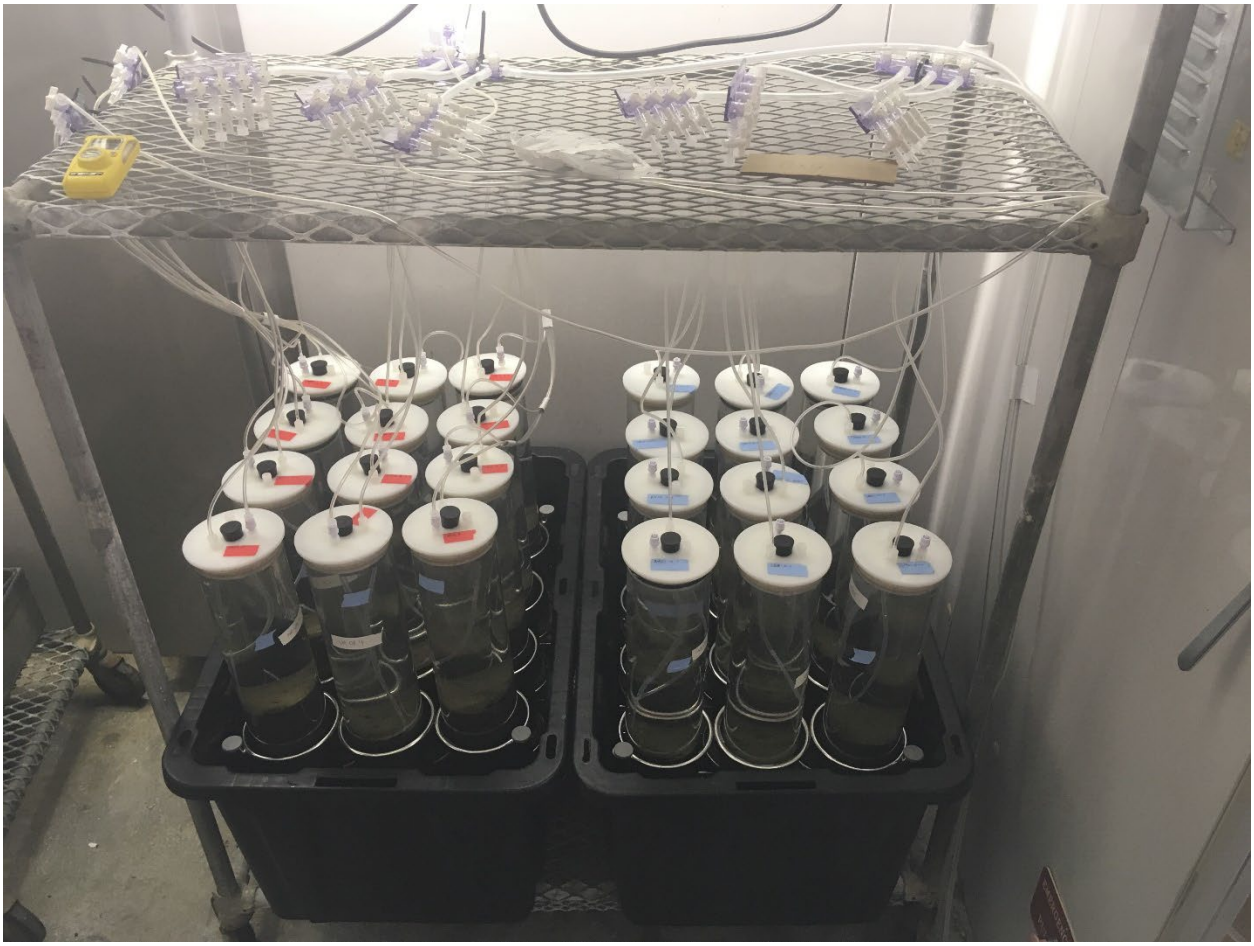

Figure 2.2: *Incubation setup inside temperature-controlled room. Cores marked with red are the anoxic treatments and cores marked in blue are the oxic treatments.*

Analytical Methods

To estimate P flux rates, we used methods similar to Moore et al. (1988) and calculated rates as the maximum slope of the linear portion of the SRP mass accumulation curves for each individual core. We then converted these to aerial rates by dividing raw rates by the sediment surface area inside the cores. To compare both theoretical and empirical anoxic internal P flux rates at summer temperatures, we applied a Q_{10} temperature correction to November 2019 rates measured at 15.2°C to reflect rates at 23°C— the average hypolimnetic temperature measured during the August 2020 experiment. To do this we used equation 2.1 (taken from Nürnberg 2009) where c =3 (this is equivalent to a Q_{10} value), which corresponds to a tripling of rates over a 10°C temperature interval. A Q_{10} value of 3 has been used in studies of P flux rates in other polymictic, hypereutrophic lakes (Liikanen et al. 2002, Nürnberg 2009), however, we acknowledge that there is some uncertainty in this parameter and it can vary among lakes. For this reason, we present temperature-adjusted P flux rates using Q_{10} values ranging from 2-3 to yield a more conservative estimate.

Equation 2.1:

$$RR_{Summer} = RR_{Incubation} \times c^{(T_{Summer} - T_{Incubation})/10}$$

Analysis of sediment and water column P coupling

To analyze seasonality in redox-sensitive sediment P pools and coupling of sediment P and the overlying water column, we analyzed Clear Lake sediment Fe+Al-P concentration data provided by Lake County DWR and water column orthophosphate data gathered from the California Environmental Data Exchange Network (CEDEN) from 2008-2017. In order to only include available pools of Fe+Al-P in the sediments, we only included concentration data from the top 6 cm of sediment based on our own observations of active P exchange with sediment depth (Fig. 2.7). We also only included water column orthophosphate concentrations from samples taken at 5m depth or greater to capture sediment-derived phosphorus. We averaged concentration values for each day for each of the three sites (locations shown in Appendix B6).

Results

Trends in pH and redox during experiments

During both incubations, pH of overlying water in sediment cores was consistently basic and relatively stable. During the November 2019 and August 2020 experiments pH ranged from 7.5-8.6 and 7.6-8.8 respectively (Appendix B2). Redox conditions (E_h) in anoxic cores ranged from -50 to 400mV and oxic cores ranged from 340 to 450mV, and were more variable during the November 2019 experiments than August 2020 experiments. Anoxic cores in the August 2020 experiment ranged from -100 to 200mV (except for one core that had an outlying measurement of 300mV) and oxic cores ranged from 340 to 410mV (Appendix B1).

Patterns in nutrient concentrations

SRP concentrations in overlaying water of anoxic cores ranged from 1200-2500 µg-SRP/L and 650-1250 µg-SRP/L during the November 2019 and August 2020 incubations respectively, and were consistently higher in anoxic cores compared to oxic cores. Oxic SRP concentrations stayed below 250 µg-SRP/L and 1000 µg-SRP/L for the November 2019 and August 2020 incubations respectively (Fig. 2.3). SRP concentrations at sites NR02 and OA04 were 2086 and 2380 µg-SRP/L respectively during the November 2019 experiment—much higher than all other sites which ranged from 1315-1719 µg-SRP/L (Fig. 2.3A).

SRP concentrations also varied between summer and autumn as maximum SRP concentrations in November 2019 cores was an average of 1768 µg-SRP/L compared to 1130 µg-SRP/L in August 2020. Cores in the November 2019 experiment took between 18-30 days to reach maximum concentrations of SRP, but concentrations in cores from the Upper Arm increased steadily until day 30 and did not show evidence of reaching maximum SRP concentrations (Fig. 2.3A). Contrastingly, cores from the August 2020 experiments achieved maximum SRP concentrations much more quickly, with cores only taking 3 days (Fig. 2.3B). Despite this result, starting concentrations of SRP in cores from August 2020 experiment

were significantly higher than November 2019 cores with average SRP concentrations of 715 and 108 µg-SRP/L respectively (Fig. 2.3).

Similar to patterns in SRP, NH_4 concentrations from the November 2019 experiment were highest in anoxic cores and ranged from 125-875 µg NH_4-N/L, while concentrations in oxic cores mostly remained under 12 µg NH_4-N /L (Fig. 2.5). Unlike patterns in SRP concentrations, however, NH_4 concentrations did not exhibit consistent increases throughout the incubation, but rather punctuated increases followed by rapid declines (Fig. 2.5). NH_4 concentrations exhibited similar spatial patterns as SRP (Fig. 2.5) with the highest observed concentrations occurring at sites OA04 and NRO2 with ~400 and 875 µg NH_4-N /L respectively. The Upper and Lower Arm sites, however, had comparatively lower NH_4 concentrations with maximum concentrations ranging from 125-250 µg NH_4-N/L (Fig. 2.5).

Patterns in NO_3 concentrations differed from those of NH_4 and SRP in that concentrations were highest in oxic cores (Fig. 2.6) where oxidative redox conditions were dominant (Appendix B1). Concentrations of NO_3 in overlying water of oxic cores ranged from 45-120 µg NO_3-N/L, but stayed between 15-20 µg NO_3-N/L in anoxic cores (Fig. 2.6). NO_3 concentrations also varied spatially as concentrations were consistently highest in cores from OA04 in both the November 2019 and August 2020 experiments (maximum concentrations were ~120 and 350 µg NO_3-N/L respectively; Fig. 2.6). All other sites showed comparatively lower levels of NO_3 release with maximum concentrations ranging from 45-60 µg NO_3-N/L during the November 2021 experiment and from 100-150 µg NO_3-N/L during the August 2020 experiment (Fig. 2.6). Seasonal variation in NO_3 concentrations was very pronounced as maximum concentrations in August 2020 cores were 3-7 times larger compared to maximum concentrations in November 2019 cores and ranged from 102-350 µg NO_3-N/L (Fig. 2.6). Site OA04 showed the largest change in maximum NO_3 concentration between November 2019 and August 2020, and August 2020 concentrations were 7 times larger than those in November 2019 (Fig. 2.6).

Seasonal differences in nutrient flux rates

Anoxic P flux rates ranged from 8.8-26.7 mg SRP m^{-2} d^{-1} and were much higher than oxic flux rates during both November and August experiments (Fig. 2.4). While anoxic P flux rates were all positive, oxic P flux rates were both positive (sediments released P) and negative (sediments absorbed P) during the November 2019 experiment and were all negative during the August 2020 experiment (Fig. 2.4). P flux rates of the Oaks Arm (OA04), the Narrows (NR02), and the Lower Arm (LA03) ranged from 21.4-26.7 mg SRP m^{-2} d^{-1}, and were 2-3 times higher than the Upper Arm sites during the November 2019 experiment (Fig 4A). Spatial variation showed different patterns during the August 2020 incubation as P flux at site OA04 was a little over 1.5 times the rates at sites LA03 and UA06 (Fig. 2.4B).

Contrary to significant seasonal patterns in SRP concentrations, anoxic SRP flux rates showed little seasonal variation, with average rates of 17 mg SRP m^{-2} d^{-1} during both the November 2019 and August 2020 experiments. Direct site-to-site comparisons between November 2019 and August 2020 indicate that anoxic P flux rates decreased for sites OA04 and LA03 by 7.2 and 2.5 mg SRP m^{-2} d^{-1} respectively, but increased at site UA06 by 2.5 mg SRP m^{-2} d^{-1} (Fig. 2.4). Oxic flux rates tended to be more negative during August 2020, with sediments absorbing 2.4-4.2 mg SRP m^{-2} d^{-1} (Fig. 2.4B). Theoretical summer P flux rates (rates measured during November 2019 at 15.2°C and adjusted to 23°C using Q_{10} = 2-3) ranged from 21-64 mg SRP m^{-2} d^{-1}, and were much larger than empirically measured summer rates with an average anoxic P flux rate of 42 mg SRP m^{-2} d^{-1}—more than double the August 2020 average of 17 mg SRP m^{-2} d^{-1} (Table 2.1). Despite this, there are some uncertainty in these estimates and they likely do not reflect true P flux values in the lake.

Sediment P profiles

Differences between sediment profiles of anoxic and oxic cores of the November 2019 experiment indicate that iron and aluminum-bound P (Fe+Al-P) was depleted in the top 6 cm of anoxic cores at 3 of the 6 sites (Fig. 2.7). On average, anoxic cores were depleted in Fe+Al-P relative to oxic

cores to a depth of 5.6 cm (excluding site NR02). Site NR02 was an outlier and exhibited differences between anoxic and oxic cores down to 21 cm depth (Fig. 2.7). Site UA06 also differed from other sites and exhibited differences in Fe+Al-P content down to 6-8 cm, and UA08 to only 0-2 cm depth (Fig. 2.7).

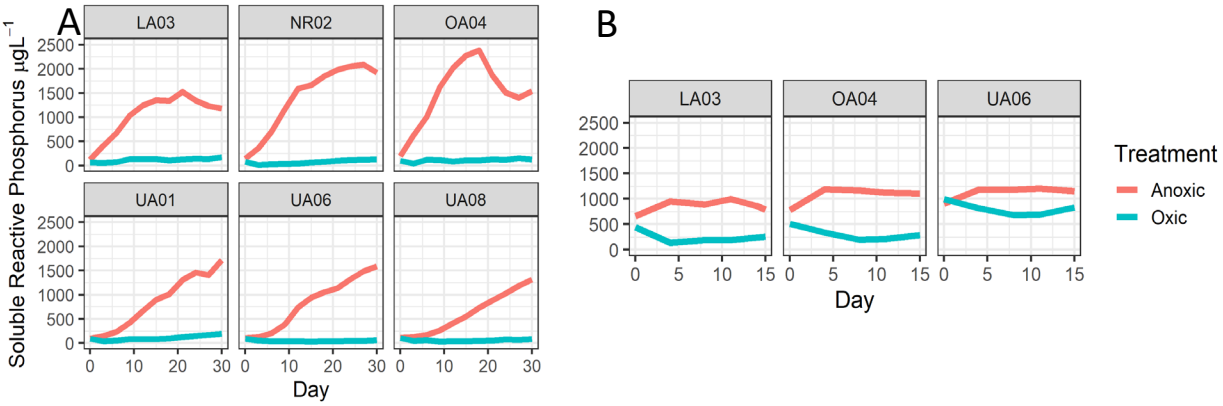

Figure 2.3: *A) Average concentrations of SRP (µg-P/L) over 30 days in duplicate cores from November 2019 experiments for both anoxic and oxic treatments, and B) average SRP concentrations over 15 days in duplicate anoxic cores and a single oxic core for the August 2020 experiment.*

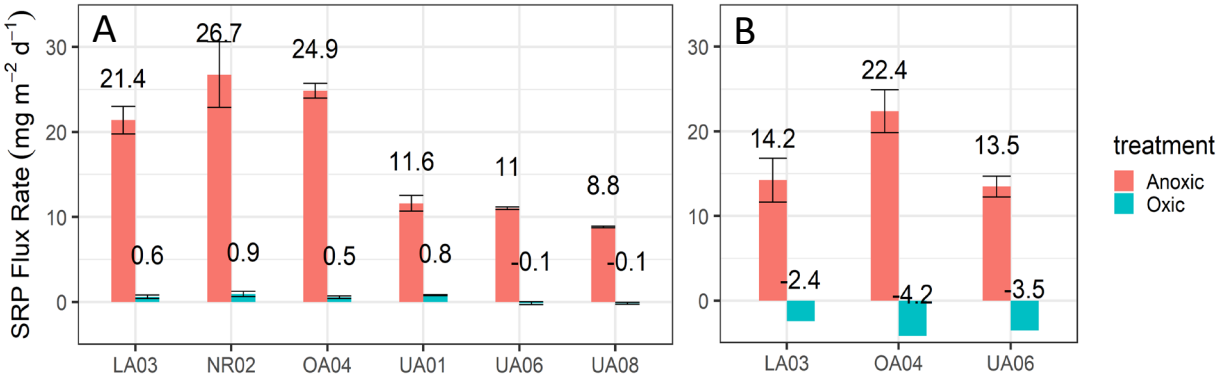

Figure 2.4: Average P-flux rates of duplicate cores measured during A) *November 2019 at 15.2°C, and B) August 2020 at 23°C. Error bars denote associated standard deviations. Oxic data in August 2020 have no error bars since data was gathered from a single sample.*

Site	treatment	Mean SRP Flux Rate (15.2°C)	sd	SRP flux at 23°C (Q_{10} = 2)	sd	SRP flux at 23°C (Q_{10} = 3)	sd
LA03	A	21.39031	1.613179	37.24269	2.808709	51.51267	3.884899

	O	0.611918	0.199458	1.065411	0.347277	1.473635	0.480341
NR02	A	26.73648	3.857979	46.55091	6.717132	64.38745	9.290881
	O	0.947029	0.30847	1.648874	0.537077	2.280659	0.742865
OA04	A	24.85397	0.85857	43.27328	1.494856	59.85395	2.067628
	O	0.549996	0.155884	0.957598	0.271411	1.324513	0.375405
UA01	A	11.62746	0.935576	20.24459	1.628932	28.00154	2.253077
	O	0.797619	0.058763	1.388735	0.102313	1.920846	0.141515
UA06	A	11.01093	0.14409	19.17114	0.250875	26.51679	0.347001
	O	-0.13617	0.160831	-0.23709	0.280023	-0.32793	0.387317
UA08	A	8.825759	0.089058	15.36654	0.155059	21.25441	0.214472
	O	-0.14491	0.116567	-0.2523	0.202955	-0.34897	0.28072

Table 2.1: *Average P flux rates at 15.2°C, with theoretical temperature adjusted P flux rates at 23°C (the same temperature of August 2020 incubations) calculated using Q_{10} values ranging from 2-3. "A" denotes anoxic cores and "O" denotes oxic cores. Averages are given and associated standard deviations of duplicate cores are shown in the adjacent column.*

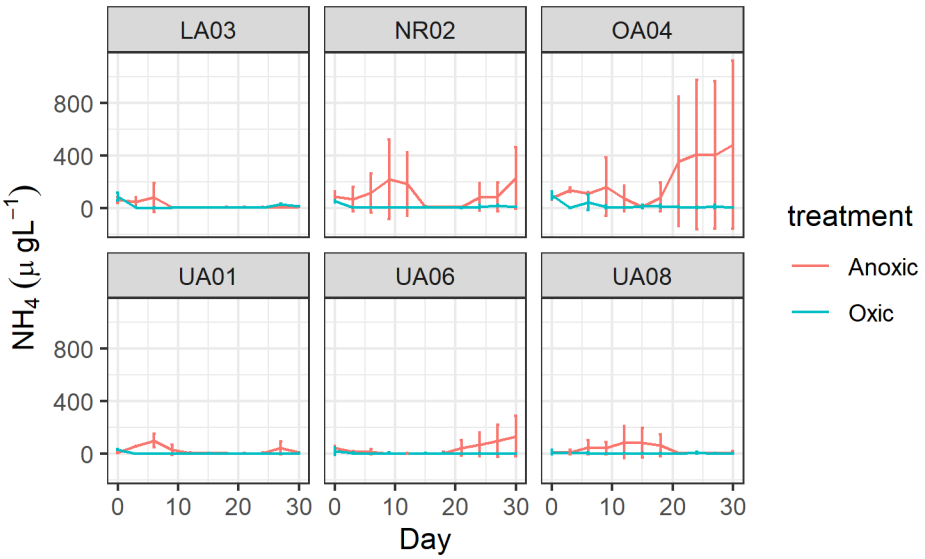

Figure 2.5: *Concentrations of NH_4 in both oxic and anoxic cores in the November 2019 experiment. Lines represent averages of duplicate cores, and vertical bars denote standard deviations. NH_4 concentrations in the August 2020 experiment were not measured.*

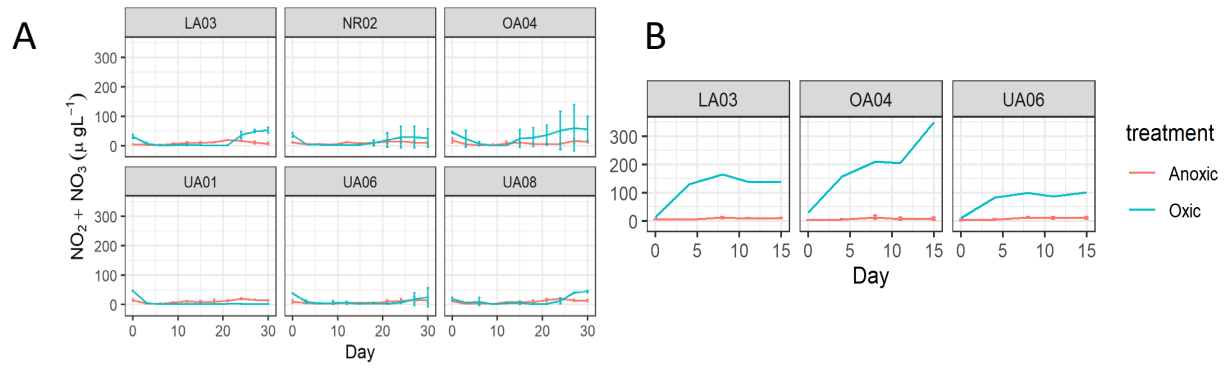

Figure 2.6: *Concentrations of NO_2 + NO_3 in anoxic and oxic cores during both the A) November 2019 and B) August 2020 experiments. Lines with error bars represent averages of duplicate cores, while those without error bars represent results from a single core.*

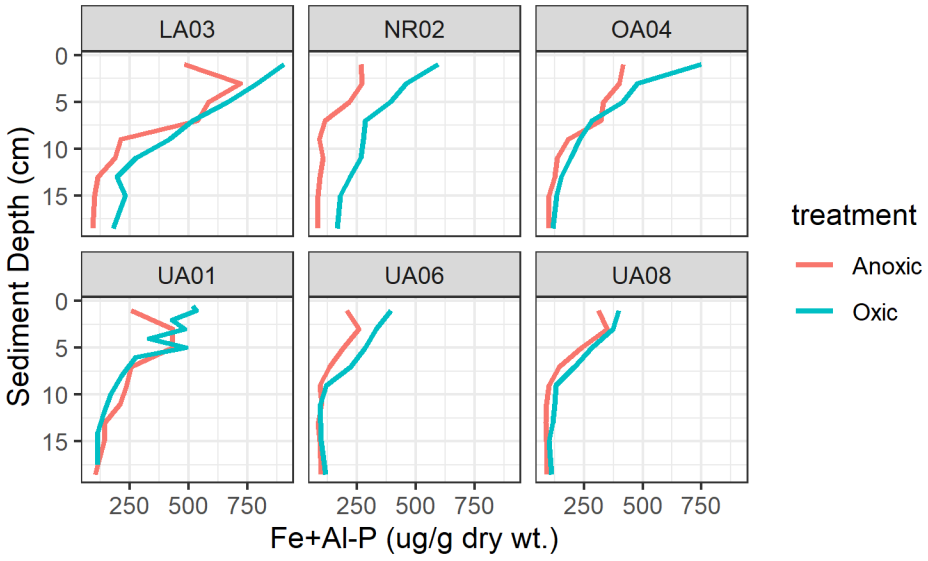

Figure 2.7: *Lines represent average sediment Fe+Al-P concentrations (µg Fe+Al-P/g dry wt.) of duplicate cores from November 2019, with red denoting anoxic treatment and blue oxic treatment. Cores were sectioned in 2 cm sections thus data points represent ±1 cm resolution except for the bottom-most depth which pooled the 5 cm of sediment from 16-21 cm depth and is ±2.5 cm resolution. An oxic core from site UA01 differed from other cores since the top layer was 1 cm thick rather than 2 cm, but all other core depths maintained the same sampling pattern and were thus 1 cm off from normal core depths.*

Discussion

Comparing P flux rates to other hypereutrophic systems

The empirically derived internal loading rates for Clear Lake that we quantified are squarely within the range of reported values for other hypereutrophic lakes. Phosphorus flux rates in Clear Lake ranged from 8.8 to 26.7mg m^{-2} d^{-1}, and typical ranges reported for other hypereutrophic lakes ranged

from 1.7 to 38 mg m^{-2} d^{-1} (Auer et al. 1993, Penn et al. 2000, Ruley and Rusch 2004, Loh et al. 2013). Our measured rates are also similar to other eutrophic/hypereutrophic lakes in California which typically range from 2.5-33.3 mg m^{-2} d^{-1} (Beutel 2000, Beutel et al. 2020). Literature reviews on internal P loading show that Canadian eutrophic lakes had a median anoxic P flux rate of ~8 mg m^{-2} d^{-1} (n = 17) and hypereutrophic lakes a median of ~5 mg m^{-2} d^{-1} (n = 3) (Orihel et al. 2017), North American and European lakes had median flux rates of ~22 mg m^{-2} d^{-1} for hypereutrophic lakes (n = 6) (Nürnberg 1997), and Midwest hypereutrophic reservoirs range from 13-40 mg P m^{-2} d^{-1} (n = 5) (Carter and Dzialowski 2012). This indicates Clear Lake P flux rates were higher than most Canadian lakes, but were on par with other North American, European, and Midwestern lakes. Average theoretical (temperature adjusted) Clear Lake summer P flux rates ranged from 15 to 46 mg m^{-2} d^{-1} among the six sites are at the higher end of most rates in the literature. The lakes in this comparison are temperate and commonly have winter ice cover with accompanying low rates of P flux during this period due to lower temperatures (Nürnberg et al. 2013); however, Clear Lake remains ice-free year-round and relatively high P flux rates may persist throughout the year. This may lead to higher annual internal P loads relative to temperate lakes despite having similar P flux rates. Taken together, Clear Lake is characterized by high P flux rates similar to other hypereutrophic systems, and internal P loading is an important driver of within-lake P concentrations.

Despite the fact that temperature adjusted rates are at the high end of values reported in the literature, there is significant uncertainty in the Q_{10} temperature adjustments. This parameter varies among lakes, and has not been calibrated for Clear Lake specifically. We thus present these temperature adjusted rates not to reflect actual *in situ* flux rates occurring in the field, but rather to contrast empirical results of August 2020 incubations.

Drivers of seasonal variability in P flux

Despite our expectations for high summer sediment P flux rates due to warmer temperatures, we observed little difference in flux rates measured between summer and autumn (Fig. 2.4). While temperature is known to have a positive effect on sediment P flux rates (Jensen and Andersen 1992, Liikanen et al. 2002, Nürnberg 2009, Nõges et al. 2011b, Søndergaard et al. 2013, Wu et al. 2014, Gibbons and Bridgeman 2020), the absence of an effect in our study indicates that other factors affected sediment P flux rates as well. pH, another critical variable in determining P flux rates, was within a suitable range for internal P flux (Appendix B2; Wu et al. 2014), however, lower summer P flux rates may have been caused by seasonal fluctuation in sediment P pools (Penn et al. 2000). As shown in other systems, prolonged anoxia may eventually exhaust redox-sensitive P species in the sediments and thus limit sediment P flux rates to those of sedimentation and diagenesis in the benthos (Penn et al. 2000, Spears et al. 2007). In fact, August 2020 sediment cores exhibited elevated initial SRP concentrations at the beginning of the experiment compared to November 2019 cores (Fig. 2.3), suggesting internal P loading was already occurring *in-situ* at the time of sampling. This evidence suggests that the sediments may have been partially depleted in redox-sensitive P during the August 2020 experiment and may have caused unexpectedly low P flux rates.

Although summer sediment P flux rates are usually expected to represent a seasonal maximum due to high temperatures and comparatively high pH levels (the latter being a product of high algal productivity; Koski-Vähälä and Hartikainen 2001, Xie 2006), our study shows that lower sediment P concentrations may negate those effects. As a result, lakes may experience so-called “bursts” of internal P flux upon initial onset of anoxia during the late spring/early summer when sediments are richest in redox-sensitive P species and temperature and pH conditions are still favorable (Penn et al. 2000).

Data for sediment P pools from 2008-2017 show that redox-sensitive P species such as Fe+Al-P and Ca-P fluctuate seasonally as sediments exchange P with the overlying water column (Fig. 2.8). Data

show that decreases in the sediment pools of redox-sensitive P often correspond to spikes in water-column orthophosphate concentrations suggesting that internal phosphorus loading drives P concentrations in the lake (Fig. 2.8). This pattern is not always consistent, and lag time between patterns in sediment P and water column P concentrations may be mediated by biological uptake of dissolved P (Lemley et al. 2021) and dilution effects from large inter-annual fluctuations in precipitation to the lake (Richerson et al. 1994). As a result, early season anoxic events in the late spring/early summer may have a disproportionate impact on within-lake phosphorus concentrations, and subsequent anoxic events in the late summer/early fall may have lesser impacts. With this in mind, theoretical summer rates in Clear Lake, predicted to range from 21 to 64 mg m^{-2} d^{-1}, may only be representative of early season internal P flux rates when sediments are P-rich and do not accurately characterize P flux rates for the entire summer. Thus, our data demonstrate that predicting seasonal variation in sediment P flux rates using temperature alone does not produce accurate results and can be misleading due to seasonal variation in sediment P pools. Therefore, seasonal variation in sediment P pools should also be taken into account when characterizing sediment P fluxes.

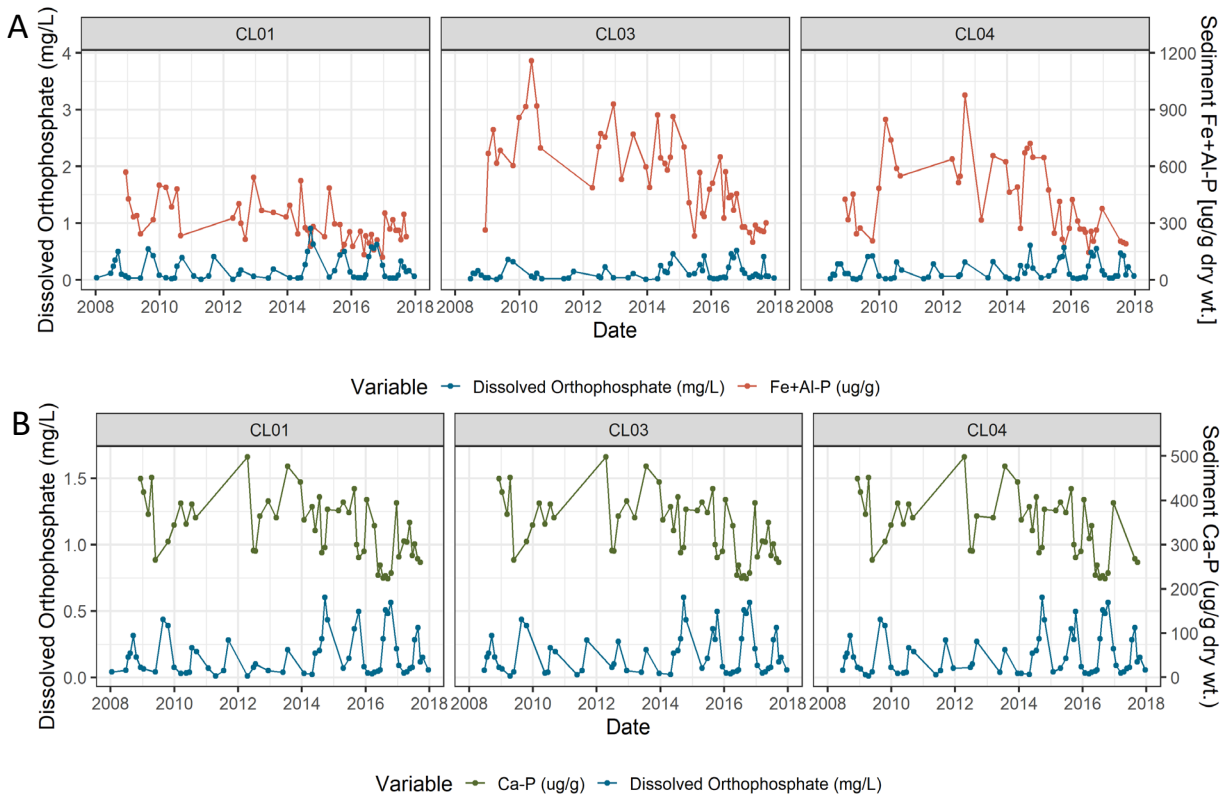

Figure 2.8: *Concentrations of sediment P species and water column orthophosphate in Clear Lake. A) Fe+Al-P in the upper 6 cm of sediment and dissolved orthophosphate in the water column below 5m depth. B) Ca-P in the upper 6 cm of sediment and dissolved orthophosphate in the water column at 5m depth and below. Sites CL01, CL03, and CL04 correspond to the Upper, Lower, and Oaks Arms respectively and are Lake County DWR long-term monitoring sites (Appendix B6).*

Implications of sediment N and P fluxes

Consistent with classical internal P loading models, SRP fluxes were consistently higher in anoxic, reducing conditions compared to oxic conditions (Welch and Cooke 1995, Nürnberg et al. 2013, Orihel et al. 2017, Osaka et al. 2022). While the focus of our analysis was on phosphorus, we noted that NH_4 flux occurred under reducing conditions, although fluxes were quite variable and were much smaller than those of other hypereutrophic lakes in California (Beutel 2006). The highest concentrations achieved (~800 µgNH_4-N/L at site OA04) were at the low end of reported anoxic NH_4 concentrations measured in

hypereutrophic San Vicente Reservoir (800-2000 μgNH_4-N/L), and were well below those of hypereutrophic Lake Elsinore (4,000-5,000 μgNH_4-N/L) (Beutel 2006).

These results were unexpected as higher NH_4 fluxes are characteristic of hypereutrophic lakes such as Clear Lake. Lower NH_4 fluxes may have been due to the following four mechanisms. 1) Anammox—or anaerobic ammonium oxidation to N_2 gas— has been shown to occur in anoxic lake sediments and can result in removal of ammonium from the system (Allgeier et al. 1932, Schubert et al. 2006, Yoshinaga et al. 2011, Zhu et al. 2013a, Yang et al. 2017, Crowe et al. 2017). 2) Changes to NH_4 concentrations during sample hold times can lead to inaccurate characterization of NH_4 concentrations (Turner and Roupas 2006, Zhu et al. 2013b). 3) Nitrification of ammonia to nitrate and/or nitrite during accidental oxygenation of sediment cores (van Luijn et al. 1999). Finally 4) the assimilation of ammonium into bacterial biomass can be a sink for NH_4, thus leading to low concentrations in the overlaying water of sediment cores (Beutel 2006). Mechanism 1, regarding removal of NH_4 via anammox reactions is possible, but research into the magnitude and significance of anammox-related N fluxes is still relatively unknown (Crowe et al. 2017). Sample hold times, which were up to 7 days in our experiments, could have altered NH_4 concentrations and led to inaccurate results of NH_4 concentrations in cores through mechanism 2 (Turner and Roupas 2006, Zhu et al. 2013b). It appears nitrification was not a significant process in anoxic cores or sample bottles during hold times due to low nitrate concentrations measured in anoxic cores (Fig. 2.6), thus, mechanism 3 can be ruled out. Mechanism 4, assimilation of ammonium into bacterial biomass was also a possible sink for NH_4 since we observed white biofilms potentially composed of bacteria forming on interior surfaces of cores. Anoxic cores were periodically oxic during the experiment (Appendix B1.A), and it is possible that aerobic bacteria assimilated significant amounts of NH_4 since they have higher rates of ammonium assimilation relative to anaerobic bacteria (Hansen and Blackburn 1991) due to faster growth rates (Moore Jr. et al. 1992). This final mechanism seems most likely given that we observed a noticeable white biofilm that

developed during the incubations on surfaces inside the cores, and bacterial biomass presumably increased.

NH_4 is mainly produced by bacterial mineralization of organic N within sediments and enters the water column via diffusion (D'Angelo and Reddy 1993, Song et al. 2003). This source of nitrogen is more readily taken up by phytoplankton relative to NO_3 (Dortch 1990, Dugdale et al. 2007), and since internal NH_4 pulses coincide with internal P loading this can have important implications for algal ecology (Beutel 2006). Past studies on Clear Lake have shown how summer pulses of NH_4 can potentially suppress proliferation of N-fixing cyanobacteria and shift dominance towards *Microcystis*, a toxin-producing cyanobacteria that is incapable of N-fixation (Goldman and Horne 1983). NO_3 flux occurred under oxidative conditions, as ammonium was oxidized via nitrification (D'Angelo and Reddy 1993). Despite this, NO_3 fluxes were smaller in magnitude compared to NH_4 (Fig. 2.6), and these fluxes may have a smaller effect on algal productivity in Clear Lake.

Other potential controls of sediment P flux

While our research indicated that sediment P pools in addition to redox (and consequently dissolved oxygen) were important controls over sediment P release, we did not test for other factors that can influence sediment P release. Bioturbation by macroinvertebrates or fish (commonly carp) represents a well-known mechanism that can increase P flux rates significantly in freshwater bodies (Holdren and Armstrong 1980, Matisoff and Wang 1998, Chaffin and Kane 2010, Huser et al. 2016) or even help retain P in the sediments (Hupfer et al. 2019). During our incubations, sediment cores maintained under anoxic conditions for long periods experienced die-offs of a significant number of chironimids and chaoborid larvae with burrows extending beyond 10 cm deep in the sediments. This pathway likely plays a large role in Clear Lake P cycling by mobilizing or burying redox-sensitive P from deeper sediments that were previously inaccessible. Clear Lake, due to its extremely high productivity, is home to a large biomass of benthic chironomid and chaoborid species (Hunt and Bischoff 1960,

Suchanek et al. 2008) making this an important potential source of P. In addition to bioturbation, wind can also cause sediment disturbance and resuspension that lead to phosphorus releases an order of magnitude higher than in the case of undisturbed sediments in lakes thus representing another important potential P source (Søndergaard et al. 1992). This process likely represents an important P source in the case of Clear Lake due to frequent resuspension caused by its shallow basin and large fetch (Rueda et al. 2003)

Another possible avenue for sediment P flux is the translocation of sediment and hypolimnetic P by vertical movement of cyanobacteria. Cyanobacteria have buoyancy control and are able to harness available P in the benthos, rise to the surface, and subsequently leak or senesce—releasing available P into the photic zone (Cottingham et al. 2015). This phenomenon has been documented with both *Aphanizomenon* (Osgood 1988, Barbiero and Welch 1992, Barbiero and Kann 1994) and *Microcystis* (Xie et al. 2003), both of which occur in high abundance in Clear Lake (Richerson et al. 1994). This potential source can result in significant increases in internal P loads to hypereutrophic lakes (Xie et al. 2003), but remains unmeasured in Clear Lake.

Implications of depth of active P exchange

Profiles of sediment iron and aluminum-bound P, an abundant redox sensitive form of P (Lukkari et al. 2007) that drives the bulk internal P loads in Clear Lake (Richerson et al. 1994), reveal that active P exchange with the overlying water column occurs down to a an average depth of 5.6 cm among the 6 sites tested in November 2019 (Fig. 2.7). This is approximately half the 10 cm active sediment layer assumed in previous studies of Clear Lake (Richerson et al. 1994). While this finding suggests the pool of available sediment P is smaller than previously assumed, it only represents the depth of short term P fluxes that occurred in the sediments. It is likely that wind-driven processes in Clear Lake periodically resuspend sediments (Rueda et al. 2003), exposing previously buried sediment layers to the water column and making more P available for exchange to the water column during anoxic events. This

complicates efforts to estimate the size of sediment P pools and the time to recovery of the system as managers seek interventions to curb internal nutrient loads.

Conclusions

We found little variability in P flux rates between incubations performed in November 2019 and August 2020 at 15.2°C and 23°C respectively, suggesting that summer drawdown of redox-sensitive sediment P led to reduced summer P flux rates. Seasonal phenology in sediment P pools can have strong influences on sediment P flux, and should be considered in addition to other variables such as pH, temperature, and redox. Characterizing seasonal patterns in P flux is important for estimating annual internal P loads to a lake, and we found using temperature to scale observations from single experiment alone can lead to inaccurate P flux estimates. Therefore it is necessary to use repeated measurements of P flux rates and sediment P content during different seasons to estimate sediment P fluxes. We also found it important to address spatial variation in nutrient flux experiments as sites in this study varied significantly between each of the lakes three basins. In all, Clear Lake's hypereutrophy is driven by high levels of internal P loads from sediments, despite these sources being largely ignored during the establishment of phosphorus TMDLs. We highlight the importance of measuring internal nutrient sources—especially within a seasonal context—before developing restoration strategies for impaired lakes.

Literature Cited

Abe, S.-I., K. Uchida, T. Nagumo, and J. Tanaka. 2007. Alterations in the biomass-specific productivity of periphyton assemblages mediated by fish grazing. Freshwater Biology 52:1486–1493.

Allgeier, R. J., W. H. Peterson, C. Juday, and E. A. Birge. 1932. The Anaerobic Fermentation of Lake deposits. Internationale Revue der gesamten Hydrobiologie und Hydrographie 26:444–461.

Aloi, J. E. 1986. Ecology and primary productivity of the eulittoral epilithon community: Lake Tahoe, California-Nevada. California Univ.

Andersen, J. M. 1975. Influence of pH on release of phosphorus from lake sediments. Arch. Hydrobiol 76:411–419.

Anderson, S. I., G. Franzè, J. D. Kling, P. Wilburn, C. T. Kremer, S. Menden-Deuer, E. Litchman, D. A. Hutchins, and T. A. Rynearson. 2022. The interactive effects of temperature and nutrients on a spring phytoplankton community. Limnology and Oceanography 67:634–645.

Arrhenius, S. 1889. Über die Reaktionsgeschwindigkeit bei der Inversion von Rohrzucker durch Säuren. Zeitschrift für Physikalische Chemie 4U:226–248.

Atkins, K. S., S. H. Hackley, B. C. Allen, S. Watanabe, J. E. Reuter, and S. G. Schladow. 2021. Variability in periphyton community and biomass over 37 years in Lake Tahoe (CA-NV). Hydrobiologia 848:1755–1772.

Auer, M. T., N. A. Johnson, M. R. Penn, and S. W. Effler. 1993. Measurement and verification of rates of sediment phosphorus release for a hypereutrophic urban lake. Hydrobiologia 253:301–309.

Barbiero, R. P., and J. Kann. 1994. The importance of benthic recruitment to the population development of Aphanizomenon flos-aquae and internal loading in a shallow lake. Journal of Plankton Research 16:1581–1588.

Barbiero, R. P., and E. Welch. 1992. Contribution of benthic blue-green algal recruitment to lake populations and phosphorus translocation 27:249--260.

Beardall, J., E. Young, and S. Roberts. 2001. Approaches for determining phytoplankton nutrient limitation. Aquatic Sciences 63:44–69.

Berg, N., and A. Hall. 2017. Anthropogenic warming impacts on California snowpack during drought. Geophysical Research Letters 44:2511–2518.

Bernhardt, E. S., and G. E. Likens. 2004. Controls on periphyton biomass in heterotrophic streams. Freshwater Biology 49:14–27.

Beutel, M., B. Fuhrmann, G. Herbon, A. Chow, S. Brower, and J. Pasek. 2020. Cycling of methylmercury and other redox-sensitive compounds in the profundal zone of a hypereutrophic water supply reservoir. Hydrobiologia 847:4425–4446.

Beutel, M. W. 2000. Dynamics and control of nutrient, metal and oxygen fluxes at the profundal sediment -water interface of lakes and reservoirs. Ph.D., University of California, Berkeley, United States -- California.

Beutel, M. W. 2006. Inhibition of ammonia release from anoxic profundal sediments in lakes using hypolimnetic oxygenation. Ecological Engineering 28:271–279.

Beutel, M. W., and A. J. Horne. 2018. Nutrient Fluxes From Profundal Sediment of Ultra-Oligotrophic Lake Tahoe, California/Nevada: Implications for Water Quality and Management in a Changing Climate. Water Resources Research 54:1549–1559.

Biggs, B. J. F., and M. E. Close. 1989. Periphyton biomass dynamics in gravel bed rivers: the relative effects of flows and nutrients. Freshwater Biology 22:209–231.

Biggs, B. J., and C. Kilroy. 2000. Stream periphyton monitoring manual. NIWA, Christchurch, N.Z.

Birch, D. G., I. R. Elrifi, and D. H. Turpin. 1986. Nitrate and Ammonium Induced Photosynthetic Suppression in N-Limited Selenastrum minutum 1: II. Effects of NO_3^- and NH_4^+ Addition to CO_2 Efflux in the Light. Plant Physiology 82:708–712.

Blumenshine, S. C., Y. Vadeboncoeur, D. M. Lodge, K. L. Cottingham, and S. E. Knight. 1997. Benthic-Pelagic Links: Responses of Benthos to Water-Column Nutrient Enrichment. Journal of the North American Benthological Society 16:466–479.

Brothers, S. M., S. Hilt, S. Meyer, and J. Köhler. 2013. Plant community structure determines primary productivity in shallow, eutrophic lakes. Freshwater Biology 58:2264–2276.

Cantonati, M., D. Metzeltin, N. Soninkhishig, and H. Lange-Bertalot. 2016. Unusual occurrence of a Didymosphenia bloom in a lentic habitat: Observation of Didymosphenia laticollis blooming on the eastern shore of Lake Hövsgöl (Mongolia). Phytotaxa 263:139–146.

Cao, Y., S. Olsen, M. F. Gutierrez, S. Brucet, T. A. Davidson, W. Li, T. L. Lauridsen, M. Søndergaard, and E. Jeppesen. 2017. Temperature effects on periphyton, epiphyton and epipelon under a nitrogen pulse in low-nutrient experimental freshwater lakes. Hydrobiologia 795:267–279.

Caraco, N. F., J. J. Cole, and G. E. Likens. 1989. Evidence for sulphate-controlled phosphorus release from sediments of aquatic systems. Nature 341:316–318.

Carter, L. D., and A. R. Dzialowski. 2012. Predicting sediment phosphorus release rates using landuse and water-quality data. Freshwater Science 31:1214–1222.

Cattaneo, A., and J. Kalff. 1980. The relative contribution of aquatic macrophytes and their epiphytes to the production of macrophyte beds1. Limnology and Oceanography 25:280–289.

Chaffin, J. D., and D. D. Kane. 2010. Burrowing mayfly (Ephemeroptera: Ephemeridae: Hexagenia spp.) bioturbation and bioirrigation: A source of internal phosphorus loading in Lake Erie. Journal of Great Lakes Research 36:57–63.

Cisneros, J., B.E., T. Oki, N. W. Arnell, G. Benito, J. G. Cogley, P. Döll, T. Jiang, and S. S. Mwakalila. 2014. Freshwater Resources. In: Climate Change 2014: Impacts, Adaptation, and Vulnerability. Part A: Global and Sectoral Aspects. Contribution of Working Group II to the Fifth Assessment Report of the Intergovernmental Panel on Climate Change [Field, C.B., V.R. Barros, D.J. Dokken, K.J. Mach, M.D. Mastrandrea, T.E. Bilir, M. Chatterjee, K.L. Ebi, Y.O. Estrada, R.C. Genova, B. Girma, E.S. Kissel, A.N. Levy, S. MacCracken, P.R. Mastrandrea, and L.L.White (eds.)]. Cambridge University Press, Cambridge, United Kingdom and New York, NY, USA:229–269.

Clarkson, D. T., M. J. Earnshaw, P. J. White, and H. D. Cooper. 1988. Temperature dependent factors influencing nutrient uptake: an analysis of responses at different levels of organization. Symposia of the Society for Experimental Biology 42:281–309.

Cole, J. J., Y. T. Prairie, N. F. Caraco, W. H. McDowell, L. J. Tranvik, R. G. Striegl, C. M. Duarte, P. Kortelainen, J. A. Downing, J. J. Middelburg, and J. Melack. 2007. Plumbing the Global Carbon Cycle: Integrating Inland Waters into the Terrestrial Carbon Budget. Ecosystems 10:172–185.

Cottingham, K. L., H. A. Ewing, M. L. Greer, C. C. Carey, and K. C. Weathers. 2015. Cyanobacteria as biological drivers of lake nitrogen and phosphorus cycling. Ecosphere 6:art1.

Cross, W. F., J. M. Hood, J. P. Benstead, A. D. Huryn, and D. Nelson. 2015. Interactions between temperature and nutrients across levels of ecological organization. Global Change Biology 21:1025–1040.

Crowe, S. A., A. H. Treusch, M. Forth, J. Li, C. Magen, D. E. Canfield, B. Thamdrup, and S. Katsev. 2017. Novel anammox bacteria and nitrogen loss from Lake Superior. Scientific Reports 7:13757.

Cyr, H., S. K. McCabe, and G. K. Nürnberg. 2009. Phosphorus sorption experiments and the potential for internal phosphorus loading in littoral areas of a stratified lake. Water Research 43:1654–1666.

D'Angelo, E. M., and K. R. Reddy. 1993. Ammonium Oxidation and Nitrate Reduction in Sediments of a Hypereutrophic Lake. Soil Science Society of America Journal 57:1156–1163.

Demars, B. O. l., J. Russell Manson, J. S. Ólafsson, G. M. Gíslason, R. Gudmundsdóttir, G. Woodward, J. Reiss, D. E. Pichler, J. J. Rasmussen, and N. Friberg. 2011. Temperature and the metabolic balance of streams. Freshwater Biology 56:1106–1121.

Dortch, Q. 1990. The interaction between ammonium and nitrate uptake in phytoplankton. Marine Ecology Progress Series 61:183–201.

Dugdale, R. C., F. P. Wilkerson, V. E. Hogue, and A. Marchi. 2007. The role of ammonium and nitrate in spring bloom development in San Francisco Bay. Estuarine, Coastal and Shelf Science 73:17–29.

Einsele, W. 1936. Über die Beziehungen des Eisenkreislaufs zum Phosphatkreislauf im eutrophen See. Archiv für Hydrobiologie 29:664–686.

Elrifi, I. R., and D. H. Turpin. 1987. Short-term physiological indicators of N deficiency in phytoplankton: a unifying model. Marine Biology 96:425–432.

Elser, J. J., M. E. S. Bracken, E. E. Cleland, D. S. Gruner, W. S. Harpole, H. Hillebrand, J. T. Ngai, E. W. Seabloom, J. B. Shurin, and J. E. Smith. 2007. Global analysis of nitrogen and phosphorus limitation of primary producers in freshwater, marine and terrestrial ecosystems. Ecology Letters 10:1135–1142.

Elser, J. J., E. R. Marzolf, and C. R. Goldman. 1990. Phosphorus and Nitrogen Limitation of Phytoplankton Growth in the Freshwaters of North America: A Review and Critique of Experimental Enrichments. Canadian Journal of Fisheries and Aquatic Sciences 47:1468–1477.

Feyrer, F., M. Young, O. Patton, and D. Ayers. 2020. Dissolved oxygen controls summer habitat of Clear Lake Hitch (Lavinia exilicauda chi), an imperilled potamodromous cyprinid. Ecology of Freshwater Fish 29:188–196.

Fishman, M., and L. Friedman. 1989. Methods for Determination of Inorganic Substances in Water and Fluvial Sediments. https://books.google.com/books?hl=en&lr=&id=3ojAFWxH0GkC&oi=fnd&pg=PA1&dq=Methods+for+the+Determination+of+Inorganic+Substances+in+Water+and+Fluvial+Sediments&ots=K6pEbY_fsq&sig=Gh4BP_B1wsCfTFxStgOpUlClMKI#v=onepage&q=Methods%20for%20the%20Determination%20of%20Inorganic%20Substances%20in%20Water%20and%20Fluvial%20Sediments&f=false.

Flint, R. W., and C. R. Goldman. 1975. The effects of a benthic grazer on the primary productivity of the littoral zone of Lake Tahoe1. Limnology and Oceanography 20:935–944.

Gibbons, K. J., and T. B. Bridgeman. 2020. Effect of temperature on phosphorus flux from anoxic western Lake Erie sediments. Water Research 182:116022.

Gillooly, J. F., J. H. Brown, G. B. West, V. M. Savage, and E. L. Charnov. 2001. Effects of Size and Temperature on Metabolic Rate. Science 293:2248–2251.

Goldman, C. R. 1988. Primary productivity, nutrients, and transparency during the early onset of eutrophication in ultra-oligotrophic Lake Tahoe, Califomia-Nevada1. Limnology and Oceanography 33:1321–1333.

Goldman, C. R., and A. J. Horne. 1983. Limnology. McGraw-Hill.

Goldman, C. R., and R. G. Wetzel. 1963. A Study of the Primary Productitivy of Clear Lake, Lake County California. Ecology 44:283–294.

Hansen, L. S., and T. H. Blackburn. 1991. Aerobic and anaerobic mineralization of organic material in marine sediment microcosms. Marine Ecology Progress Series 75:283–291.

Hargrave, B. T. 1969. Similarity of Oxygen Uptake by Benthic Communities. Limnology and Oceanography 14:801–805.

Hauck, S., M. Benz, A. Brune, and B. Schink. 2001. Ferrous iron oxidation by denitrifying bacteria in profundal sediments of a deep lake (Lake Constance). FEMS Microbiology Ecology 37:127–134.

Hawes, I., and R. Smith. 1994. Seasonal dynamics of epilithic periphyton in oligotrophic Lake Taupo, New Zealand. New Zealand Journal of Marine and Freshwater Research 28:1–12.

Hay, M. E. 1981. The Functional Morphology of Turf-Forming Seaweeds: Persistence in Stressful Marine Habitats. Ecology 62:739–750.

Healey, F. P. 1973. Inorganic Nutrient Uptake and Deficiency in Algae. CRC Critical Reviews in Microbiology 3:69–113.

Healey, F. P. 1979. Short-Term Responses of Nutrient-Deficient Algae to Nutrient Addition1. Journal of Phycology 15:289–299.

Hecky, R. E., and R. H. Hesslein. 1995. Contributions of Benthic Algae to Lake Food Webs as Revealed by Stable Isotope Analysis. Journal of the North American Benthological Society 14:631–653.

Hecky, R. E., and P. Kilham. 1988. Nutrient limitation of phytoplankton in freshwater and marine environments: A review of recent evidence on the effects of enrichment1. Limnology and Oceanography 33:796–822.

Hieltjes, A. H. M., and L. Lijklema. 1980. Fractionation of Inorganic Phosphates in Calcareous Sediments. Journal of Environmental Quality 9:405–407.

Higgins, S. N., S. Y. Malkin, E. Todd Howell, S. J. Guildford, L. Campbell, V. Hiriart-Baer, and R. E. Hecky. 2008. An Ecological Review of Cladophora Glomerata (chlorophyta) in the Laurentian Great Lakes1. Journal of Phycology 44:839–854.

Higley, H. J. Carrick, M. T. Brett, C. Luecke, and C. R. Goldman. 2001. The effects of ultraviolet radiation and nutrient additions on periphyton biomass and composition in a sub-alpine lake (Castle Lake, USA). International Review of Hydrobiology 86:147–163.

Holdren, G. C., and D. E. Armstrong. 1980. Factors affecting phosphorus release from intact lake sediment cores. Environmental Science & Technology 14:79–87.

Hood, J. M., J. P. Benstead, W. F. Cross, A. D. Huryn, P. W. Johnson, G. M. Gíslason, J. R. Junker, D. Nelson, J. S. Ólafsson, and C. Tran. 2018. Increased resource use efficiency amplifies positive response of aquatic primary production to experimental warming. Global Change Biology 24:1069–1084.

Horne, A. J. 1975. The ecology of Clear Lake phytoplankton. Clear Lake Algal Research Unit, Lakeport, Calif.

Horne, A. J., and C. R. Goldman. 1972. Nitrogen Fixation in Clear Lake, California. I. Seasonal Variation and the Role of Heterocysts. Limnology and Oceanography 17:678–692.

Hunt, E. G., and A. I. Bischoff. 1960. Inimical effects on wildlife of periodic DDD applications to Clear Lake 46:91.

Hupfer, M., S. Jordan, C. Herzog, C. Ebeling, R. Ladwig, M. Rothe, and J. Lewandowski. 2019. Chironomid larvae enhance phosphorus burial in lake sediments: Insights from long-term and short-term experiments. Science of The Total Environment 663:254–264.

Huser, B. J., P. G. Bajer, C. J. Chizinski, and P. W. Sorensen. 2016. Effects of common carp (Cyprinus carpio) on sediment mixing depth and mobile phosphorus mass in the active sediment layer of a shallow lake. Hydrobiologia 763:23–33.

Hyacinthe, C., and P. Van Cappellen. 2004. An authigenic iron phosphate phase in estuarine sediments: composition, formation and chemical reactivity. Marine Chemistry 91:227–251.

Hyne, N. J., P. Chelminski, J. E. Court, D. S. Gorsline, and C. R. Goldman. 1972. Quaternary History of Lake Tahoe, California-Nevada. GSA Bulletin 83:1435–1448.

IPCC. 2013. Climate Change 2013: The Physical Science Basis. Contribution of Working Group I to the Fifth Assessment Report of the Intergovernmental Panel on Climate Change. Cambridge University Press, Cambridge, United Kingdom and New York, NY, USA.

Jacoby, J. M., D. D. Bouchard, and C. R. Patmont. 1991. Response of Periphyton to Nutrient Enrichment in Lake Chelan, WA. Lake and Reservoir Management 7:33–43.

Jassby, A. D., C. R. Goldman, J. E. Reuter, and R. C. Richards. 1999. Origins and scale dependence of temporal variability in the transparency of Lake Tahoe, California–Nevada. Limnology and Oceanography 44:282–294.

Jensen, H. S., and F. O. Andersen. 1992. Importance of temperature, nitrate, and pH for phosphate release from aerobic sediments of four shallow, eutrophic lakes. Limnology and Oceanography 37:577–589.

Johnson, F. H., S. Johnson, H. Eyring, and B. J. Stover. 1974. The Theory of Rate Processes in Biology and Medicine. Wiley.

Jones, J. G., S. Gardener, and B. M. Simon. 1983. Bacterial Reduction of Ferric Iron in a Stratified Eutrophic Lake. Microbiology, 129:131–139.

Kamphake, L. J., S. A. Hannah, and J. M. Cohen. 1967. Automated analysis for nitrate by hydrazine reduction. Water Research 1:205–216.

Kennard, R. A. 2021. Safe and Affordable Drinking Water for Sources Impaired by Harmful Algal Blooms: Clear Lake, California. UC Davis.

Koski-Vähälä, J., and H. Hartikainen. 2001. Assessment of the Risk of Phosphorus Loading Due to Resuspended Sediment. Journal of Environmental Quality 30:960–966.

Kravtsova, L. S., L. A. Izhboldina, I. V. Khanaev, G. V. Pomazkina, E. V. Rodionova, V. M. Domysheva, M. V. Sakirko, I. V. Tomberg, T. Ya. Kostornova, O. S. Kravchenko, and A. B. Kupchinsky. 2014. Nearshore benthic blooms of filamentous green algae in Lake Baikal. Journal of Great Lakes Research 40:441–448.

Lake County Water Resources Department. 2017. Sediment Nitrogen and Phosphorus Monitoring.

Lean, D. R. S., and F. R. Pick. 1981. Photosynthetic response of lake plankton to nutrient enrichment: A test for nutrient limitation. Limnology and Oceanography 26:1001–1019.

Lemley, D. A., J. B. Adams, and J. L. Largier. 2021. Harmful algal blooms as a sink for inorganic nutrients in a eutrophic estuary. Marine Ecology Progress Series 663:63–76.

Lenth, R. V., P. Buerkner, M. Herve, J. Love, F. Miguez, H. Riebl, and H. Singmann. 2022, March 27. emmeans: Estimated Marginal Means, aka Least-Squares Means.

Liddicoat, M. I., S. Tibhitts, and E. I. Butler. 1975. The determination of ammonia in seawater. Limnology and Oceanography 20:131–132.

Liikanen, A., T. Murtoniemi, H. Tanskanen, T. Väisänen, and P. J. Martikainen. 2002. Effects of temperature and oxygenavailability on greenhouse gas and nutrient dynamics in sediment of a eutrophic mid-boreal lake. Biogeochemistry 59:269–286.

Lindeman, R. L. 1942. The Trophic-Dynamic Aspect of Ecology. Ecology 23:399–417.

Loeb, S. L. 1980. The Production of the Epilithic Periphyton Community in Lake Tahoe.

Loeb, S. L. 1987. Groundwater Quality within the Tahoe Basin, Institute of Ecology. Groundwater Quality Within the Tahoe Basin University of California.

Loeb, S. L., J. E. Reuter, and C. R. Goldman. 1983. Littoral zone production of oligotrophic lakes. Pages 161–167 *in* R. G. Wetzel, editor. Periphyton of Freshwater Ecosystems. Springer Netherlands, Dordrecht.

Loh, P. S., L. A. Molot, E. Nowak, G. K. Nürnberg, S. B. Watson, and B. Ginn. 2013. Evaluating relationships between sediment chemistry and anoxic phosphorus and iron release across three different water bodies: Inland Waters: Vol 3, No 1. https://www.tandfonline.com/doi/abs/10.5268/IW-3.1.533.

van Luijn, F., P. C. M. Boers, L. Lijklema, and J.-P. R. A. Sweerts. 1999. Nitrogen fluxes and processes in sandy and muddy sediments from a shallow eutrophic lake. Water Research 33:33–42.

Lukkari, K., H. Hartikainen, and M. Leivuori. 2007. Fractionation of sediment phosphorus revisited. I: Fractionation steps and their biogeochemical basis. Limnology and Oceanography: Methods 5:433–444.

Matisoff, G., and X. Wang. 1998. Solute transport in sediments by freshwater infaunal bioirrigators. Limnology and Oceanography 43:1487–1499.

Matthews, D. A., D. B. Babcock, J. G. Nolan, A. R. Prestigiacomo, S. W. Effler, C. T. Driscoll, S. G. Todorova, and K. M. Kuhr. 2013. Whole-lake nitrate addition for control of methylmercury in mercury-contaminated Onondaga Lake, NY. Environmental Research 125:52–60.

Mazumder, A., W. D. Taylor, D. J. McQueen, and D. R. S. Lean. 1989. Effects of nutrients and grazers on periphyton phosphorus in lake enclosures. Freshwater Biology 22:405–415.

McCormick, P. V., R. B. E. Shuford III, J. G. Backus, and W. C. Kennedy. 1997. Spatial and seasonal patterns of periphyton biomass and productivity in the northern Everglades, Florida, U.S.A. Hydrobiologia 362:185–210.

McCulloch, J., A. Gudimov, G. Arhonditsis, A. Chesnyuk, and M. Dittrich. 2013. Dynamics of P-binding forms in sediments of a mesotrophic hard-water lake: Insights from non-steady state reactive-transport modeling, sensitivity and identifiability analysis. Chemical Geology 354:216–232.

McCullough, I. M., K. S. Cheruvelil, S. M. Collins, and P. A. Soranno. 2019. Geographic patterns of the climate sensitivity of lakes. Ecological Applications 29:e01836.

Melack, J. M., S. Sadro, J. O. Sickman, and J. Dozier. 2020. Lakes and Watersheds in the Sierra Nevada of California: Responses to Environmental Change. Univ of California Press.

Melton, E. D., C. Schmidt, and A. Kappler. 2012. Microbial Iron(II) Oxidation in Littoral Freshwater Lake Sediment: The Potential for Competition between Phototrophic vs. Nitrate-Reducing Iron(II)-Oxidizers. Frontiers in Microbiology 3.

Moore Jr., P. A., K. R. Reddy, and D. A. Graetz. 1992. Nutrient Transformations in Sediments as Influenced by Oxygen Supply. Journal of Environmental Quality 21:387–393.

Mortimer, C. H. 1941. The Exchange of Dissolved Substances Between Mud and Water in Lakes. Journal of Ecology 29:280–329.

Mortimer, C. H. 1942. The Exchange of Dissolved Substances between Mud and Water in Lakes. Journal of Ecology 30:147–201.

Mountain Research Initiative Edw Working Group, N. Pepin, R. S. Bradley, H. F. Diaz, M. Baraer, E. B. Caceres, N. Forsythe, H. Fowler, G. Greenwood, M. Z. Hashmi, X. D. Liu, J. R. Miller, L. Ning, A. Ohmura, E. Palazzi, I. Rangwala, W. Schöner, I. Severskiy, M. Shahgedanova, M. B. Wang, S. N.

Williamson, and D. Q. Yang. 2015. Elevation-dependent warming in mountain regions of the world. Nature Climate Change 5:424–430.

Mulholland, P. J., A. D. Steinman, A. V. Palumbo, J. W. Elwood, and D. B. Kirschtel. 1991. Role of Nutrient Cycling and Herbivory in Regulating Periphyton Communities in Laboratory Streams. Ecology 72:966–982.

Murphy, J., and J. P. Riley. 1962. A modified single solution method for the determination of phosphate in natural waters. Analytica Chimica Acta 27:31–36.

Naranjo, R. C., R. G. Niswonger, D. Smith, D. Rosenberry, and S. Chandra. 2019. Linkages between hydrology and seasonal variations of nutrients and periphyton in a large oligotrophic subalpine lake. Journal of Hydrology 568:877–890.

Nõges, P., T. Nõges, M. Ghiani, F. Sena, R. Fresner, M. Friedl, and J. Mildner. 2011a. Increased nutrient loading and rapid changes in phytoplankton expected with climate change in stratified South European lakes: sensitivity of lakes with different trophic state and catchment properties. Hydrobiologia 667:255–270.

Nõges, P., T. Nõges, M. Ghiani, F. Sena, R. Fresner, M. Friedl, and J. Mildner. 2011b. Increased nutrient loading and rapid changes in phytoplankton expected with climate change in stratified South European lakes: sensitivity of lakes with different trophic state and catchment properties. Hydrobiologia 667:255–270.

Nürnberg, G. 1997. Coping with Water Quality Problems due to Hypolimnetic Anoxia in Central Ontario Lakes. Water Quality Research Journal 32:391–405.

Nürnberg, G. K. 2009. Assessing internal phosphorus load – Problems to be solved. Lake and Reservoir Management 25:419–432.

Nürnberg, G. K., B. D. LaZerte, P. S. Loh, and L. A. Molot. 2013. Quantification of internal phosphorus load in large, partially polymictic and mesotrophic Lake Simcoe, Ontario. Journal of Great Lakes Research 39:271–279.

Oleksy, I. A., J. S. Baron, and W. S. Beck. 2020. Nutrients and warming alter mountain lake benthic algal structure and function. Freshwater Science 40:88–102.

Orihel, D. M., H. M. Baulch, N. J. Casson, R. L. North, C. T. Parsons, D. C. M. Seckar, and J. J. Venkiteswaran. 2017. Internal phosphorus loading in Canadian fresh waters: a critical review and data analysis. Canadian Journal of Fisheries and Aquatic Sciences 74:2005–2029.

Osaka, K., R. Yokoyama, T. Ishibashi, and N. Goto. 2022. Effect of dissolved oxygen on nitrogen and phosphorus fluxes from lake sediments and their thresholds based on incubation using a simple and stable dissolved oxygen control method. Limnology and Oceanography: Methods 20:1–14.

Osgood, R. A. 1988. A hypothesis on the role of Aphanizomenon in translocating phosphorus. Hydrobiologia 169:69–76.

Ozersky, T., E. A. Volkova, N. A. Bondarenko, O. A. Timoshkin, V. V. Malnik, V. M. Domysheva, and S. E. Hampton. 2018. Nutrient limitation of benthic algae in Lake Baikal, Russia. Freshwater Science 37:472–482.

Parsons, C., F. Rezanezhad, D. W. O'Connell, and P. van Cappellen. 2017. Sediment phosphorus speciation and mobility under dynamic redox conditions.

Penn, M. R., M. T. Auer, S. M. Doerr, C. T. Driscoll, C. M. Brooks, and S. W. Effler. 2000. Seasonality in phosphorus release rates from the sediments of a hypereutrophic lake under a matrix of pH and redox conditions. Canadian Journal of Fisheries and Aquatic Sciences 57:1033–1041.

Pepin, N. C., E. Arnone, A. Gobiet, K. Haslinger, S. Kotlarski, C. Notarnicola, E. Palazzi, P. Seibert, S. Serafin, W. Schöner, S. Terzago, J. M. Thornton, M. Vuille, and C. Adler. 2022. Climate Changes

and Their Elevational Patterns in the Mountains of the World. Reviews of Geophysics 60:e2020RG000730.

Phinney, H. K., and C. D. McIntire. 1965. Effect of Temperature on Metabolism of Periphyton Communities Developed in Laboratory Streams1. Limnology and Oceanography 10:341–345.

Pinheiro, J., D. Bates, S. DebRoy, D. Sarkar, and R Core Team. 2020. _nlme: Linear and Nonlinear Mixed Effects Models_. R package version 3.1-150, <URL: https://CRAN.R-project.org/package=nlme>.

Pinheiro, J., D. Bates, and R Core Team. 2022, March 25. nlme: Linear and Nonlinear Mixed Effects Models.

Power, M. E., A. J. Stewart, and W. J. Matthews. 1988. Grazer Control of Algae in an Ozark Mountain Stream: Effects of Short-Term Exclusion. Ecology 69:1894–1898.

Quinn, P. J. 1988. Effects of temperature on cell membranes. Symposia of the Society for Experimental Biology 42:237–258.

R Core Team. 2020. R: A language and environment for statistical computing. R Foundation for Statistical Computing, Vienna, Austria. URL https://www.R-project.org/.

Reay, D. S., D. B. Nedwell, J. Priddle, and J. C. Ellis-Evans. 1999. Temperature Dependence of Inorganic Nitrogen Uptake: Reduced Affinity for Nitrate at Suboptimal Temperatures in Both Algae and Bacteria. Applied and Environmental Microbiology 65:2577–2584.

Reuter, J. E., S. L. Loeb, and C. R. Goldman. 1986. Inorganic nitrogen uptake by epilithic periphyton in a N-deficient lake1. Limnology and Oceanography 31:149–160.

Rhee, G.-Y., and I. J. Gotham. 1981. The effect of environmental factors on phytoplankton growth: Temperature and the interactions of temperature with nutrient limitation1. Limnology and Oceanography 26:635–648.

Richerson, P., T. H. Suchanek, R. A. Zierenberg, D. A. Osleger, A. C. Heyvaert, D. G. Slotton, C. A. Eagles-Smith, and C. E. Vaughn. 2008. Anthropogenic Stressors and Changes in the Clear Lake Ecosystem as Recorded in Sediment Cores. Ecological Applications 18:A257–A283.

Richerson, P., T. Suchanek, and W. Steven. 1994. The Causes And Control of Algal Blooms in Clear Lake. University of California Davis.

Roberts, D. C., P. Moreno-Casas, F. A. Bombardelli, S. J. Hook, B. R. Hargreaves, and S. G. Schladow. 2019. Predicting Wave-Induced Sediment Resuspension at the Perimeter of Lakes Using a Steady-State Spectral Wave Model. Water Resources Research 55:1279–1295.

Roden, E. E., and J. W. Edmonds. 1997. Phosphate mobilization in iron-rich anaerobic sediments : microbial Fe(III) oxide reduction versus iron-sulfide formation. Phosphate mobilization in iron-rich anaerobic sediments : microbial Fe(III) oxide reduction versus iron-sulfide formation 139:347–378.

Roldán, R., V. Barrón, and J. Torrent. 2002. Experimental alteration of vivianite to lepidocrocite in a calcareous medium. Clay Minerals 37:709–718.

Rosa, J., V. Ferreira, C. Canhoto, and M. A. S. Graça. 2013. Combined effects of water temperature and nutrients concentration on periphyton respiration – implications of global change. International Review of Hydrobiology 98:14–23.

Rueda, F. J., and G. S. Schladow. 2003. Dynamics of Large Polymictic Lake. II: Numerical Simulations. Journal of Hydraulic Engineering 129:92–101.

Rueda, F. J., G. S. Schladow, S. G. Monismith, and M. T. Stacey. 2003. Dynamics of Large Polymictic Lake. I: Field Observations. Journal of Hydraulic Engineering 129:82–91.

Ruley, J. E., and K. A. Rusch. 2004. Development of a simplified phosphorus management model for a shallow, subtropical, urban hypereutrophic lake. Ecological Engineering 22:77–98.

Sadro, S., J. M. Melack, J. O. Sickman, and K. Skeen. 2019. Climate warming response of mountain lakes affected by variations in snow. Limnology and Oceanography Letters 4:9–17.

Schindler, D. W., F. A. J. Armstrong, S. K. Holmgren, and G. J. Brunskill. 1971. Eutrophication of Lake 227, Experimental Lakes Area, Northwestern Ontario, by Addition of Phosphate and Nitrate. Journal of the Fisheries Research Board of Canada 28:1763–1782.

Schubert, C. J., E. Durisch-Kaiser, B. Wehrli, B. Thamdrup, P. Lam, and M. M. M. Kuypers. 2006. Anaerobic ammonium oxidation in a tropical freshwater system (Lake Tanganyika). Environmental Microbiology 8:1857–1863.

Solórzano, L. 1969. DETERMINATION OF AMMONIA IN NATURAL WATERS BY THE PHENOLHYPOCHLORITE METHOD 1 1 This research was fully supported by U.S. Atomic Energy Commission Contract No. ATS (11-1) GEN 10, P.A. 20. Limnology and Oceanography 14:799–801.

Solórzano, L., and J. H. Sharp. 1980. Determination of total dissolved phosphorus and particulate phosphorus in natural waters1. Limnology and Oceanography 25:754–758.

Søndergaard, M., R. Bjerring, and E. Jeppesen. 2013. Persistent internal phosphorus loading during summer in shallow eutrophic lakes. Hydrobiologia 710:95–107.

Søndergaard, M., J. P. Jensen, and E. Jeppesen. 2003. Role of sediment and internal loading of phosphorus in shallow lakes. Hydrobiologia 506:135–145.

Søndergaard, M., P. Kristensen, and E. Jeppesen. 1992. Phosphorus release from resuspended sediment in the shallow and wind-exposed Lake Arresø, Denmark. Hydrobiologia 228:91–99.

Song, J., Y. M. Luo, Q. G. Zhao, and P. Christie. 2003. Novel use of soil moisture samplers for studies on anaerobic ammonium fluxes across lake sediment–water interfaces. Chemosphere 50:711–715.

Spears, B. M., L. Carvalho, R. Perkins, A. Kirika, and D. M. Paterson. 2007. Sediment phosphorus cycling in a large shallow lake: spatio-temporal variation in phosphorus pools and release. Pages 37–48

in R. D. Gulati, E. Lammens, N. De Pauw, and E. Van Donk, editors. Shallow Lakes in a Changing World. Springer Netherlands, Dordrecht.

Spears, B. M., E. B. Mackay, S. Yasseri, I. D. M. Gunn, K. E. Waters, C. Andrews, S. Cole, M. De Ville, A. Kelly, S. Meis, A. L. Moore, G. K. Nürnberg, F. van Oosterhout, J.-A. Pitt, G. Madgwick, H. J. Woods, and M. Lürling. 2016. A meta-analysis of water quality and aquatic macrophyte responses in 18 lakes treated with lanthanum modified bentonite (Phoslock®). Water Research 97:111–121.

Sterner, R. W., and J. J. Elser. 2002. Ecological Stoichiometry.

Straub, K. L., M. Benz, B. Schink, and F. Widdel. 1996. Anaerobic, nitrate-dependent microbial oxidation of ferrous iron. Applied and Environmental Microbiology 62:1458–1460.

Strickland, J. D. H., and T. R. Parsons. 1972. A Practical Handbook of Seawater Analysis. https://scholar.googleusercontent.com/scholar?q=cache:w2MKn3yIK-gJ:scholar.google.com/&hl=en&as_sdt=0,5.

Suchanek, T., C. Eagles-Smith, D. G. Slotton, E. Harner, D. P. Adam, A. E. Colwell, N. L. Anderson, and D. L. Woodward. 2008. Mine-derived mercury: Effects on lower trophic species in Clear Lake, California. Ecological Applications 18(8) Supplement:A158–A176.

Sulzberger, B., D. Suter, C. Siffert, S. Banwart, and W. Stumm. 1989. Dissolution of fe(iii)(hydr)oxides in natural waters; laboratory assessment on the kinetics controlled by surface coordination. Marine Chemistry 28:127–144.

Swain, D. L., B. Langenbrunner, J. D. Neelin, and A. Hall. 2018. Increasing precipitation volatility in twenty-first-century California. Nature Climate Change 8:427–433.

TERC. 2019. Tahoe: State of the Lake Report 2019.

Tetra Tech. 2009. Clear Lake Watershed TMDL Monitoring Program. Lake County Watershed Protection District.

Thomas, M. K., M. Aranguren-Gassis, C. T. Kremer, M. R. Gould, K. Anderson, C. A. Klausmeier, and E. Litchman. 2017. Temperature–nutrient interactions exacerbate sensitivity to warming in phytoplankton. Global Change Biology 23:3269–3280.

Trochine, C., M. E. Guerrieri, L. Liboriussen, T. L. Lauridsen, and E. Jeppesen. 2014. Effects of nutrient loading, temperature regime and grazing pressure on nutrient limitation of periphyton in experimental ponds. Freshwater Biology 59:905–917.

Turner, E., and J. Roupas. 2006. Analyze Free Ammonia Before It's Too Late. Opflow 32:18–20.

US EPA, O. 2017, April. Field Measurement of Oxidation-Reduction Potential. Policies and Guidance. https://www.epa.gov/quality/field-measurement-oxidation-reduction-potential.

Vadeboncoeur, Y., M. V. Moore, S. D. Stewart, S. Chandra, K. S. Atkins, J. S. Baron, K. Bouma-Gregson, S. Brothers, S. N. Francoeur, L. Genzoli, S. N. Higgins, S. Hilt, L. R. Katona, D. Kelly, I. A. Oleksy, T. Ozersky, M. E. Power, D. Roberts, A. P. Smits, O. Timoshkin, F. Tromboni, M. J. V. Zanden, E. A. Volkova, S. Waters, S. A. Wood, and M. Yamamuro. 2021. Blue Waters, Green Bottoms: Benthic Filamentous Algal Blooms Are an Emerging Threat to Clear Lakes Worldwide. BioScience 71:1011–1027.

Vadeboncoeur, Y., and A. D. Steinman. 2002. Periphyton Function in Lake Ecosystems. Review Article. https://www.hindawi.com/journals/tswj/2002/923031/.

Vinebrooke, R. D., and P. R. Leavitt. 1996. Effects of ultraviolet radiation on periphyton in an alpine lake. Limnology and Oceanography 41:1035–1040.

Ward, N. K., B. G. Steele, K. C. Weathers, K. L. Cottingham, H. A. Ewing, P. C. Hanson, and C. C. Carey. 2020. Differential Responses of Maximum Versus Median Chlorophyll-a to Air Temperature and Nutrient Loads in an Oligotrophic Lake Over 31 Years. Water Resources Research 56:e2020WR027296.

Welch, E. B., and G. D. Cooke. 1995. Internal Phosphorus Loading in Shallow Lakes: Importance and Control. Lake and Reservoir Management 11:273–281.

Wu, Y., Y. Wen, J. Zhou, and Y. Wu. 2014. Phosphorus release from lake sediments: Effects of pH, temperature and dissolved oxygen. KSCE Journal of Civil Engineering 18:323–329.

Xie, P. 2006. Biological mechanisms driving the seasonal changes in the internal loading of phosphorus in shallow lakes. Science in China Series D 49:14–27.

Xie, P. Q., P. Xie, and H. J. Tang. 2003. Enhancement of dissolved phosphorus release from sediment to lake water by Microcystis blooms—an enclosure experiment in a hyper-eutrophic, subtropical Chinese lake 122:391--399.

Yang, Y., Y. Dai, N. Li, B. Li, S. Xie, and Y. Liu. 2017. Temporal and Spatial Dynamics of Sediment Anaerobic Ammonium Oxidation (Anammox) Bacteria in Freshwater Lakes. Microbial Ecology 73:285–295.

Yoshii, K. 1999. Stable isotope analyses of benthic organisms in Lake Baikal:15.

Yoshinaga, I., T. Amano, T. Yamagishi, K. Okada, S. Ueda, Y. Sako, and Y. Suwa. 2011. Distribution and Diversity of Anaerobic Ammonium Oxidation (Anammox) Bacteria in the Sediment of a Eutrophic Freshwater Lake, Lake Kitaura, Japan. Microbes and Environments 26:189–197.

Yvon-Durocher, G., J. I. Jones, M. Trimmer, G. Woodward, and J. M. Montoya. 2010. Warming alters the metabolic balance of ecosystems. Philosophical Transactions of the Royal Society B: Biological Sciences 365:2117–2126.

Zhu, G., S. Wang, W. Wang, Y. Wang, L. Zhou, B. Jiang, H. J. M. Op den Camp, N. Risgaard-Petersen, L. Schwark, Y. Peng, M. M. Hefting, M. S. M. Jetten, and C. Yin. 2013a. Hotspots of anaerobic ammonium oxidation at land–freshwater interfaces. Nature Geoscience 6:103–107.

Zhu, Y., D. Yuan, Y. Huang, J. Ma, and S. Feng. 2013b. A sensitive flow-batch system for on board determination of ultra-trace ammonium in seawater: Method development and shipboard application. Analytica Chimica Acta 794:47–54.

Zuur, A. F., E. N. Ieno, N. Walker, A. A. Saveliev, and G. M. Smith. 2009. Mixed effects models and extensions in ecology with R. Springer New York, New York, NY.

Appendix

Appendix A

A1: Rock surface area measurements

Our calculations are show below in equation A1 in which S represents the rock surface area in square meters, a is the radius of axis a of the rock in meters, b is the radius of axis b, and so on with c. The assumed 67% coverage of rocks by periphyton was empirically measured on rocks from the 4/7/21 experiment and are shown in table A1.

Equation A1:

$$S = 0.67 \times 4\pi \left(\frac{((ab)^{1/6} + (ac)^{1/6} + (bc)^{1/6})^{1/1.6}}{3} \right)$$

chamber	periphyton percent cover
1	50
2	60
3	NA
4	75
5	75
6	75
7	50
8	50
9	80
10	50
11	75

12	NA
13	75
14	75
15	70
16	75
Avg. Perc. Cover	66.78571

Table A1: Percent periphyton cover on rocks collected from the 4/07/2021 experiment. This average was used to calculate rock surface areas since only 67% of rocks were covered with periphyton on average.

A2: Background metabolic rate tests

Background metabolic rates of both ambient and enriched samples from the August-February experiments. Metabolic rates in these chambers correspond to residual bacterioplankton or nanoplankton that were not able to be removed by filtering to 0.45µm, were considered negligible relative to periphyton rates, and did not need to be adjusted for in the analysis.

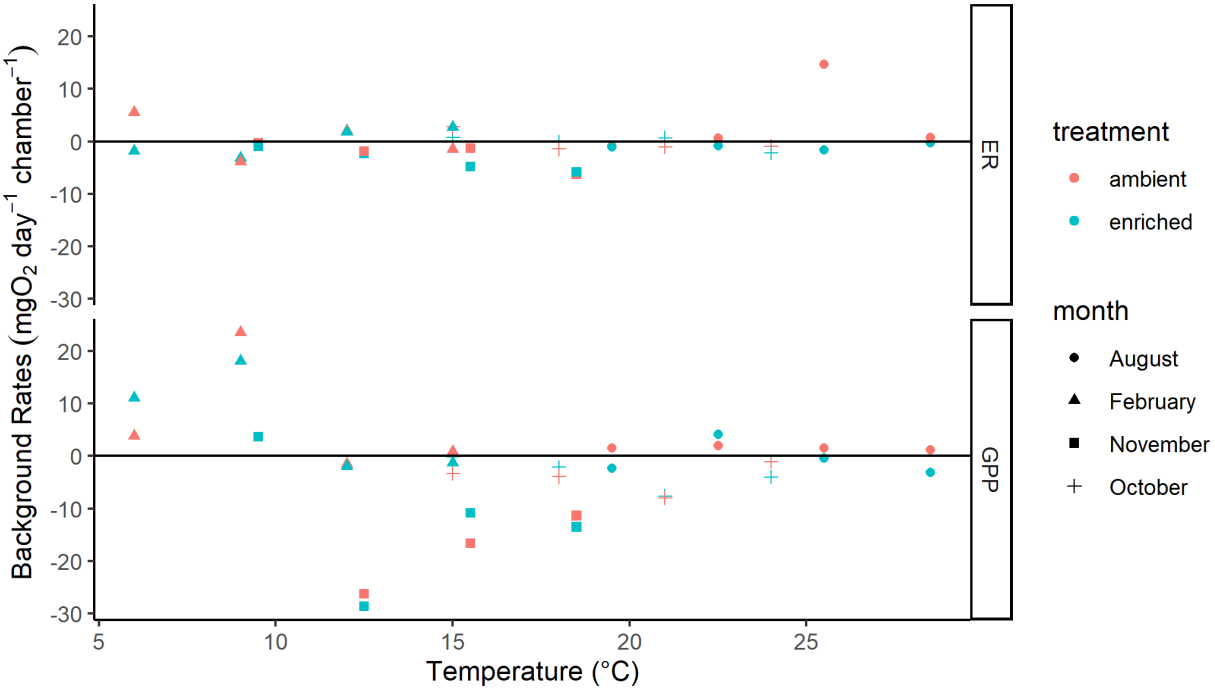

A3: Background nutrient uptake rate tests

Background nutrient uptake rates from August-February experiments measured in jars filled with incubation water only and no periphyton. Nutrient uptake rates in these chambers correspond to residual bacterioplankton or nanoplankton that were not able to be removed by filtering to 0.45µm, were considered negligible relative to periphyton rates, and did not need to be adjusted for in the analysis.

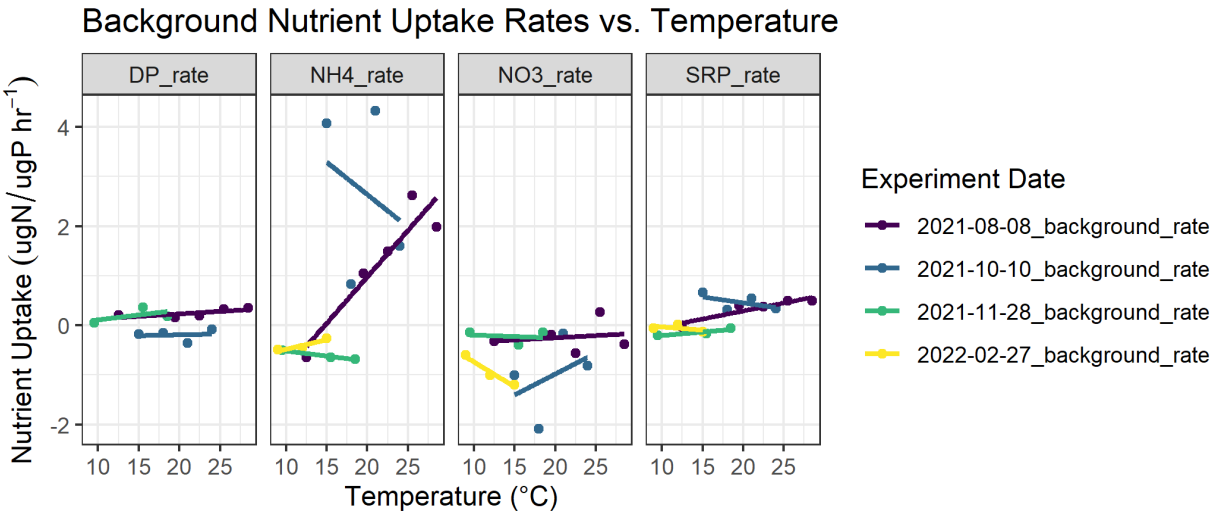

A4: Model selection

GPP models:

Predictors	Model0 Estimates	Model1 Estimates	Model2 Estimates	Model3 Estimates	Model4 Estimates
(Intercept)	-1.61 ***	-1.60 ***	-1.01 ***	-1.01 ***	-1.01 ***
temp C		0.09 ***	0.04 ***	0.03 ***	0.04 ***
nutrient on [ambient]		0.21			
month [June]		0.91			
month [August]		0.69			
month [October]		0.18			
month [November]		0.41 *			
temp C * nutrient on [ambient]		-0.01			
temp C * month [June]		0.04 *			
temp C * month [August]		-0.04			
temp C * month [October]		-0.04			
temp C * month [November]		0.04 *			
nutrient on [ambient] * month [June]		0.06			
nutrient on [ambient] * month [August]		-0.49			
nutrient on [ambient] * month [October]		-1.05			
nutrient on [ambient] * month [November]		-1.31 *			
(temp C * nutrient on [ambient]) * month [June]		0.01			
(temp C * nutrient on [ambient]) * month [August]		0.01			
(temp C * nutrient on [ambient]) * month [October]		0.04			
(temp C * nutrient on [ambient]) * month [November]		0.10 *			
nutrient on [1]			0.04	0.04	0.04
month [1]			-0.17 ***	-0.17 ***	-0.17 ***
month [2]			-0.11 **	-0.10 **	-0.06 **
month [3]			0.75 ***	0.78 ***	0.78 ***
month [4]			0.48 ***	0.49 ***	0.51 ***
temp C * nutrient on [1]			0.00	0.00	0.00
temp C * month [1]			0.04 ***	0.04 ***	0.04 ***
temp C * month [2]			0.01 ***	0.01 ***	0.01 ***
temp C * month [3]			0.01 ***	0.01 ***	0.01 ***
temp C * month [4]			0.01	0.01	0.00
nutrient on [1] * month [1]			0.04	0.04	0.04
nutrient on [1] * month [2]			-0.11	-0.11	-0.11
nutrient on [1] * month [3]			0.04	0.04	0.07
nutrient on [1] * month [4]			0.04	0.04	0.04
(temp C * nutrient on [1]) * month [1]			0.01	0.01	0.00
(temp C * nutrient on [1]) * month [2]			0.01	0.01	0.01
(temp C * nutrient on [1]) * month [3]			0.00	0.00	0.00
(temp C * nutrient on [1]) * month [4]			0.00	0.00	0.00
Random Effects					
σ^2			0.01	0.01	0.01
τ_{00}			0.06 $_{\text{mesocosm}}$	0.06 $_{\text{mesocosm}}$	0.17 $_{\text{mesocosm}}$
τ_{11}					0.00 $_{\text{mesocosm}}$ temp_C
ρ_{01}					-0.83 $_{\text{mesocosm}}$
ICC			0.89	0.88	0.93
N			78 $_{\text{mesocosm}}$	78 $_{\text{mesocosm}}$	78 $_{\text{mesocosm}}$
Observations	143	143	143	143	143
Marginal R^2 / Conditional R^2	NA	NA	0.668 / 0.963	0.661 / 0.961	0.661 / 0.971
AIC	1961.799	1957.811	1595.913	1574.987	1569.117

*p<0.05 **p<0.01 ***p<0.001

ER Models:

Predictors	Model0 Estimates	Model1 Estimates	Model2 Estimates	Model3 Estimates
(Intercept)	3.08***	2.83***	3.04***	3.04***
temp.C		0.04**	0.03***	0.03***
nutrient.ox [ambient]		-0.40		
month [june]		1.11*		
month [august]		0.16		
month [october]		-0.08		
month [november]		0.56		
temp.C * nutrient.ox [ambient]		0.02		
temp.C * month [june]		-0.04		
temp.C * month [august]		-0.01		
temp.C * month [october]		-0.05		
temp.C * month [november]		-0.03		
nutrient.ox [ambient] * month [june]		0.56		
nutrient.ox [ambient] * month [august]		-0.13		
nutrient.ox [ambient] * month [october]		-0.77		
nutrient.ox [ambient] * month [november]		-0.70		
(temp.C * nutrient.ox [ambient]) * month [june]		-0.03		
(temp.C * nutrient.ox [ambient]) * month [august]		0.00		
(temp.C * nutrient.ox [ambient]) * month [october]		0.01		
(temp.C * nutrient.ox [ambient]) * month [november]		0.01		
nutrient.ox [1]			0.11***	0.11**
month [1]			0.41***	0.49**
month [2]			0.63***	0.78***
month [3]			0.17	0.41*
month [4]			-0.11	0.31**
temp.C * nutrient.ox [1]			0.01*	0.01*
temp.C * month [1]			0.04***	0.04**
temp.C * month [2]			0.01**	0.01***
temp.C * month [3]			0.03	0.02*
temp.C * month [4]			0.01	0.01
nutrient.ox [1] * month [1]			0.00	0.01
nutrient.ox [1] * month [2]			0.04	0.05
nutrient.ox [1] * month [3]			-0.10	0.11
nutrient.ox [1] * month [4]			0.04	0.09
(temp.C * nutrient.ox [1]) * month [1]			0.00	0.00
(temp.C * nutrient.ox [1]) * month [2]			0.01	0.00
(temp.C * nutrient.ox [1]) * month [3]			0.00	0.00
(temp.C * nutrient.ox [1]) * month [4]			0.01	0.01
Random Effects				
σ^2			0.02	0.01
τ_{00}			0.00 $_{site\_ID}$	0.00 $_{site\_ID}$
ICC			0.02	0.01
N			78 $_{site\_ID}$	78 $_{site\_ID}$
Observations	141	141	141	141
Marginal R^2 / Conditional R^2	NA	NA	0.759 / 0.940	0.814 / 0.943
AIC	1248.481	1074.809	994.904	970.944

* p<0.05 ** p<0.01 *** p<0.001

NEP Models:

Predictors	Model0 Estimates	Model1 Estimates	Model2 Estimates	Model3 Estimates	Model4 Estimates	Model5 Estimates
(Intercept)	4.36 ***	3.56 ***	3.91 ***	3.92 ***	3.88 ***	3.91 ***
temp C		0.10 ***	0.05 ***	0.05 ***	0.04 ***	0.05 ***
station ws [ambient]		0.78				
month [june]		0.92				
month [august]		0.69				
month [october]		0.71				
month [november]		0.66 *				
temp C * station ws [ambient]		-0.01				
temp C * month [june]		-0.06 ***				
temp C * month [august]		0.06 *				
temp C * month [october]		0.06 *				
temp C * month [november]		-0.10 ***				
station ws [ambient] * month [june]		0.07				
station ws [ambient] * month [august]		-0.88				
station ws [ambient] * month [october]		-1.17				
station ws [ambient] * month [november]		-1.41 *				
(temp C * station ws [ambient]) * month [june]		0.02				
(temp C * station ws [ambient]) * month [august]		0.04				
(temp C * station ws [ambient]) * month [october]		0.06				
(temp C * station ws [ambient]) * month [november]		0.12 *				
station ws [1]			0.02	0.04	0.02	0.04
month [1]			-0.42 ***	0.41 ***	-0.41 ***	0.40 ***
month [2]			0.17 ***	0.17 *	0.18 *	0.11 *
month [3]			0.92 ***	0.91 ***	0.88 ***	0.91 ***
month [4]			-0.61 ***	0.61 ***	-0.61 ***	0.61 ***
temp C * station ws [1]			0.00	0.00	0.00	0.00
temp C * month [1]			0.06 ***	0.06 ***	0.06 ***	0.06 ***
temp C * month [2]			-0.04 ***	0.04 ***	-0.04 ***	0.03 ***
temp C * month [3]			-0.04 ***	0.04 ***	-0.04 ***	0.04 ***
temp C * month [4]			0.01	0.01 *	0.01	0.01 *
station ws [1] * month [1]			-0.06	0.06	-0.09	0.04
station ws [1] * month [2]			-0.20	0.19	-0.18	0.17
station ws [1] * month [3]			-0.04	0.04	-0.07	0.06
station ws [1] * month [4]			0.11	0.11	0.13	0.11
(temp C * station ws [1]) * month [1]			0.01	0.01	0.01	0.01
(temp C * station ws [1]) * month [2]			0.01	0.01	0.01	0.01
(temp C * station ws [1]) * month [3]			0.01	0.00	0.01	0.01
(temp C * station ws [1]) * month [4]			-0.01	0.00	-0.00	0.00
Random Effects						
σ^2			0.01	0.02	0.01	0.01
τ_{00}			0.08 [illegible]	0.08 [illegible]	0.18 [illegible]	0.17 [illegible]
τ_{11}					0.00 [illegible]	0.00 [illegible]
ρ_{01}					-0.97 [illegible]	0.80 [illegible]
ICC			0.87	0.81	0.89	0.88
N			78 [illegible]	78 [illegible]	78 [illegible]	78 [illegible]
Observations	193	193	181	181	181	181
Marginal R^2 / Conditional R^2	NA	NA	0.620 / 0.946	0.686 / 0.918	0.668 / 0.962	0.689 / 0.917
AIC	1497.790	1418.850	1520.156	1111.736	1117.301	1109.411

* p<0.05 ** p<0.01 *** p<0.001

A5: Ambient nutrient concentrations

Ambient concentrations of dissolved phosphorus (DP), soluble reactive phosphorus (SRP), nitrate-nitrite, and ammonium at Pineland at 0.5m depth.

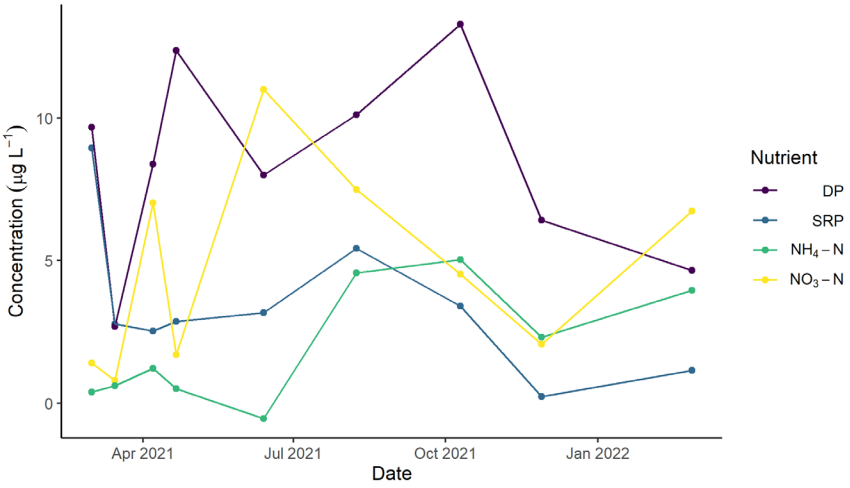

A6. Periphyton nutrient uptake rates vs. ambient nutrient concentration

Periphyton nutrient uptake rates as a function of ambient A) NH_4, B) NO_2 + NO_3, and C) SRP concentrations measured at the sediment-water interface at 0.5m depth at Pineland.

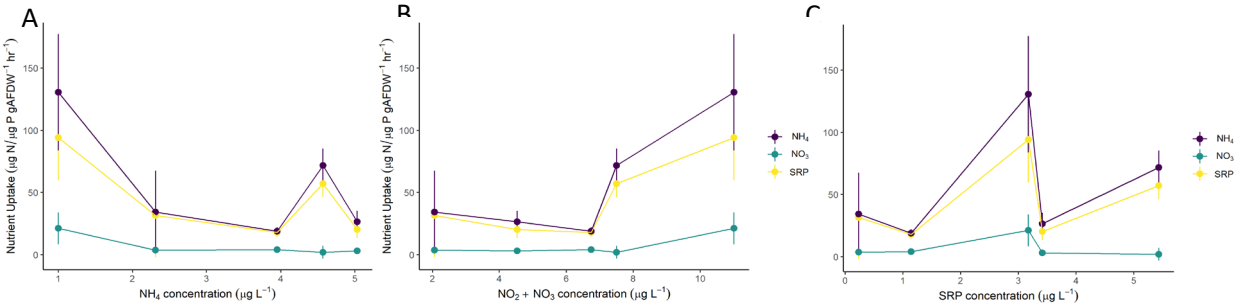

A7. Nutrient uptake vs. temperature

Temperature effects on nutrient uptake (in moles) of periphyton.

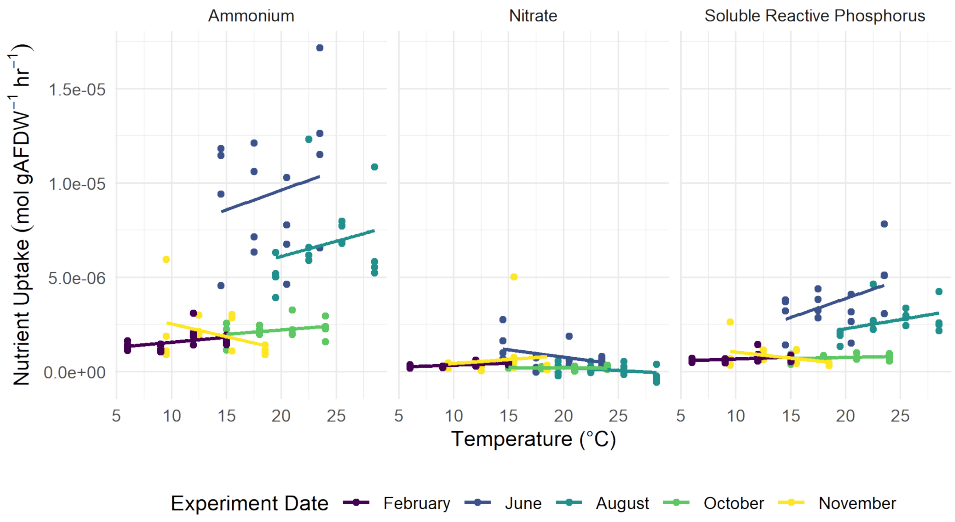

A8. Temperature effects on nutrient uptake molar N:P ratio

Molar N:P ratios of periphyton nutrient uptake vs. temperature.

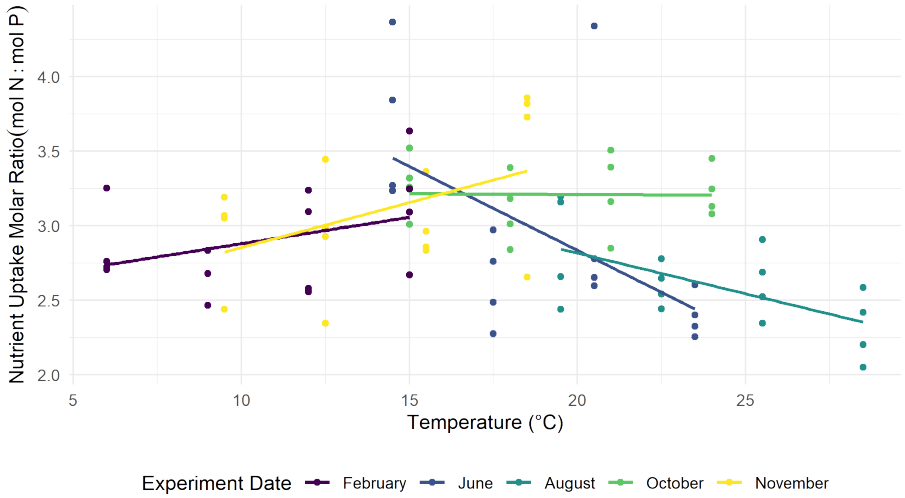

A9: Periphtyon Community Composition

Qualitative analysis of periphyton community composition measured from preserved periphyton samples from a single rock from 6 experiments ranging from April 2021-February 2022.

Lahontan Periphyton ID				
Sample Date	**Site Description**	**Preserved?**	**Abundance**	**Algal Community**
4/21/2021	Pineland, 0.5m, Comm. Comp	N	dominant	diatoms,
			moderate	stalked diatoms
			minimal	green filamentous (zygnema)
4/21/2021	Pineland, 0.5m	Lugols	dominant	stalked diatoms (gomph)
			moderate	green filamentous (zygnema)
			minimal	diatoms
6/13/2021	Pineland, 0.5m	Lugols	dominant	stalked diatoms, diatoms
			moderate	green filamentous (zygnema, mougeotia)
			very minimal	cyanobacteria (calothrix), small amount pine tr
8/8/2021	Pineland, 0.5m	Lugols	dominant	cyanobacteria (tolypothrix)
			dominant	green filamentous (spirogyra)
			dominant	diatoms
10/10/2021	Pineland, 0.5m	Lugols	dominant	cyanobacteria (calothrix maybe gloeotrichia)
			moderate	green filamentous (mougeotia, spirogyra)
			minimal	diatoms (epithemia), pine tree pollen
11/28/2021	Pineland, 0.5m	Lugols	dominant	cyanobacteria (calothrix, tolypothrix))
			moderate	diatoms
			minimal	stalked diatooms
2/27/2022	Pineland, 0.5m	Lugols	dominant	cyanobacteria (calothrix, tolypothrix))
			moderate	diatoms (gomphoneis)
			minimal	

A10. Lake Tahoe water level

Water level in Lake Tahoe from 2007-2022 measured at the Tahoe City gauge maintained by the USGS.

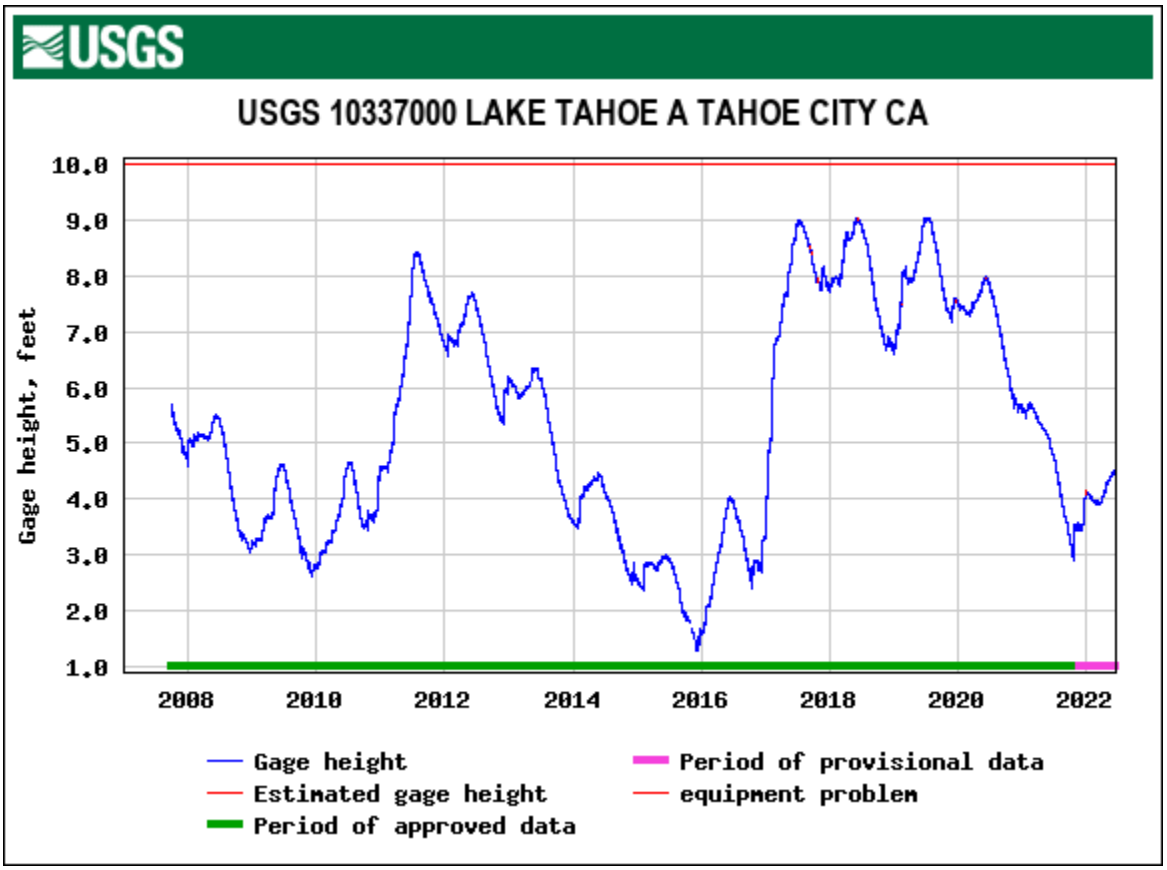

Appendix B

B1. Redox Measurements

Redox (E_h) values for oxic (blue), anoxic (red), and Phoslock® cores (gold) for the duration of the A) November 2019 and B) August 2020 experiments. Lines represent measurements made on a single core.

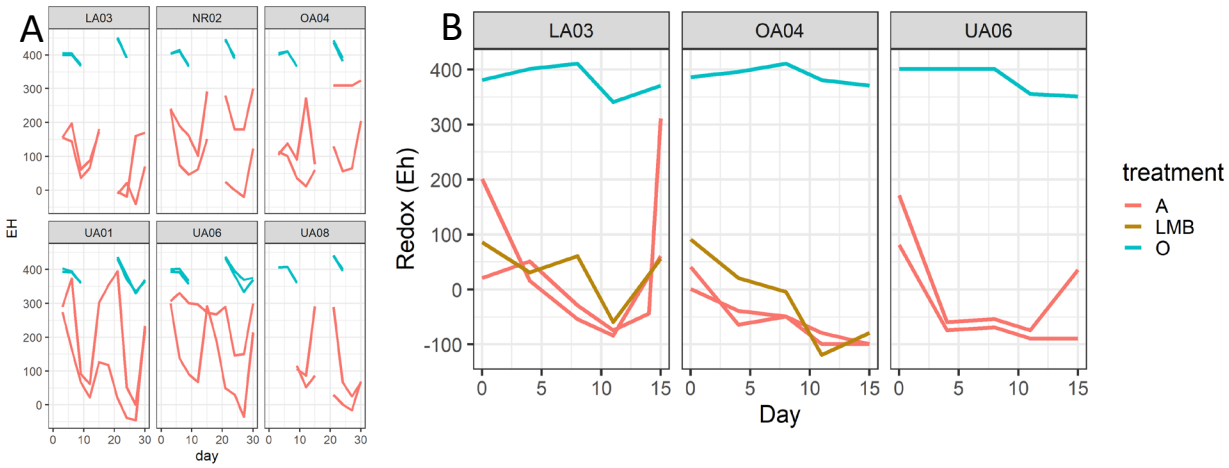

Despite large fluctuations in redox conditions in anoxic cores, potentially due to accidental introduction of oxygen during samplings, anoxic P release remained consistent during both incubations (Fig. 3). This may be due to the high biological oxygen demand (BOD) of Clear Lake sediments as the lake is such a highly productive system and sediments are rich in organic matter. This high BOD of sediments may maintain anoxic, reducing conditions near the sediment water interface even when the overlying water is slightly oxidative.

B2. pH measurements

pH conditions plotted over time for the oxic (blue), anoxic (red), and Phoslock® cores (gold) during the A) November 2019 and B) August 2020 experiments. Lines represent measurements for a single core.

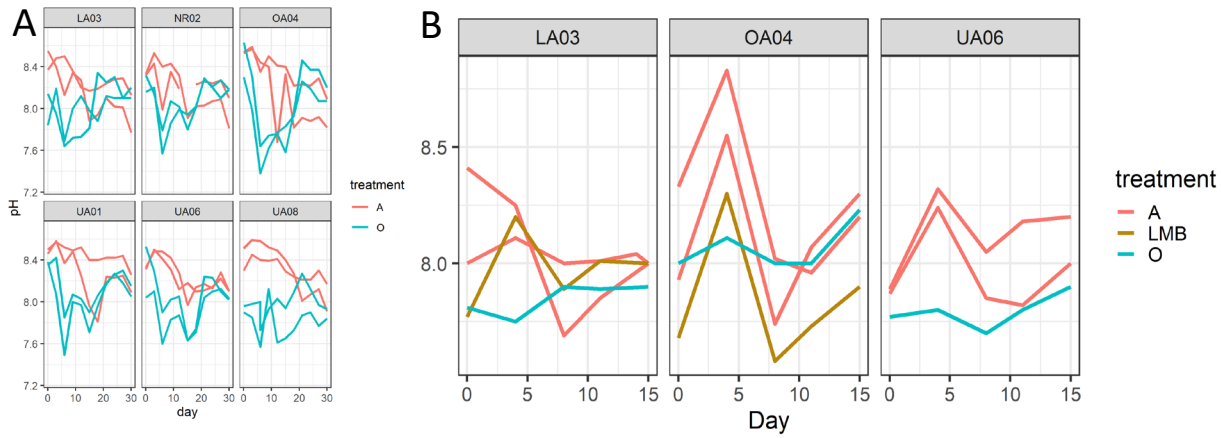

B3. Phoslock® effects on sediment NO_3 Release

Concentrations of NO_2 + NO_3 in anoxic (red), oxic (blue), and Phoslock® cores (green) during both the August 2020 experiments. Lines with error bars represent averages of duplicate cores, while those without error bars represent results from a single core.

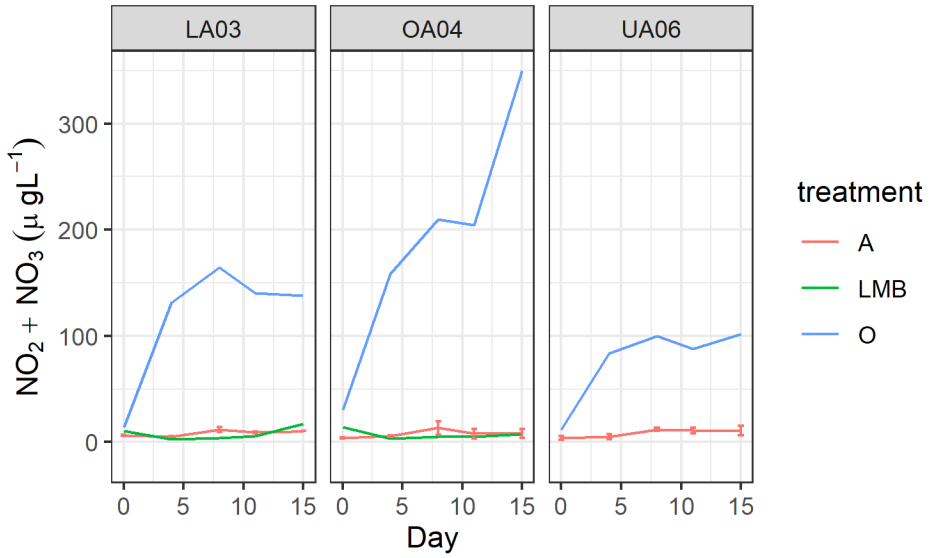

To test the efficacy of a potential phosphorus mitigation strategy, we collected 2 additional cores during August 2020 from sites LA03 and OA04 and added Phoslock® (Lanthanum-modified

Bentonite [LMB])—a chemical treatment that is known to sequester phosphorus into the sediments by increasing P sorption capacity of sediments.

The Phoslock® treatment did not appear to have an effect on NO_3 release during the August 2020 experiment as NO_3 concentrations remained low and mostly resembled patterns of non-Phoslock® treated anoxic cores.

B4. Phoslock® effects on sediment SRP Release

Concentrations of SRP (µg/L) in duplicate cores for anoxic (red), oxic (blue), and Phoslock® (green) treatments for the August 2020 experiment. Lines represent average concentrations for duplicate anoxic cores and a single oxic and Phoslock® core.

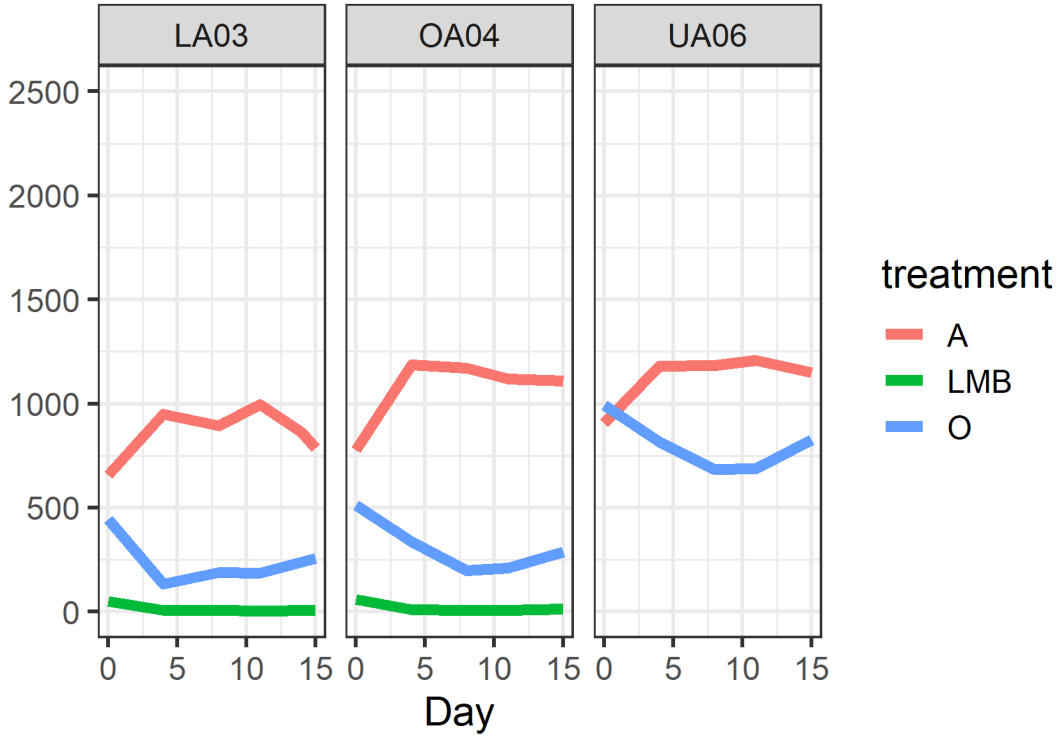

B5. Effectiveness of Phoslock® for restoration

The LMB, or Phoslock®, treatment was effective at removing almost all SRP in the overlying water in cores despite anoxic conditions, and exhibited lower SRP concentrations than oxic cores (Supplemental Fig. 4). This treatment is promising for applications in eutrophic lakes, with a meta-analysis of n = 15 lakes showing decreases in TP following Phoslock® application; however, there was considerable variation in the responses between lakes (Spears et al. 2016). If applied to 2/3 of the surface area of Clear Lake (11,700ha)—the area of fine sediments actively exchanging P (Richerson et al. 1994)—at the minimum Phoslock® load listed in the previous meta-analysis (1.4MT/ha; Spears et al. 2016), then Clear Lake would need approximately 16380MT of Phoslock® which comes to a price of $157 million. This may not be a viable application for Clear Lake as the large surface area makes costs prohibitive.

B6. Map of Lake County DWR water quality and sediment sampling sites

Map of Clear Lake, CA, with Lake County DWR long-term monitoring sites indicated with red points.